

สนาามความเร็วการไหลแบบลามินาร์จากฟังก์ชันของกรีน



นาย สกล แสันทรงสิริ

สถาบันวิทยบริการ

จุฬาลงกรณ์มหาวิทยาลัย

วิทยานิพนธ์นี้เป็นส่วนหนึ่งของการศึกษาตามหลักสูตรปริญญาวิทยาศาสตรมหาบัณฑิต

สาขาวิชาฟิสิกส์ ภาควิชาฟิสิกส์

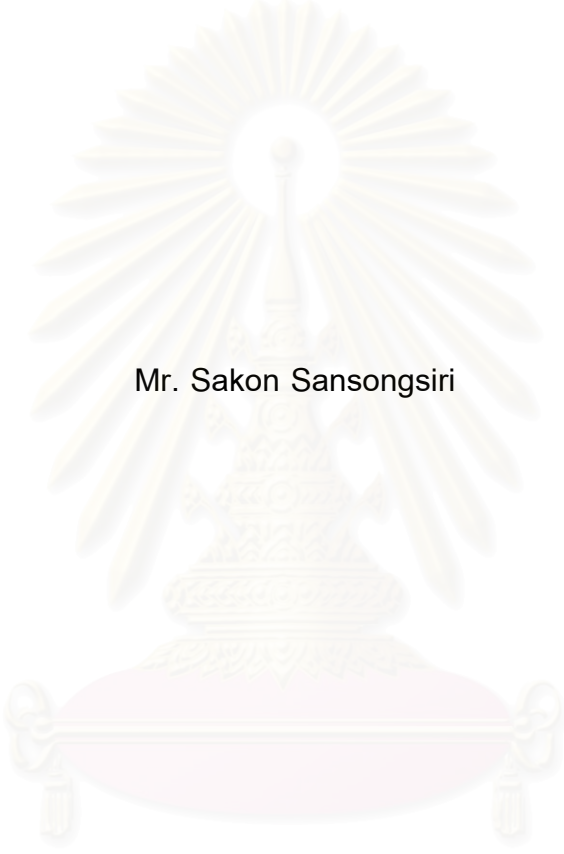
คณะวิทยาศาสตร์ จุฬาลงกรณ์มหาวิทยาลัย

ปีการศึกษา 2545

ISBN 974-17-2257-5

ลิขสิทธิ์ของจุฬาลงกรณ์มหาวิทยาลัย

LAMINAR FLOW VELOCITY FIELD FROM A GREEN'S FUNCTION



Mr. Sakon Sansongsiri

สถาบันวิทยบริการ
จุฬาลงกรณ์มหาวิทยาลัย

A Thesis Submitted in Partial Fulfillment of the Requirements
for the Degree of Master of Science in Physics

Department of Physics
Faculty of Science
Chulalongkorn University
Academic Year 2002
ISBN 974-17-2257-5

Thesis Title LAMINAR FLOW VELOCITY FIELD FROM A GREEN'S FUNCTION
By Mr. Sakon Sansongsiri
Field of Study Physics
Thesis Advisor Associate Professor Mayuree Natenapit, Ph.D.

Accepted by the Faculty of Science, Chulalongkorn University in Partial
Fulfillment of the Requirements for the Master's Degree

..... Dean of Faculty of Science
(Associate Professor Dr. Wanchai Phothiphichitr)

THESIS COMMITTEE

..... Chairman
(Assistant Professor Dr. Pisistha Ratanavararak)

..... Thesis Advisor
(Associate Professor Dr. Mayuree Natenapit)

..... Member
(Dr. Rujikom Dhanawittayapol)

..... Member
(Dr. Patcha Chatraphorn)

สกล แสตนทรงศิริ: สนามความเร็วการไหลแบบลามินาร์จากฟังก์ชันของกรีน. (LAMINAR FLOW VELOCITY FIELD FROM A GREEN'S FUNCTION) อ. ที่ปรึกษา: รศ. ดร. มยุรี เนตรธนภิส, 105 หน้า. ISBN 974-17-2257-5.

งานวิจัยนี้กล่าวถึงการคำนวณหาสนามความเร็วการไหลของของไหลที่มีรูปแบบการไหลแบบลามินาร์ผ่านกลุ่มทรงกลมที่กระจายอย่างสุ่ม ซึ่งใช้วิธีตัวกลางยังผลเป็นแบบจำลอง โดยแทนระบบของของไหลและกลุ่มทรงกลมที่กระจายอยู่ในของไหลนั้นด้วยทรงกลมประกอบ ซึ่งประกอบด้วยทรงกลมตัวแทนอันหนึ่งให้มีรัศมี a ปกคลุมด้วยชั้นของไหลรัศมี b อยู่ในตัวกลางยังผลที่กำหนดให้มีค่าความหนืดต่างไปจากของไหลเดิม การไหลของของไหลที่พิจารณาซึ่งเป็นแบบลามินาร์อธิบายได้ด้วยสมการของนาวิเออร์-สโตคส์ ซึ่งมีรูปแบบสมการเทียบได้กับสมการของปัวส์ซอง ดังนั้นสนามความเร็วในชั้นของไหลและในบริเวณตัวกลางยังผลคำนวณได้โดยใช้ทฤษฎีของกรีนร่วมกับเงื่อนไขขอบที่เหมาะสม โดยมีสัดส่วนการบรรจุ ($\gamma^3 = a^3/b^3$) หรือความหนาแน่นโดยปริมาตรของทรงกลมในของไหลเป็นพารามิเตอร์ และได้คำนวณสมการความเร็วของของไหลรูปแบบเชิงวิเคราะห์โดยการประมาณในสองช่วง คือ กรณีสัดส่วนการบรรจุค่าน้อย $\gamma^3 < 0.1$ และ กรณี $\gamma^3 > 0.1$ กระแสการไหลในชั้นของไหลที่ได้จากงานวิจัยนี้ถูกนำไปเปรียบเทียบกับกระแสการไหลของฮัพเปิลโดยมี γ เป็นพารามิเตอร์ นอกจากนี้ยังได้ประยุกต์ใช้สมการความเร็วที่คำนวณได้เพื่อศึกษาการดักจับอนุภาคแม่เหล็กที่ปะปนมากับของไหลโดยกลุ่มทรงกลมแม่เหล็ก โดยใช้โปรแกรมสำเร็จรูปแมทเทมทิคาคำนวณเส้นทางการเคลื่อนที่ของอนุภาคแม่เหล็กเพื่อหารัศมีการจับอนุภาคในรูปของ γ และนำไปเปรียบเทียบกับผลการศึกษาที่ผ่านมานบนพื้นฐานของทฤษฎีของฮัพเปิล

ผลการวิจัยพบว่ากระแสการไหลภายในชั้นของไหลมีลักษณะใกล้เคียงกันกับกระแสการไหลของฮัพเปิล โดยเฉพาะที่สัดส่วนการบรรจุเบาบาง สำหรับรัศมีการจับอนุภาคแม่เหล็กพบว่ามีการผันแปรที่ขึ้นกับ γ คล้ายกันสำหรับสนามการไหลวิธีตัวกลางยังผลและสนามการไหลของฮัพเปิล แต่ที่ γ ค่ามาก รัศมีการจับอนุภาคที่คำนวณได้นี้มีค่าน้อยกว่าที่ได้จากแบบจำลองของฮัพเปิล

ภาควิชา...ฟิสิกส์..... ลายมือชื่อนิสิต.....
 สาขาวิชา...ฟิสิกส์..... ลายมือชื่ออาจารย์ที่ปรึกษา.....
 ปีการศึกษา...2545.....

4372430423 : MAJOR PHYSICS

KEY WORD: GREEN'S FUNCTION / LAMINAR FLOW / FLUID SHELL / EFFECTIVE MEDIUM

SAKON SANSONGSIRI: LAMINAR FLOW VELOCITY FIELD FROM A GREEN'S FUNCTION. THESIS ADVISOR: ASSOC. PROF. MAYUREE NATENAPIT, Ph.D.,
105 pp. ISBN 974-17 -2257 -5.

The determination of velocity field of the fluid with laminar flow through randomly distributed spheres using an effective medium treatment (EMT) is presented. In the EMT, the system of fluid and spheres is replaced by a composite sphere -- a representative sphere of radius a enclosed by a fluid shell of radius b -- embedded in an effective medium of different viscosity. This type of fluid flow is described by Navier-Stokes equation which is equivalent to Poisson's equation, so that the velocity field in the fluid shell and in the effective medium as a function of sphere volume packing fraction ($\gamma^3 = a^3/b^3$) or density of spheres in the fluid can be determined by using Green's theorem and proper boundary conditions. The approximate fluid velocity in analytic closed form is obtained for low packing fraction ($\gamma^3 < 0.1$) and for the other range of $\gamma^3 > 0.1$. The comparison of flow fields in the fluid shell obtained in this research with Happel flow fields is shown for varying γ . The results of fluid velocity are applied to study the capture of magnetic particles by an assemblage of magnetic spheres by using Mathematica program. The capture radius as a function of γ is obtained and compared with the results from previous study based on Happel's theory.

The investigation shows that the flow fields within the fluid shell are very similar to Happel flow fields especially for the dilute range of packing fractions. The general features of the variation of capture radii with γ for the EMT and Happel flow fields are also similar, but for higher γ our results are lower than the corresponding Happel model results.

Department....Physics..... Student's signature.....
Field of study....Physics..... Advisor's signature.....
Academic year....2002.....

Acknowledgements

I wish to express my sincere gratitude to Associate Professor Dr. Mayuree Natenapit, for her helpful suggestions and supports throughout this research and also to the thesis committee, Assistant Professor Dr. Pisistha Ratanavararak, Dr. Rujikorn Dhanawittayapol and Dr. Patcha Chatraphorn for their valuable comments and also useful suggestions.

Sincere thanks are also expressed to the Ministry of University Affairs for the scholarship under the lecturer development project and to the staff of the Physics Department, Chulalongkorn University for their assistance and providing a teaching assistantship in the second year.

Lastly, I would like to give a special thank to my parents for their love and encouragement, and to my friends for their support throughout this study. I am also grateful to every one who has contributed suggestions and support during this study.



สถาบันวิทยบริการ
จุฬาลงกรณ์มหาวิทยาลัย

Contents

	page
Abstract in Thai	iv
Abstract in English	v
Acknowledgements	vi
Contents	vii
List of Tables	ix
List of Figures	x
List of Notations	xiii
Chapter	
I Introduction	1
II Green's function for Poisson's equation	3
2.1 Formal solution to Poisson's equation	3
2.1.1 Green's identities and methods	3
2.1.2 Green's theorem for electrostatics	8
2.2 Green's function in a spherical shell	9
III Laminar flow velocity field	15
3.1 Happel flow field	15
IV Laminar flow velocity field from a Green's function	21
4.1 Effective medium treatment	21
4.2 Laminar flow velocity field from a Green's function	23
4.2.1 Velocity field outside the shell	25
4.2.2 Velocity field in the shell region	28

	page
4.3 Closed form of velocity fields	33
4.3.1 For low packing fraction	33
4.3.2 For higher packing fraction	36
4.4 Comparing velocity profiles	41
V Capture of magnetic particles in laminar flow	54
5.1 Equation of motion	54
5.2 Mathematica program for particle trajectories	56
5.3 Capture radius	63
VI Conclusion and discussion	68
References	71
Appendices	73
Appendix A Solution for the constants A, B, C, D and δ	74
Appendix B Curve fitting of the constants	84
Appendix C Particle trajectories by Mathematica program	91
Biography	105

สถาบันวิทยบริการ
จุฬาลงกรณ์มหาวิทยาลัย

List of Tables

Table	page
4.1 The numerical values of relative viscosity ($\delta = \eta^* / \eta$) and constants in Equations (4.30) and (4.31) for various packing fraction (γ^3)	32
4.2 The numerical values of the constants from Equations (4.36a)-(4.36d) for various γ	36
5.1 Capture radii of magnetic particles for varying γ taken from the EMT velocity field in closed form. Characteristic constants are $v_{ma} = 571.5 \text{ s}^{-1}$, $v_{0a} = 6.65 \text{ s}^{-1}$ and $K_s = 0.58$. $\vec{H}_0 // \vec{v}_0$ and $\vec{H}_0 \perp \vec{v}_0$ denote longitudinal and transverse mode design, respectively	64

List of Figures

Figure	page
2.1 Surfaces and appropriate cuts used in Green's theorem	4
2.2 Discontinuity in slope of the radial Green's function	13
4.1 A representative sphere in the effective medium	22
4.2 The effective viscosity as a function of γ (γ^3 = packing fraction)	33
4.3 The fitted curve of parameter A (solid line) superimposed on the numerical values of A (points)	38
4.4 The fitted curve of parameter B (solid line) superimposed on the numerical values of B (points)	38
4.5 The fitted curve of parameter C (solid line) superimposed on the numerical values of C (points)	39
4.6 The fitted curve of parameter D (solid line) superimposed on the numerical values of D (points)	39
4.7 Comparison of EMT velocity profiles (dash lines) with Happel flow profile (solid lines) for low packing fraction at $\gamma^3 = 0.001$ and $v_{0a} = 6.65 \text{ s}^{-1}$	42
4.8 Comparison of EMT velocity profiles (dash lines) with Happel flow profile (solid lines) for low packing fraction at $\gamma^3 = 0.008$ and $v_{0a} = 6.65 \text{ s}^{-1}$	43
4.9 Comparison of EMT velocity profiles (dash lines) with Happel flow profile (solid lines) for low packing fraction at $\gamma^3 = 0.027$ and $v_{0a} = 6.65 \text{ s}^{-1}$	44
4.10 Comparison of EMT velocity profiles (dash lines) with Happel flow profile (solid lines) for low packing fraction at $\gamma^3 = 0.064$ and $v_{0a} = 6.65 \text{ s}^{-1}$	45
4.11 Comparison of EMT velocity profiles (dash lines) with Happel flow profile (solid lines) for higher packing fraction at $\gamma^3 = 0.216$ and $v_{0a} = 6.65 \text{ s}^{-1}$	46

4.12 Comparison of EMT velocity profiles (dash lines) with Happel flow profile (solid lines) for higher packing fraction at $\gamma^3 = 0.343$ and $v_{0a} = 6.65 \text{ s}^{-1}$	47
4.13 Comparison of EMT velocity profiles Equation (4.29) (dash lines) with Happel flow profile (solid lines) at $\gamma^3 = 0.001$, and $v_{0a} = 6.65 \text{ s}^{-1}$	48
4.14 Comparison of EMT velocity profiles Equation (4.29) (dash lines) with Happel flow profile (solid lines) at $\gamma^3 = 0.008$, and $v_{0a} = 6.65 \text{ s}^{-1}$	49
4.15 Comparison of EMT velocity profiles Equation (4.29) (dash lines) with Happel flow profile (solid lines) at $\gamma^3 = 0.027$, and $v_{0a} = 6.65 \text{ s}^{-1}$	50
4.16 Comparison of EMT velocity profiles Equation (4.29) (dash lines) with Happel flow profile (solid lines) at $\gamma^3 = 0.064$, and $v_{0a} = 6.65 \text{ s}^{-1}$	51
4.17 Comparison of EMT velocity profiles Equation (4.29) (dash lines) with Happel flow profile (solid lines) at $\gamma^3 = 0.216$, and $v_{0a} = 6.65 \text{ s}^{-1}$	52
4.18 Comparison of EMT velocity profiles Equation (4.29) (dash lines) with Happel flow profile (solid lines) at $\gamma^3 = 0.343$, and $v_{0a} = 6.65 \text{ s}^{-1}$	53
5.1 Capture radius r_c and particle trajectories of paramagnetic particles for a longitudinal mode ($\vec{H}_0 // \vec{v}_0$) with $\gamma^3 = 0.001$, $v_{0a} = 6.65 \text{ s}^{-1}$, $v_{ma}^* = 572.16 \text{ s}^{-1}$ and $K_s = 0.58$	57
5.2 Capture radius r_c and particle trajectories of paramagnetic particles for a transverse mode ($\vec{H}_0 \perp \vec{v}_0$) with $\gamma^3 = 0.001$, $v_{0a} = 6.65 \text{ s}^{-1}$, $v_{ma}^* = 572.16 \text{ s}^{-1}$ and $K_s = 0.58$	58
5.3 Capture radius r_c and particle trajectories of diamagnetic particles for a longitudinal mode ($\vec{H}_0 // \vec{v}_0$) with $\gamma^3 = 0.001$, $v_{0a} = 6.65 \text{ s}^{-1}$, $v_{ma}^* = -572.16 \text{ s}^{-1}$ and $K_s = 0.58$	59
5.4 Capture radius r_c and particle trajectories of diamagnetic particles for a transverse mode ($\vec{H}_0 \perp \vec{v}_0$) with $\gamma^3 = 0.001$, $v_{0a} = 6.65 \text{ s}^{-1}$, $v_{ma}^* = -572.16 \text{ s}^{-1}$ and $K_s = 0.58$	60
5.5 Capture radius r_c and particle trajectories of paramagnetic particles for a longitudinal mode ($\vec{H}_0 // \vec{v}_0$) with $\gamma^3 = 0.125$, $v_{0a} = 6.65 \text{ s}^{-1}$, $v_{ma}^* = 664.34 \text{ s}^{-1}$ and $K_s = 0.58$	61

- 5.6 Capture radius r_c and particle trajectories of paramagnetic particles for a transverse mode ($\vec{H}_0 \perp \vec{v}_0$) with $\gamma^3 = 0.125$, $v_{0a} = 6.65 \text{ s}^{-1}$, $v_{ma}^* = 664.34 \text{ s}^{-1}$ and $K_s = 0.58$ 62
- 5.7 Capture radius for paramagnetic particles as a function of γ based on Happel and EMT flow fields in closed form. Characteristic constants are $v_{ma} = 571.5 \text{ s}^{-1}$, $v_{0a} = 6.65 \text{ s}^{-1}$ and $K_s = 0.58$ 65
- 5.8 Capture radius for diamagnetic particles as a function of γ based on Happel and EMT flow fields in closed form. Characteristic constants are $v_{ma} = 571.5 \text{ s}^{-1}$, $v_{0a} = 6.65 \text{ s}^{-1}$ and $K_s = 0.58$ 66



สถาบันวิทยบริการ
จุฬาลงกรณ์มหาวิทยาลัย

List of Notations

a	= radius of solid sphere
b	= radius of fluid shell
A, B, C, D	= constants
$G(\vec{r}, \vec{r}')$	= Green's function
\vec{H}	= magnetic field
p	= pressure
$P_l(\cos \theta)$	= Legendre polynomial of order l
$p_{r\theta}$	= stress component in θ direction
r_c	= capture radius
r_p	= particle radius
Re	= Reynolds number
\vec{v}_0	= fluid entrance velocity
\vec{v}_1	= velocity field in fluid shell
\vec{v}_2	= velocity field in effective medium
\vec{v}_{1h}	= velocity field in fluid shell for higher packing fraction ($\gamma^3 > 0.1$)
\vec{v}_{2h}	= velocity field in effective medium for higher packing fraction ($\gamma^3 > 0.1$)
\vec{v}_{1l}	= velocity field in fluid shell for low packing fraction ($\gamma^3 < 0.1$)
\vec{v}_{2l}	= velocity field in effective medium for low packing fraction ($\gamma^3 < 0.1$)
$Y_{lm}(\theta, \phi)$	= spherical harmonics

Greek Letters

Φ	= electrostatic potential
χ_f	= fluid susceptibility
χ_p	= particle susceptibility
$\delta = \eta^* / \eta$	= relative viscosity
ϵ_0	= permittivity of free space
$\gamma^3 = a^3 / b^3$	= volume packing fraction
η	= fluid viscosity
φ	= velocity potential
ρ	= fluid density
$\rho(\vec{r})$	= charge density
$\nu = \mu_p / \mu_f$	= relative permeability of particle and fluid



สถาบันวิทยบริการ
จุฬาลงกรณ์มหาวิทยาลัย

CHAPTER I

INTRODUCTION

The problem of fluid flow through various shapes of obstacles is interesting in many applications. Especially, the determination of fluid velocity field has been investigated by many approaches, for example the flow around multiple aligned cylinders [1, 2] and the flow past arrays of spheres [3]. When the fluid flows around solid objects, the characteristic of fluid flows is indicated by Reynolds number. There are two types of fluid flow, laminar and turbulent [4]. Laminar flow occurs when the fluid stream around the object is smooth, while turbulent flow occurs when the fluid stream breaks up and causes little whirlwind currents next to the object which occurs at high Reynolds number. In between, fluid flow is in the transition range. In this research, the velocity profiles for laminar flow through randomly distributed spheres are considered. This type of fluid flow occurs for values of Reynolds number $\mathbf{Re} = \rho v_0 a / \eta < 1$, where ρ , v_0 , η , and a are the fluid density, entrance velocity, viscosity, and the sphere radius, respectively. For $\mathbf{Re} > 1$, the fluid flow which is incompressible and irrotational is called potential flow which is an ideal fluid. The potential flow is described by Laplace's equation, $\nabla^2 \phi = 0$, where ϕ is the velocity potential. At steady state, the laminar flow velocity field is described by the Navier-Stokes equation which is Poisson's nonhomogeneous equation. This equation can be explored by using Green's function techniques to obtain the velocity field describing laminar flow around random spheres.

Several models have been developed to describe the system of fluid flow pass individual type of obstacles [3, 5, 6, 7, 8]. The simplest and most successful model to determine velocity profiles of laminar flow through randomly distributed spheres is the free-surface model due to Happel [9]. The model consists of two concentric spheres; the inner sphere represents one of the spheres in the assemblage and the outer sphere is a fluid envelope. The surface of the outer sphere is assumed to be frictionless; its size is fixed by sphere volume packing fraction or density of the spheres in the system. In this research, we used an effective medium treatment (EMT). In the EMT, the system of fluid and spheres is replaced by a composite sphere -- a

representative sphere of radius a enclosed by a fluid shell of radius b -- embedded in an effective medium of different viscosity. The velocity fields in the fluid shell and in the effective medium as a function of sphere volume packing fraction ($\gamma^3 = a^3/b^3$) or density of the spheres in liquid are determined by using Green's theorem and proper boundary conditions.

This thesis begins with a review of Green's function for Poisson's equation as given in the second chapter. The determination of the formal solution to Poisson's equation with Dirichlet boundary conditions and Green's function in a spherical shell are reported.

In Chapter 3, we discuss the Happel model and demonstrate the derivation of the laminar velocity field of fluid flow around random particles moving in the fluid at rest. Then the transformation of this velocity field to the reference coordinate system fixed on a representative particle is performed.

In Chapter 4, the derivation of fluid flow fields by using effective medium treatment (EMT) with Green's function technique reviewed in Chapter 2, and proper boundary conditions is discussed in detail. Two regions are considered: outside the shell (in the effective medium) and in the shell regions. We consider for the cases of low packing fraction ($\gamma^3 < 0.1$) and $\gamma^3 > 0.1$ separately. Then our results are compared with Happel flow fields for varying various packing fractions.

In Chapter 5, the flow fields obtained in this research as presented in the previous chapter are applied to describe the trajectories of magnetic particles carried by the fluid of laminar flow type. Finally, the capture radii are investigated for varying γ and presented in comparison with the results based on Happel flow fields.

The last chapter is devoted to the conclusion and discussion of the velocity flow fields obtained in this research and its applications. There, the comparison of velocity profiles and capture radius (r_c) with the results based on Happel's theory are discussed.

CHAPTER II

GREEN'S FUNCTION FOR POISSON'S EQUATION

Our research concerns the solution to Poisson's equation in any region of a spherical shell with Dirichlet boundary conditions. Poisson's equation is a special case of Helmholtz equation which is amenable to the method of Green's function technique. In this chapter, the development of the formal solution to Poisson's equation with Dirichlet boundary conditions is reviewed with the construction of Green's function in a spherical shell of radii a and b .

2.1 Formal Solution to Poisson's Equation

In this section the use of Green's theorem to construct the formal solution for Dirichlet boundary value problems is presented. First we discuss the general solution of Helmholtz equation and next the Poisson's equation in electrostatics.

2.1.1 Green's Identities and Methods

We now consider the general solution of the three-dimensional scalar Helmholtz partial differential equation [10]

$$\nabla^2 \varphi(\vec{r}) + \beta^2 \varphi(\vec{r}) = f(\vec{r}) \quad (2.1)$$

subject to the generalized homogeneous boundary conditions

$$\alpha_1 \varphi(\vec{r}_s) + \alpha_2 \frac{\partial \varphi(\vec{r}_s)}{\partial n} = 0. \quad (2.2)$$

Here \vec{r}_s is on surface S with \hat{n} an outward directed unit vector, and α_1 and α_2 are constants. The Green's function $G(\vec{r}, \vec{r}')$ of Equation (2.1) must satisfy the partial differential equation

$$\nabla^2 G(\vec{r}, \vec{r}') + \beta^2 G(\vec{r}, \vec{r}') = \delta(\vec{r} - \vec{r}') \quad (2.3)$$

subject to the generalized homogeneous boundary condition [10]

$$\alpha_1 G(\vec{r}_s, \vec{r}') + \alpha_2 \frac{\partial G(\vec{r}_s, \vec{r}')}{\partial n} = 0. \quad (2.4)$$

To accomplish this we need two identities from vector calculus that are usually referred to as Green's first and second identities.

Consider a volume V enclosing the surfaces $S_1, S_2, S_3, \dots, S_n$ as shown in Figure 2.1. By introducing appropriate cuts, the volume V is bounded by a regular surface S that consists of surfaces $S_1 - S_n$, the surfaces along the cuts, and the spherical surface S_a of infinite radius which encloses all the smaller surfaces. A unit vector \hat{n} normal to S is directed outwards the volume V , as shown in Figure 2.1.

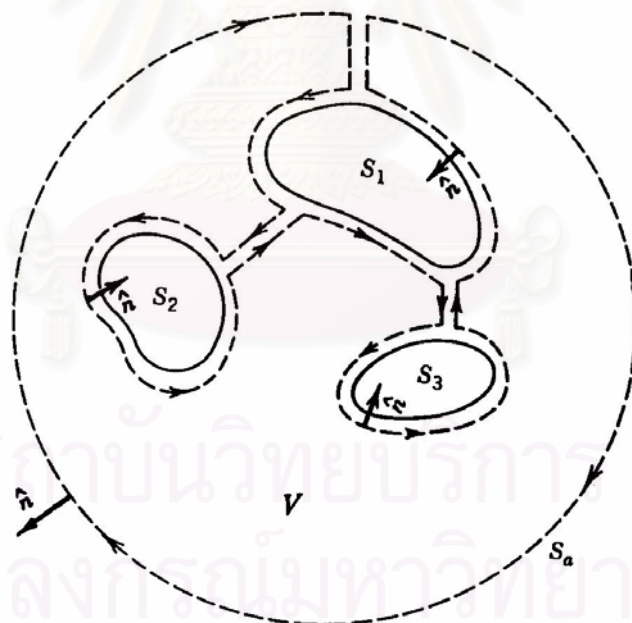


Figure 2.1 Surfaces and appropriate cuts used in Green's theorem [10].

Let us introduce within V two scalar functions ϕ and ψ which their first and second derivatives are continuous within V and on the surface S . To the vector $\phi \bar{\nabla} \psi$ we apply the divergence theorem

$$\oint \bar{A}.d\bar{s} = \int \bar{\nabla}.\bar{A}dv ,$$

$$\text{thus} \quad \oint (\phi \bar{\nabla} \psi).d\bar{s} = \oint (\phi \bar{\nabla} \psi).\hat{n}da = \int \bar{\nabla}.\phi \bar{\nabla} \psi dv . \quad (2.5)$$

When expanded, the integrand of the volume integral can be written as

$$\bar{\nabla}.\phi \bar{\nabla} \psi = \phi \bar{\nabla}.\bar{\nabla} \psi + \bar{\nabla} \phi.\bar{\nabla} \psi = \phi \nabla^2 \psi + \bar{\nabla} \phi.\bar{\nabla} \psi . \quad (2.6)$$

Thus Equation (2.5) can be expressed as

$$\oint (\phi \bar{\nabla} \psi).d\bar{s} = \int (\phi \nabla^2 \psi)dv + \int (\bar{\nabla} \phi.\bar{\nabla} \psi)dv \quad (2.7)$$

which is referred to as *Green's first identity*. Since

$$(\bar{\nabla} \psi).\hat{n} = \frac{\partial \psi}{\partial n} , \quad (2.8)$$

where the derivative $\partial \psi / \partial n$ is taken in the direction of positive normal, equation (2.7) can also be written as

$$\begin{aligned} \oint \phi \frac{\partial \psi}{\partial n} ds &= \int (\phi \nabla^2 \psi)dv + \int (\bar{\nabla} \phi.\bar{\nabla} \psi)dv \\ &= \int (\phi \nabla^2 \psi + \bar{\nabla} \phi.\bar{\nabla} \psi)dv , \end{aligned} \quad (2.9)$$

which is an *alternative form of Green's first identity*.

If we repeat the procedure but apply the divergence theorem of Equation (2.5) to the vector $\psi \bar{\nabla} \phi$, then we can write, respectively, Green's first identity of Equation (2.7) and its alternative form of Equation (2.9) as

$$\oint (\psi \bar{\nabla} \phi).ds = \int (\psi \nabla^2 \phi)dv + \int (\bar{\nabla} \psi.\bar{\nabla} \phi)dv \quad (2.10)$$

and

$$\oint (\psi \frac{\partial \phi}{\partial n}) ds = \int (\psi \nabla^2 \phi) dv + \int (\bar{\nabla} \psi \cdot \bar{\nabla} \phi) dv . \quad (2.11)$$

Subtracting Equation (2.10) from Equation (2.7) we can write

$$\oint (\phi \bar{\nabla} \psi - \psi \bar{\nabla} \phi) . ds = \int (\phi \nabla^2 \psi - \psi \nabla^2 \phi) dv \quad (2.12)$$

which is referred to as *Green's second identity*. Its alternative form

$$\oint (\phi \frac{\partial \psi}{\partial n} - \psi \frac{\partial \phi}{\partial n}) ds = \int (\phi \nabla^2 \psi - \psi \nabla^2 \phi) dv \quad (2.13)$$

is obtained by subtracting Equation (2.11) from Equation (2.9).

With Green's first and second identities, we now develop the formulation of the generalized Green's function method for the partial differential equation (2.1) whose Green's function $G(\vec{r}, \vec{r}')$ satisfies Equation (2.3).

Let us multiply Equation (2.1) by $G(\vec{r}, \vec{r}')$ and Equation (2.3) by $\phi(\vec{r})$. Doing this leads to

$$G \nabla^2 \phi + \beta^2 \phi G = fG \quad (2.14a)$$

$$\text{and} \quad \phi \nabla^2 G + \beta^2 \phi G = \phi \delta(\vec{r} - \vec{r}') . \quad (2.14b)$$

Subtracting Equation (2.14a) from Equation (2.14b) and integrating over the volume V , we can write

$$\int \phi \delta(\vec{r} - \vec{r}') dv - \int fG dv = \int (\phi \nabla^2 G - G \nabla^2 \phi) dv \quad (2.15a)$$

or

$$\begin{aligned} \phi(\vec{r} = \vec{r}') &= \phi(\vec{r}') \\ &= \int f(\vec{r}) G(\vec{r}, \vec{r}') dv + \int [\phi(\vec{r}) \nabla^2 G(\vec{r}, \vec{r}') - G(\vec{r}, \vec{r}') \nabla^2 \phi(\vec{r})] dv . \end{aligned} \quad (2.15b)$$

Applying Green's second identity (2.12) reduces Equation (2.15b) to

$$\varphi(\vec{r}') = \int f(\vec{r})G(\vec{r}, \vec{r}')dv + \oint [\varphi(\vec{r})\vec{\nabla}G(\vec{r}, \vec{r}') - G(\vec{r}, \vec{r}')\vec{\nabla}\varphi(\vec{r})].d\vec{s} . \quad (2.16)$$

Since \vec{r}' is an arbitrary point within V and \vec{r} is a dummy variable. By the mathematical symmetry property $G(\vec{r}, \vec{r}') = G(\vec{r}', \vec{r})$, we can also write Equation (2.16) as

$$\varphi(\vec{r}) = \int f(\vec{r}')G(\vec{r}, \vec{r}')dv' + \oint [\varphi(\vec{r}')\vec{\nabla}'G(\vec{r}, \vec{r}') - G(\vec{r}, \vec{r}')\vec{\nabla}'\varphi(\vec{r}')].d\vec{s}' , \quad (2.17)$$

where $\vec{\nabla}'$ indicates differentiation with respect to the prime coordinates.

Equation (2.17) is a generalized formula for the solution of a three-dimensional scalar Helmholtz equation. It can be simplified depending on the boundary conditions of φ and G , and their derivatives on S .

If the nonhomogeneous partial differential equation (2.1) satisfies the nonhomogeneous Dirichlet boundary condition

$$\varphi(\vec{r}_s) = g(\vec{r}_s) , \quad (2.18a)$$

where \vec{r}_s is on S , then we can still construct a Green's function that satisfies the boundary condition

$$G(\vec{r}_s, \vec{r}') = 0 , \quad (2.18b)$$

where \vec{r}_s is on S .

For these boundary conditions on φ and G the second term in the surface integral of Equation (2.17) vanishes, so that Equation (2.17) reduces to

$$\varphi(\vec{r}) = \int f(\vec{r}')G(\vec{r}, \vec{r}')dv' + \oint \varphi(\vec{r}')\vec{\nabla}'G(\vec{r}_s, \vec{r}') .d\vec{s}' , \quad (2.19)$$

φ is scalar function which along with its first and second derivatives are continuous within V and on the surface S . In the next section we will considered this formal solution in a specific case for electrostatics.

2.1.2 Green's Theorem for Electrostatics

This section we review the construction of formal solution to Dirichlet boundary value problems for Poisson's equation in electrostatics.

For the special case of Helmholtz equation (2.1), Poisson's equation for the electrostatics potential Φ takes the form

$$\nabla^2 \Phi = -\frac{\rho(\vec{r})}{\epsilon_0}, \quad (2.20)$$

where $\rho(\vec{r})$ is the charge density found within volume V . The contributions of charges that might be found outside the volume of interest are represented by the boundary conditions, either the potential or its normal derivatives on the bounding surface. It is useful to define the Green's function $G(\vec{r}, \vec{r}')$ to be the potential at \vec{r} produced by a unit point charge at \vec{r}' satisfying the partial differential equation (2.3) as the solution to

$$\nabla^2 G(\vec{r}, \vec{r}') = -4\pi\delta(\vec{r} - \vec{r}') \quad (2.21)$$

subject to appropriate boundary conditions to be specified later. Next we apply Green's second identity (2.13) by choosing ϕ to be the electrostatic potential Φ and ψ to be the Green's function $G(\vec{r}, \vec{r}')$, so that

$$\begin{aligned} & \int \left(\Phi(\vec{r}') \nabla'^2 G(\vec{r}, \vec{r}') - G(\vec{r}, \vec{r}') \nabla'^2 \Phi(\vec{r}') \right) dv' \\ &= \oint \left(\Phi(\vec{r}') \frac{\partial G(\vec{r}, \vec{r}')}{\partial n'} - G(\vec{r}, \vec{r}') \frac{\partial \Phi(\vec{r}')}{\partial n'} \right) ds' \end{aligned} \quad (2.22)$$

Using Poisson's equation (2.20) and the definition of the Green's function in Equation (2.21), this becomes

$$\begin{aligned} & -4\pi \int \left(\Phi(\vec{r}') \delta(\vec{r} - \vec{r}') - G(\vec{r}, \vec{r}') \frac{\rho(\vec{r}')}{4\pi\epsilon_0} \right) dv' \\ &= \oint \left(\Phi(\vec{r}') \frac{\partial G(\vec{r}, \vec{r}')}{\partial n'} - G(\vec{r}, \vec{r}') \frac{\partial \Phi(\vec{r}')}{\partial n'} \right) ds' \end{aligned} \quad (2.23)$$

Thus, a formal solution to Poisson's equation is [11]

$$\begin{aligned}\Phi(\vec{r}) &= \frac{1}{4\pi\epsilon_0} \int \rho(\vec{r}') G(\vec{r}, \vec{r}') dv' \\ &+ \frac{1}{4\pi} \oint \left(G(\vec{r}, \vec{r}') \frac{\partial \Phi(\vec{r}')}{\partial n'} - \Phi(\vec{r}') \frac{\partial G(\vec{r}, \vec{r}')}{\partial n'} \right) ds'. \quad (2.24)\end{aligned}$$

If there were no boundary surfaces, the first term would represent the familiar electrostatic potential produced by a specified charge distribution. The second term then represents the contribution made by external charges that determine the conditions on the boundary surfaces.

For Dirichlet boundary conditions specifying Φ on S , it is required that Green's function vanishes on S so that [11]

$$\Phi(\vec{r}) = \frac{1}{4\pi\epsilon_0} \int \rho(\vec{r}') G(\vec{r}, \vec{r}') dv' - \frac{1}{4\pi} \oint \Phi(\vec{r}') \frac{\partial G(\vec{r}, \vec{r}')}{\partial n'} ds'. \quad (2.25)$$

This equation is a formal solution to Poisson's equation with Dirichlet boundary conditions. The Green's function $G(\vec{r}, \vec{r}')$ in this equation will be determined in the next section.

2.2 Green's Function in a Spherical Shell

We seek to construct a Green's function for Poisson's equation that vanishes on the concentric spherical surfaces of radii a and b . A Green's function for a Dirichlet potential problem satisfies the equation

$$\nabla^2 G(\vec{r}, \vec{r}') = -4\pi\delta(\vec{r} - \vec{r}'). \quad (2.26)$$

The Laplacian in spherical coordinates, (r, θ, ϕ) , has the form

$$\nabla^2 = \frac{1}{r^2} \frac{\partial}{\partial r} \left(r^2 \frac{\partial}{\partial r} \right) + \frac{1}{r^2 \sin \theta} \left(\frac{\partial}{\partial \theta} \left(\sin \theta \frac{\partial}{\partial \theta} \right) + \frac{1}{\sin \theta} \frac{\partial^2}{\partial \phi^2} \right) \quad (2.27a)$$

and

$$\delta(\vec{r} - \vec{r}') = \frac{1}{r^2 \sin \theta} \delta(r - r') \delta(\theta - \theta') \delta(\phi - \phi').$$

(2.27b) Using Equations (2.27a) and (2.27b) into equation (2.26) which takes the form

$$\begin{aligned} \frac{1}{r^2} \frac{\partial}{\partial r} \left(r^2 \frac{\partial G}{\partial r} \right) + \frac{1}{r^2 \sin \theta} \left[\frac{\partial}{\partial \theta} \left(\sin \theta \frac{\partial G}{\partial \theta} \right) + \frac{1}{\sin \theta} \frac{\partial^2 G}{\partial \phi^2} \right] \\ = - \frac{4\pi}{r^2 \sin \theta} \delta(r - r') \delta(\theta - \theta') \delta(\phi - \phi'). \end{aligned} \quad (2.28)$$

We define the operator

$$L^2 \equiv - \left[\frac{1}{\sin \theta} \frac{\partial}{\partial \theta} \left(\sin \theta \frac{\partial}{\partial \theta} \right) + \frac{1}{\sin^2 \theta} \frac{\partial^2}{\partial \phi^2} \right]. \quad (2.29)$$

The eigenfunctions of L^2 subject to the boundary conditions that these eigenfunctions are finite at $\theta = 0$ and $\theta = \pi$ are the spherical harmonics $Y_{lm}(\theta, \phi)$. The corresponding eigenvalues are $l(l+1)$ where $l = 0, 1, 2, \dots$ etc. and m is an integer whose values are from $-l$ to l [12],

$$L^2 Y_{lm}(\theta, \phi) = l(l+1) Y_{lm}(\theta, \phi). \quad (2.30)$$

From the above condition, Equation (2.28) can be written as

$$\frac{1}{r^2} \frac{\partial}{\partial r} \left(r^2 \frac{\partial G}{\partial r} \right) - \frac{L^2}{r^2} G = - \frac{4\pi}{r^2 \sin \theta} \delta(r - r') \delta(\theta - \theta') \delta(\phi - \phi'). \quad (2.31)$$

We expand $G(\vec{r}, \vec{r}')$ in terms of these eigenfunctions;

$$G(\vec{r}, \vec{r}') = \sum_{l'=0}^{\infty} \sum_{m'=-l'}^{l'} g_{lm'}(\vec{r}, \vec{r}') Y_{lm'}(\theta, \phi). \quad (2.32)$$

By substituting Equation (2.32) into Equation (2.31) and using Equation (2.30) one obtains

$$\begin{aligned} & \sum_{l'=0}^{\infty} \sum_{m'=-l'}^{l'} \left[\frac{1}{r^2} \frac{d}{dr} \left(r^2 \frac{dg_{lm'}}{dr} \right) - \frac{l(l+1)}{r^2} g_{lm'} \right] Y_{lm'}(\theta, \phi) \\ & = -\frac{4\pi}{r^2 \sin \theta} \delta(r-r') \delta(\theta-\theta') \delta(\phi-\phi'). \end{aligned} \quad (2.33)$$

Multiplying both sides of Equation (2.33) by $r^2 Y_{lm}^*(\theta, \phi) \sin \theta$ and integrating over θ from 0 to π and over ϕ from 0 to 2π , one obtains

$$\frac{d}{dr} \left(r^2 \frac{dg_{lm}}{dr} \right) - l(l+1)g_{lm} = -4\pi \delta(r-r') Y_{lm}^*(\theta', \phi'). \quad (2.34)$$

In obtaining Equation (2.34), we have used the orthogonality property of the spherical harmonics,

$$\int_{\theta=0}^{\pi} \int_{\phi=0}^{2\pi} Y_{lm'}(\theta, \phi) Y_{lm}^*(\theta', \phi') \sin \theta d\theta d\phi = \delta_{ll'} \delta_{mm'}. \quad (2.35)$$

Let

$$g_{lm}(r, r') = G_l(r, r') Y_{lm}^*(\theta', \phi'). \quad (2.36)$$

Equation (2.34) becomes

$$\frac{d}{dr} \left(r^2 \frac{dG_l}{dr} \right) - l(l+1)G_l = -4\pi \delta(r-r'). \quad (2.37)$$

Multiply both sides of Equation (2.37) by $1/r^2$

$$\frac{1}{r^2} \frac{d}{dr} \left(r^2 \frac{d}{dr} G_l(r, r') \right) - \frac{l(l+1)}{r^2} G_l(r, r') = -\frac{4\pi}{r^2} \delta(r-r')$$

which is the same as [11]

$$\frac{1}{r} \frac{d^2}{dr^2} (rG_l(r, r')) - \frac{l(l+1)}{r^2} G_l(r, r') = -\frac{4\pi}{r^2} \delta(r-r'). \quad (2.38)$$

The radial Green's function, $G_l(r, r')$, satisfying the homogeneous radial equation for $r \neq r'$. Thus its general solution can be written as

$$G_l(r, r') = \begin{cases} (Ar^l + Br^{-(l+1)}) & \text{for } r < r', \\ (A'r^l + B'r^{-(l+1)}) & \text{for } r > r'. \end{cases}$$

The coefficients A , B , A' , B' are functions of r' to be determined by the boundary conditions, the requirement implied by $\delta(r - r')$ in Equation (2.38), and the symmetry of $G_l(r, r')$ in r and r' . Suppose that the boundary surfaces are concentric spherical surfaces at $r = a$ and $r = b$. The vanishing of $G(\bar{r}, \bar{r}')$ for \bar{r} on the surfaces implies the vanishing of $G_l(r, r')$ for $r = a$ and $r = b$. Consequently $G_l(r, r')$ becomes

$$G_l(r, r') = \begin{cases} A \left(r^l - \frac{a^{2l+1}}{r^{l+1}} \right) & \text{for } r < r' \\ B' \left(\frac{1}{r^{l+1}} - \frac{r^l}{b^{2l+1}} \right) & \text{for } r > r'. \end{cases} \quad (2.39)$$

The symmetry in r and r' requires that the coefficients $A(r')$ and $B(r')$ be such that $G_l(r, r')$ can be written

$$G_l(r, r') = C \left(r_{<}^l - \frac{a^{2l+1}}{r_{<}^{l+1}} \right) \left(\frac{1}{r_{>}^{l+1}} - \frac{r_{>}^l}{b^{2l+1}} \right), \quad (2.40)$$

where $r_{<}$ ($r_{>}$) is the smaller (larger) of r and r' . To determine the constant C we must consider the effect of the delta function in Equation (2.38). If we multiply both sides of Equation (2.38) by r and integrate over the interval from $r = r' - \varepsilon$ to $r = r' + \varepsilon$, where ε is very small, we obtain

$$\left\{ \frac{d}{dr} (rG_l(r, r')) \right\}_{r'+\varepsilon} - \left\{ \frac{d}{dr} (rG_l(r, r')) \right\}_{r'-\varepsilon} = -\frac{4\pi}{r'}. \quad (2.41)$$

Thus there is a discontinuity in slope at $r = r'$, as indicated in Figure 2.2.

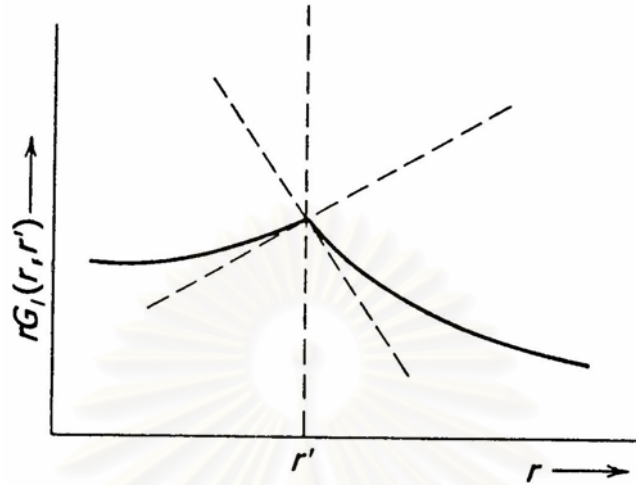


Figure 2.2 Discontinuity in slope of the radial Green's function [11].

For $r = r' + \varepsilon$ and $r_> = r$, $r_< = r'$. Hence

$$\begin{aligned} \left\{ \frac{d}{dr} [rG_l(r, r')] \right\}_{r=r'+\varepsilon} &= C \left(r'^l - \frac{a^{2l-1}}{r'^{l-1}} \right) \left[\frac{d}{dr} \left(\frac{1}{r^l} - \frac{r^{l-1}}{b^{2l-1}} \right) \right]_{r=r'} \\ &= -\frac{C}{r'} \left[1 - \left(\frac{a}{r'} \right)^{2l-1} \right] \left[l + (l+1) \left(\frac{r'}{b} \right)^{2l+1} \right]. \end{aligned}$$

Similarly for $r = r' - \varepsilon$,

$$\left\{ \frac{d}{dr} [rG_l(r, r')] \right\}_{r=r'-\varepsilon} = \frac{C}{r'} \left[l + 1 + l \left(\frac{a}{r'} \right)^{2l+1} \right] \left[1 - \left(\frac{r'}{b} \right)^{2l-1} \right].$$

Substituting these derivatives into Equation (2.41), we find

$$C = \frac{4\pi}{(2l+1) \left[1 - \left(\frac{a}{b} \right)^{2l+1} \right]}. \quad (2.42)$$

Combination of Equations (2.42), (2.40), (2.36), and (2.32) yields the expansion of Green's function for a spherical shell bounded by $r = a$ and $r = b$ [11]:

$$G(\vec{r}, \vec{r}') = 4\pi \sum_{l=0}^{\infty} \sum_{m=-l}^l \frac{Y_{lm}^*(\theta', \phi') Y_{lm}(\theta, \phi)}{(2l+1) \left[1 - \left(\frac{a}{b} \right)^{2l+1} \right]} \left(r_{<}^l - \frac{a^{2l+1}}{r_{<}^{l+1}} \right) \left(\frac{1}{r_{>}^{l+1}} - \frac{r_{>}^l}{b^{2l+1}} \right), \quad (2.43)$$

where $r_{<} (r_{>})$ is the smaller (larger) of r and r' , ($a \leq r \leq b$).

For the "exterior" problem with a spherical boundary at $r = b$, we merely let $b \rightarrow \infty$ and $a \rightarrow b$, then the Green's function (2.43) becomes

$$G(\vec{r}, \vec{r}') = 4\pi \sum_{l=0}^{\infty} \sum_{m=-l}^l \frac{1}{(2l+1)} \left[\frac{r_{<}^l}{r_{>}^{l+1}} - \frac{1}{b} \left(\frac{b^2}{rr'} \right)^{l+1} \right] Y_{lm}^*(\theta', \phi') Y_{lm}(\theta, \phi), \quad (2.44)$$

where $r_{<} (r_{>})$ is the smaller (larger) of r and r' , $r \geq b$.

CHAPTER III

LAMINAR FLOW VELOCITY FIELD

As mentioned in the first chapter, the simplest and successful model to determine velocity profiles for laminar flow through randomly distributed spheres is the free surface model due to Happel [9]. This cell model consists of a concentric spheres, which corresponds to EMT model as mentioned in Chapter 1. It is, therefore, useful to attest EMT results with Happel velocity field. In this chapter, the derivation of Happel flow field of particles moving in the rest fluid is reviewed.

3.1 Happel Flow Field

The motion of particles relative to a fluid is often of interest in the two cases where either the particles move and there is no average motion of the fluid or alternatively the particles remain more or less stationary and fluid passes around them. In this section, we consider particles that are spheres of average radius a moving through stationary fluid. In Happel model, the system of fluid and spheres is replaced by a composite sphere. Each composite sphere consists of a representative sphere of radius a enclosed by a fluid shell of radius b . The fluid shell radius b was chosen such that $\gamma^3 = a^3/b^3$ is the volume packing fraction or the volume density of spheres in the fluid.

At steady state, the fluid is described by the Navier-Stokes equation

$$\eta \nabla^2 \vec{v} = \vec{\nabla} p \quad (3.1)$$

and the continuity equation for an incompressible fluid is

$$\vec{\nabla} \cdot \vec{v} = 0, \quad (3.2)$$

where η , \vec{v} , and p are the viscosity of fluid, the fluid velocity inside the spherical shell, and the pressure, respectively.

The internal sphere moves in a positive direction along the z-axis with a constant velocity \vec{v}_0 inside the fluid shell with the outer free surface and thus

$$v_x = 0, \quad v_y = 0, \quad v_z = v_0 \quad \text{at } r = a \quad (3.3)$$

$$\left. \begin{array}{l} v_r = 0 \\ \left. \begin{array}{l} \\ \\ \end{array} \right\} \end{array} \right\} \quad \text{at } r = b, \quad (3.4)$$

$$p_{r\theta} = \eta_0 \left(\frac{1}{r} \frac{\partial v_r}{\partial \theta} + \frac{\partial v_\theta}{\partial r} - \frac{v_\theta}{r} \right) = 0 \quad]$$

η_0 is the viscosity of a suspension and $p_{r\theta}$ is the stress component in θ direction. The condition of no tangential stress component on the surface of the outer sphere corresponds to the vanishing of the stress tensor component $p_{r\theta}$. The condition $v_r = 0$ at $r = b$ corresponds to no flow across the boundary of the fluid envelope. Because of the symmetry $v_\phi = 0$ in the entire spherical shell $a \leq r \leq b$. At $r = b$, $\frac{\partial v_r}{\partial \theta} = 0$ and so the vanishing of $p_{r\theta}$ corresponds to

$$\frac{\partial v_\theta}{\partial r} - \frac{v_\theta}{r} = 0. \quad (3.5)$$

A general solution of the laminar flow equations is given by Lamb [13]. It is as follows

$$\vec{v} = \sum_{n=-\infty}^{\infty} \vec{\nabla} \times (\vec{r} \chi_n) + \vec{\nabla} \Phi_n + \frac{n+3}{2(n+1)(2n+3)} r^2 \vec{\nabla} p_n - \vec{r} \frac{np_n}{(n-1)(2n+3)}, \quad (3.6)$$

$$p = \eta \sum_{n=-\infty}^{\infty} p_n \quad (3.7)$$

where χ_n , Φ_n , and p_n are Legendre polynomials of order n .

An appropriate form of \vec{v} satisfying the present boundary value problem is obtained by setting $\chi_n = 0$ and retaining Legendre polynomials, p_n and Φ_n of orders -2 and 1 ,

$$\vec{v} = \vec{\nabla}\Phi_1 + \vec{\nabla}\Phi_{-2} + \frac{1}{5}r^2\vec{\nabla}p_1 - \frac{1}{10}\vec{r}p_1 + \frac{1}{2}r^2\vec{\nabla}p_{-2} + 2\vec{r}p_{-2}. \quad (3.8)$$

Using the explicit form of Legendre polynomials, we write

$$\Phi_1 = Az \quad (3.9a)$$

$$p_1 = Bz \quad (3.9b)$$

$$\Phi_{-2} = \frac{Cz}{r^3} \quad (3.9c)$$

$$p_{-2} = \frac{Dz}{r^3}. \quad (3.9d)$$

Substituting Equations (3.9a), (3.9b), (3.9c) and (3.9d) into Equation (3.8), we obtain

$$\begin{aligned} \vec{v} &= \vec{\nabla}Az + \vec{\nabla}\left(\frac{Cz}{r^3}\right) + \frac{r^2}{5}\vec{\nabla}Bz - \frac{\vec{r}}{10}Bz + \frac{r^2}{2}\vec{\nabla}\left(\frac{Dz}{r^3}\right) + 2\vec{r}\frac{Dz}{r^3} \\ &= A\hat{k} + zC\left(-\frac{3}{r^5}\right)\vec{r} + \frac{C}{r^3}\hat{k} + \frac{r^2}{5}B\hat{k} - \frac{Bz}{10}\vec{r} - \frac{3Dz}{2r^3}\vec{r} + \frac{D}{2r}\hat{k} + \frac{2Dz}{r^3}\vec{r}. \end{aligned} \quad (3.10)$$

Let $\vec{r} = r\hat{r}$, Equation (3.10) can be put in the form

$$\vec{v} = \left(A + \frac{C}{r^3} + \frac{r^2B}{5} + \frac{D}{2r}\right)\hat{k} + \left(-\frac{3Cz}{r^4} - \frac{Bzr}{10} - \frac{3Dz}{2r^2} + \frac{2Dz}{r^2}\right)\hat{r}. \quad (3.11)$$

Because $\hat{r} = \frac{1}{r}(x\hat{i} + y\hat{j} + z\hat{k})$, we get

$$\vec{v} = \left(A + \frac{C}{r^3} + \frac{r^2B}{5} + \frac{D}{2r}\right)\hat{k} + \left(-\frac{3Cz}{r^5} - \frac{Bz}{10} + \frac{Dz}{2r^3}\right)(x\hat{i} + y\hat{j} + z\hat{k}). \quad (3.12)$$

Using the boundary condition (3.3), we obtain

$$\frac{3C}{a^3} + \frac{Ba^2}{10} - \frac{D}{2a} = 0 \quad (3.13)$$

and
$$A + \frac{C}{a^3} + \frac{a^2B}{5} + \frac{D}{2a} = v_0. \quad (3.14)$$

In spherical coordinates, Equation (3.11) can be written as

$$\begin{aligned}
 \vec{v} &= \left(A + \frac{C}{r^3} + \frac{r^2 B}{5} + \frac{D}{2r} \right) (\cos \theta \hat{r} - \sin \theta \hat{\theta}) + \\
 &\quad \left(-\frac{3Cr \cos \theta}{r^4} - \frac{Br^2 \cos \theta}{10} - \frac{3Dr \cos \theta}{2r^2} + \frac{2Dr \cos \theta}{r^2} \right) \hat{r} \\
 &= \left(A + \frac{C}{r^3} + \frac{r^2 B}{5} + \frac{D}{2r} - \frac{3C}{r^3} - \frac{Br^2}{10} + \frac{D}{2r} \right) \cos \theta \hat{r} - \\
 &\quad \left(A + \frac{C}{r^3} + \frac{r^2 B}{5} + \frac{D}{2r} \right) \sin \theta \hat{\theta} \\
 \vec{v} &= \left(A - \frac{2C}{r^3} + \frac{r^2 B}{10} + \frac{D}{r} \right) \cos \theta \hat{r} - \left(A + \frac{C}{r^3} + \frac{r^2 B}{5} + \frac{D}{2r} \right) \sin \theta \hat{\theta}. \quad (3.15)
 \end{aligned}$$

From Equations (3.4) and (3.5), we have

$$A - \frac{2C}{b^3} + \frac{b^2 B}{10} + \frac{D}{b} = 0 \quad (3.16)$$

and
$$A + \frac{4C}{b^3} - \frac{b^2 B}{5} + \frac{D}{b} = 0. \quad (3.17)$$

From Equations (3.13), (3.14), (3.16), and (3.17), we obtain

$$A = -\frac{(3 + 2\gamma^5)\gamma v_0}{(2 - 3\gamma + 3\gamma^5 - 2\gamma^6)}, \quad (3.18a)$$

$$B = \frac{10\gamma^5 v_0}{a^2(2 - 3\gamma + 3\gamma^5 - 2\gamma^6)}, \quad (3.18b)$$

$$C = \frac{a^3 v_0}{2(2 - 3\gamma + 3\gamma^5 - 2\gamma^6)}, \quad (3.18c)$$

$$D = \frac{a(3 + 2\gamma^5)v_0}{(2 - 3\gamma + 3\gamma^5 - 2\gamma^6)}, \quad (3.18d)$$

where $\gamma = a/b$.

Substituting Equations (3.18a)-(3.18d) into Equation (3.15), we get the factors of v_r and v_θ as

$$\left(A - \frac{2C}{r^3} + \frac{r^2 B}{10} + \frac{D}{r} \right) = \left[-\frac{(3+2\gamma^5)\gamma v_0}{M} - \frac{v_0}{r_a^3 M} + \frac{\gamma^5 v_0 r_a^2}{M} + \frac{v_0(3+2\gamma^5)}{r_a M} \right]$$

$$= -\frac{2v_0}{M} \left(\frac{1}{2r_a^3} - \frac{(3+2\gamma^5)}{2r_a} + \frac{3\gamma}{2} + \gamma^6 - \frac{\gamma^5}{2} r_a^2 \right),$$

and

$$\left(A + \frac{C}{r^3} + \frac{r^2 B}{5} + \frac{D}{2r} \right) = -\frac{2v_0}{M} \left(-\frac{1}{4r_a^3} - \gamma^5 r_a^2 - \frac{(3+2\gamma^5)}{4r_a} + \frac{3\gamma}{2} + \gamma^6 \right),$$

where $r_a = r/a$, and $M = 2 - 3\gamma + 3\gamma^5 - 2\gamma^6$. Therefore the fluid velocity is obtained

$$\vec{v} = a_s v_0 \left[p(r_a, \gamma) \cos \theta \hat{r} - q(r_a, \gamma) \sin \theta \hat{\theta} \right], \quad (3.19)$$

where $p(r_a, \gamma)$ and $q(r_a, \gamma)$ are functions of r_a and γ given as

$$p(r_a, \gamma) = \left(\frac{1}{2r_a^3} - \frac{(3+2\gamma^5)}{2r_a} + \frac{3\gamma}{2} + \gamma^6 - \frac{\gamma^5}{2} r_a^2 \right) \quad (3.20a)$$

$$q(r_a, \gamma) = \left(-\frac{1}{4r_a^3} - \gamma^5 r_a^2 - \frac{(3+2\gamma^5)}{4r_a} + \frac{3\gamma}{2} + \gamma^6 \right) \quad (3.20b)$$

and

$$a_s = -\frac{2}{2 - 3\gamma + 3\gamma^5 - 2\gamma^6}.$$

The fluid velocity field which has been solved is for the case of the particles moving in the fluid at rest.

In the case that fluid flows through the randomly distributed spherical particles at rest, the above velocity flow field has to be transformed into a frame of reference or coordinate system which is fixed on the representative sphere. Let the fluid entrance velocity at far away from the spheres be $v_0 \hat{k}$. Therefore the fluid velocity around the sphere is

$$\vec{v}_f = -\vec{v} + \vec{v}_0, \quad (3.21)$$

where \vec{v}_f is the fluid velocity in the reference frame in which the particle is at rest, and \vec{v} is the fluid velocity obtained from Equation (3.19). Substituting Equation (3.19) into Equation (3.21), we obtain

$$\vec{v}_f = v_0 \left[(-a_s p(r_a, \gamma) + 1) \cos \theta \hat{r} - (-a_s q(r_a, \gamma) + 1) \sin \theta \hat{\theta} \right]. \quad (3.22)$$

Substituting Equation (3.20) into Equation (3.22), we obtain the components v_r and v_θ as

$$\begin{aligned} v_r &= v_0 (-a_s p(r_a, \gamma) + 1) \cos \theta \\ &= v_0 \left[\frac{2}{2 - 3\gamma + 3\gamma^5 - 2\gamma^6} \left(\frac{1}{2r_a^3} - \frac{(3 + 2\gamma^5)}{2r_a} + 1 + \frac{3\gamma}{2} - \frac{\gamma^5}{2} r_a^2 \right) \right] \cos \theta \end{aligned}$$

and

$$\begin{aligned} v_\theta &= v_0 (-a_s q(r_a, \gamma) + 1) \sin \theta \\ &= v_0 \left[\frac{2}{2 - 3\gamma + 3\gamma^5 - 2\gamma^6} \left(-\frac{1}{4r_a^3} - \frac{(3 + 2\gamma^5)}{4r_a} + 1 + \frac{3}{2}\gamma^5 - \frac{\gamma^5}{2} r_a^2 \right) \right] \sin \theta. \end{aligned}$$

So the fluid velocity is obtained as

$$\vec{v}_f = A_s v_0 [P(r_a, \gamma) \cos \theta \hat{r} - Q(r_a, \gamma) \sin \theta \hat{\theta}], \quad (3.23)$$

where

$$P(r_a, \gamma) = \frac{1}{2r_a^3} - \frac{(3 + 2\gamma^5)}{2r_a} + 1 + \frac{3}{2}\gamma^5 - \frac{\gamma^5}{2} r_a^2 \quad (3.24)$$

$$Q(r_a, \gamma) = -\frac{1}{4r_a^3} - \frac{(3 + 2\gamma^5)}{4r_a} + 1 + \frac{3}{2}\gamma^5 - \frac{\gamma^5}{2} r_a^2 \quad (3.25)$$

and

$$A_s = \frac{2}{2 - 3\gamma + 3\gamma^5 - 2\gamma^6}.$$

CHAPTER IV

LAMINAR FLOW VELOCITY FIELD FROM A GREEN'S FUNCTION

This chapter begins with an introduction of the effective medium treatment (EMT), the method used in this research. Then the determination of the velocity field for laminar flow through randomly distributed spheres is considered in next sections. As explained in Chapter 1, this type of fluid flow occurs for a Reynolds number $\text{Re} = \frac{\rho v_0 a}{\eta} < 1$, where ρ , v_0 , η and a are the fluid density, entrance velocity, viscosity and the sphere radius, respectively. The fluid velocity (in laminar flow) is described by the Navier-Stokes equation which is in the form of Poisson's equation. We, therefore, use Green's theorem to solve Navier-Stokes equation in this chapter and the comparison of EMT velocity profiles with Happel flow velocity fields is performed in the final section.

4.1 Effective Medium Treatment

In determining the velocity field, the effective medium treatment (EMT) is employed. In the EMT, the system of fluid and spheres is replaced by a composite sphere -- a representative sphere of radius a enclosed by a fluid shell of radius b -- embedded in an effective medium of different viscosity. The composite sphere consists of the collector sphere enclosed by a fluid shell with viscosity η (medium 1) embedded in an effective medium of viscosity η^* (medium 2) to be assigned. The ratio of the small sphere and the large sphere volume (a^3/b^3) is set to be equal to the sphere volume packing fraction (γ^3) or the density of spheres in the liquid. The velocity fields in the fluid shell and in the effective medium are determined by using Green's theorem and proper boundary conditions. We assume that the fluid enters the system of random spheres with a uniform velocity \vec{v}_0 along the polar (symmetry) axis of a spherical coordinate system. As shown in Figure 3.1, the representative sphere enclosed by a fluid shell is in the effective medium and the entering fluid has uniform entrance velocity \vec{v}_0 .

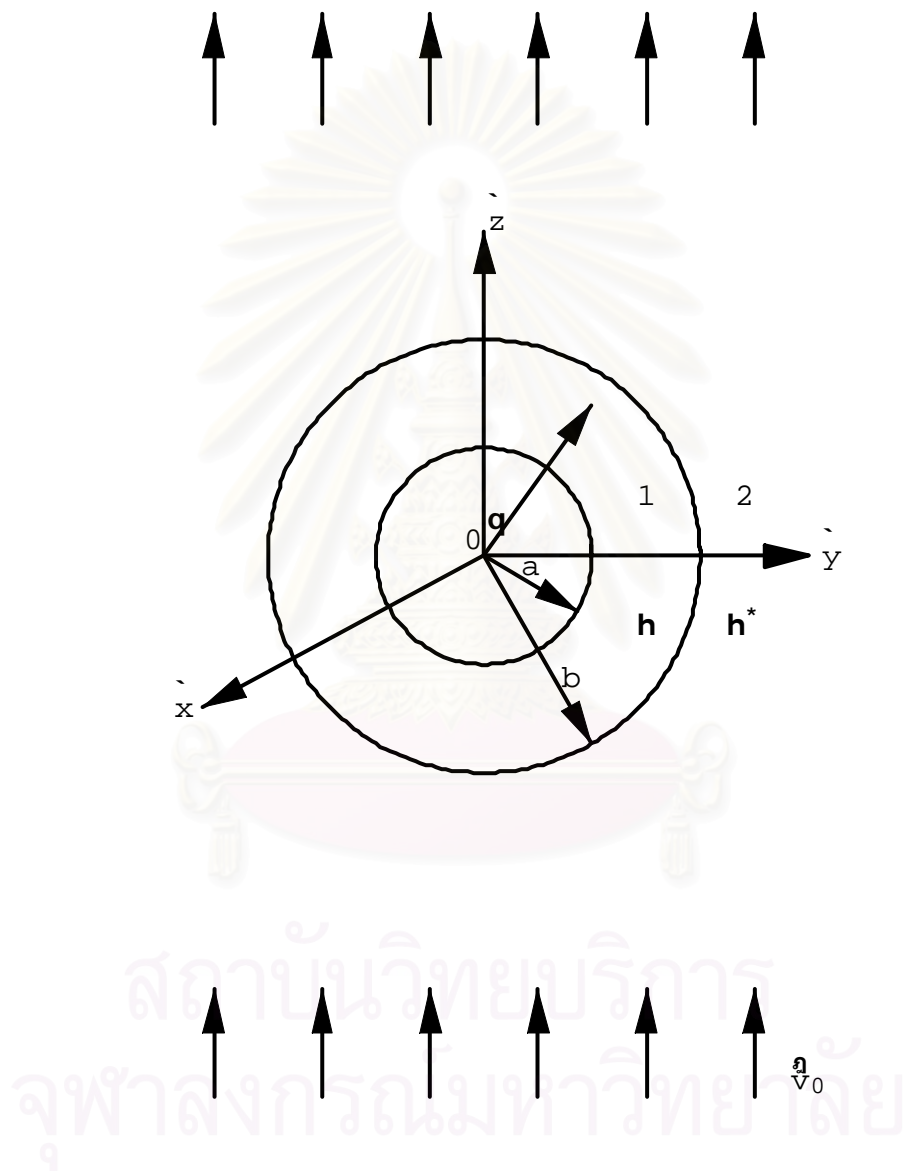


Figure 4.1 A representative sphere in the effective medium.

4.2 Laminar Flow Velocity Field from a Green's Function

At steady state, the laminar flow is described by the Navier-Stokes equation

$$\nabla^2 \bar{v} = \frac{\bar{\nabla} p}{\eta} \quad (4.1)$$

and by the continuity equation $\bar{\nabla} \cdot \bar{v} = -\partial \rho / \partial t$. For an incompressible fluid with steady flow

$$\bar{\nabla} \cdot \bar{v} = 0, \quad (4.2)$$

where p is the pressure, ρ is fluid density and η the fluid viscosity. If the divergence of Equation (4.1) is taken, we get

$$\eta \nabla^2 (\bar{\nabla} \cdot \bar{v}) = 0 = \nabla^2 p, \quad (4.3)$$

showing that the pressure satisfies Laplace's equation and the general solution in polar coordinates (r, θ) is

$$p(\bar{r}) = \sum_{l=0}^{\infty} [A_l r^l + B_l r^{-(l+1)}] P_l(\cos \theta), \quad (4.4)$$

where $P_l(\cos \theta)$ is the Legendre Polynomial of order l . With the help of Equation (4.4), the right hand side of Equation (4.1) can be determined in terms of unknown constants A_l and B_l . The form of Equation (4.1) is that of Poisson's equation. For the Dirichlet boundary condition,

$$G(\bar{r}, \bar{r}') = 0 \quad \text{for } \bar{r}' \text{ on } S,$$

where S is the boundary surface of the volume V . Referring to the solution of Poisson's equation, Equation (2.25), thus the velocity field \bar{v} in Equation (4.1) can be written as

$$\bar{v}(\bar{r}) = -\frac{1}{4\pi} \int_V \frac{\bar{\nabla}' p(\bar{r}')}{\eta} G(\bar{r}, \bar{r}') d^3 r' - \frac{1}{4\pi} \oint_S \bar{v}(\bar{r}') \frac{\partial G(\bar{r}, \bar{r}')}{\partial n'} da', \quad (4.5)$$

where $G(\vec{r}, \vec{r}')$ is the Green's function for a spherical shell bounded by $r = a$ and $r = b$ as shown in Equation (2.43):

$$G(\vec{r}, \vec{r}') = 4\pi \sum_{l=0}^{\infty} \sum_{m=-l}^l \frac{Y_{lm}^*(\theta', \phi') Y_{lm}(\theta, \phi)}{(2l+1) \left[1 - \left(\frac{a}{b}\right)^{2l+1} \right]} \left(r_{<}^l - \frac{a^{2l+1}}{r_{<}^{l+1}} \right) \left(\frac{1}{r_{>}^{l+1}} - \frac{r_{>}^l}{b^{2l+1}} \right), \quad (4.6)$$

where $r_{<} (r_{>})$ is the smaller (larger) of r and r' , ($a \leq r \leq b$).

In determining \vec{v} , we impose the following boundary conditions [14]:

1) Far away from the composite sphere, the velocity field ($\vec{v} = \vec{v}_2$) is uniform and equal to \vec{v}_0 (the entrance velocity). Thus,

$$\vec{v}_2 = \vec{v}_0 \quad \text{at } r = \infty. \quad (4.7)$$

2) In the far region, the pressure is constant and equal to p_{∞} , i.e.,

$$p = p_{\infty} \quad \text{at } r = \infty. \quad (4.8)$$

3) In the fluid shell region, $\vec{v} = \vec{v}_1$ and at the surface of the representative sphere, the fluid velocity is zero, i.e.,

$$\vec{v}_1 = 0 \quad \text{at } r = a. \quad (4.9)$$

4) At the fluid interface, the tangential and normal components of the stress tensor and all velocity components are continuous. These are the no-slip boundary conditions. Specifically, they are

$$\eta \left[\frac{1}{r} \frac{\partial v_{1r}}{\partial \theta} + \frac{\partial v_{1\theta}}{\partial r} - \frac{v_{1\theta}}{r} \right]_{r=b} = \eta^* \left[\frac{1}{r} \frac{\partial v_{2r}}{\partial \theta} + \frac{\partial v_{2\theta}}{\partial r} - \frac{v_{2\theta}}{r} \right]_{r=b}, \quad (4.10)$$

$$\left[-p_1 + 2\eta \frac{\partial v_{1r}}{\partial r} \right]_{r=b} = \left[-p_2 + 2\eta^* \frac{\partial v_{2r}}{\partial r} \right]_{r=b} \quad (4.11)$$

$$\text{and } \vec{v}_1 = \vec{v}_2 = \vec{v}(b, \theta) \quad \text{at } r = b. \quad (4.12)$$

Finally, it is necessary to write $\bar{v}^-(b, \theta)$, the boundary condition equation (4.12), in a specific form in order that the surface term of \bar{v}^- in Equation (4.5) can be integrated. Generally, the angular dependence of $\bar{v}^-(b, \theta)$ can be expressed as series in Legendre Polynomials. However, in order to minimize the mathematical complexity of our problem, a simple assumption for $\bar{v}^-(b, \theta)$ will be made.

5) The angular dependence of the normal and the tangential components of $\bar{v}^-(b, \theta)$ were $\cos \theta$ and $\sin \theta$, respectively. This form incorporates both the isolated sphere result, for the limiting case $a/b = 1/\gamma \rightarrow \infty$, and the Happel flow field results at the outer shell boundary. Thus it is assumed that [14]

$$\bar{v}^-(b, \theta) = v_0 (a_1 \cos \theta + a_2 \sin \theta), \quad (4.13)$$

where a_1 and a_2 are dimensionless constants to be determined.

4.2.1 Velocity Field outside the Shell

We first determine the velocity field in the effective medium $\bar{v}_2(\bar{r})$. For exterior problem outside the sphere of radius b , in Equation (4.6) we set $b \rightarrow \infty$ and $a \rightarrow b$, then Green's function in the effective medium is

$$G_2(\bar{r}, \bar{r}') = 4\pi \sum_{lm} \frac{1}{(2l+1)} \left[\frac{r_{<}^l}{r_{>}^{l+1}} - \frac{1}{b} \left(\frac{b^2}{rr'} \right)^{l+1} \right] Y_{lm}^*(\theta', \phi') Y_{lm}(\theta, \phi). \quad (4.14)$$

From Equation (4.4) with the boundary condition (4.8), the pressure in the effective medium is [14]

$$p_2(\bar{r}') = p_\infty + \frac{c_0}{r'} + \frac{c_1 \cos \theta'}{r'^2}, \quad (4.15)$$

where $l \geq 2$ terms are neglected and c_0 and c_1 are constants. The gradient of pressure is found to be

$$\bar{\nabla}' p_2(\bar{r}') = \left(-\frac{c_0}{r'^2} - \frac{2c_1 \cos \theta'}{r'^3} \right) \hat{r}' + \frac{1}{r'} \left(-\frac{c_1 \sin \theta'}{r'^2} \right) \hat{\theta}'. \quad (4.16)$$

In Equation (4.14) at the boundary $r' = b$, set $r_< = r'$ and $r_> = r$ and then we have

$$\begin{aligned} \left. \frac{\partial G_2}{\partial n'} \right|_{r'=b} &= - \left. \frac{\partial G_2}{\partial r'} \right|_{r'=b} \\ &= -4\pi \sum_{lm} Y_{lm}^*(\theta', \phi') Y_{lm}(\theta, \phi) \frac{b^{l-1}}{r^{l+1}} \end{aligned} \quad (4.17)$$

while at $r' \rightarrow \infty$, we let $r_< = r$, $r_> = r'$ then

$$\begin{aligned} \left. \frac{\partial G_2}{\partial n'} \right|_{r' \rightarrow \infty} &= \left. \frac{\partial G_2}{\partial r'} \right|_{r' \rightarrow \infty} \\ &= \frac{4\pi}{(2l+1)} \sum_{lm} Y_{lm}^*(\theta', \phi') Y_{lm}(\theta, \phi) \left(r^l - \frac{b^{2l+1}}{r^{l+1}} \right) \frac{(-1)(l+1)}{r'^{l+2}} \Big|_{r' \rightarrow \infty}. \end{aligned} \quad (4.18)$$

The velocity field in the effective medium is determined by substituting Equations (4.16), (4.17) and (4.18) into the right hand side of Equation (4.5).

$$\begin{aligned} \vec{v}_2(\vec{r}) &= \frac{1}{4\pi} \int \frac{1}{\eta^*} \left[\left(\frac{c_0}{r'^2} + \frac{2c_1 \cos \theta'}{r'^3} \right) \hat{r}' + \frac{c_1}{r'^3} \sin \theta' \hat{\theta}' \right] G_2(\vec{r}, \vec{r}') d^3 r' \\ &- \frac{1}{4\pi} \int_{r'=b} \vec{v}(b, \theta') \left[-4\pi \sum_{lm} Y_{lm}^*(\theta', \phi') Y_{lm}(\theta, \phi) \frac{b^{l-1}}{r^{l+1}} \right] da' \\ &- \frac{1}{4\pi} \int_{r' \rightarrow \infty} v_0 \hat{z} \left[\frac{4\pi}{(2l+1)} \sum_{lm} Y_{lm}^*(\theta', \phi') Y_{lm}(\theta, \phi) \left(r^l - \frac{b^{2l+1}}{r^{l+1}} \right) \frac{(-1)(l+1)}{r'^{l+2}} \right] da', \end{aligned} \quad (4.19)$$

where $G_2(\vec{r}, \vec{r}')$ is the Green's function in Equation (4.14) and $\vec{v}(b, \theta')$ from Equation (4.13). Finally, we have

$$\vec{v}_2(\vec{r}) = v_{2x} \hat{x} + v_{2y} \hat{y} + v_{2z} \hat{z} \quad (4.20)$$

where

$$v_{2x} = \frac{c_0}{2\eta^*} \left[1 - \left(\frac{b}{r} \right)^2 \right] \frac{x}{r} + v_0 (a_1 + a_2) \frac{b^3}{r^5} xz + \frac{c_1}{2\eta^*} \left[1 - \left(\frac{b}{r} \right)^2 \right] \frac{zx}{r^3}$$

$$\begin{aligned}
v_{2y} &= \frac{c_0}{2\eta^*} \left[1 - \left(\frac{b}{r} \right)^2 \right] \frac{y}{r} + v_0 (a_1 + a_2) \frac{b^3}{r^5} yz + \frac{c_1}{2\eta^*} \left[1 - \left(\frac{b}{r} \right)^2 \right] \frac{zy}{r^3} \\
v_{2z} &= \frac{c_0}{2\eta^*} \left[1 - \left(\frac{b}{r} \right)^2 \right] \frac{z}{r} + v_0 (a_1 + a_2) \frac{b^3}{r^5} \left(z^2 - \frac{r^2}{3} \right) \\
&\quad + \frac{v_0 b}{3r} (a_1 - 2a_2) + \frac{1}{6r^3} \frac{c_1}{\eta^*} \left[1 - \left(\frac{b}{r} \right)^2 \right] (3z^2 - r^2) + v_0 \left(1 - \frac{b}{r} \right).
\end{aligned}$$

We now use the continuity equation (4.2) to find the constants c_0 and c_1 in the pressure $p_2(\vec{r})$, Equation (4.15). Taking divergence of Equation (4.20), we have

$$\begin{aligned}
\bar{\nabla} \cdot \vec{v}_2(\vec{r}) &= \frac{c_0}{r\eta^*} + \frac{z}{r^3} \left(\frac{2c_1}{3\eta^*} + v_0 b - \frac{v_0 b}{3} (a_1 - 2a_2) \right) \\
&= 0.
\end{aligned}$$

Then we get $c_0 = 0$

and
$$c_1 = -\frac{3}{2} \eta^* b v_0 \left(1 - \frac{1}{3} (a_1 - 2a_2) \right).$$

Substituting c_0 and c_1 into Equation (4.15) and replacing $a_1 + a_2$ by C , $a_1 - 2a_2$ by D , the pressure can be written as

$$p_2(\vec{r}') = p_\infty - \frac{3}{2} \eta^* b v_0 \left(1 - \frac{D}{3} \right) \frac{\cos \theta'}{r'^2}. \quad (4.21)$$

Recall Equation (4.20) and change to spherical coordinates. The velocity field in the effective medium is found to be

$$\vec{v}_2(\vec{r}) = v_0 [P^*(r_a, \gamma) \cos \theta \hat{r} + Q^*(r_a, \gamma) \sin \theta \hat{\theta}], \quad (4.22)$$

where $r_a = r/a$, $\gamma = a/b$

$$P^*(r_a, \gamma) = 1 - \frac{3}{2r_a \gamma} + \frac{1}{2r_a^3 \gamma^3} + \frac{2C}{3r_a^3 \gamma^3} + D \left(\frac{1}{2r_a \gamma} - \frac{1}{6r_a^3 \gamma^3} \right) \quad (4.23)$$

$$Q^*(r_a, \gamma) = -1 + \frac{3}{4r_a \gamma} + \frac{1}{4r_a^3 \gamma^3} + \frac{C}{3r_a^3 \gamma^3} - D \left(\frac{1}{4r_a \gamma} + \frac{1}{12r_a^3 \gamma^3} \right). \quad (4.24)$$

We will determine the constants C , D and find \bar{v}_2 in closed form after we know \bar{v}_1 .

4.2.2 Velocity Field in the Shell Region

For the fluid shell region enclosed by concentric spheres of radii a and b , the Green's function is in Equation (4.6). Using Equation (4.4) and the boundary condition (4.11), the pressure within the fluid shell, Equation (4.4), is [14]

$$p_1(\bar{r}') = p_\infty + \eta v_0 \left(\frac{Ar'}{a^2} + \frac{Ba}{r'^2} \right) \cos \theta', \quad (4.25)$$

where A and B are constants. The gradient of equation (4.25) is

$$\bar{\nabla}' p_1(\bar{r}') = \eta v_0 \left(\frac{A}{a^2} - \frac{2Ba}{r'^3} \right) \cos \theta' \hat{r}' - \eta v_0 \left(\frac{A}{a^2} + \frac{Ba}{r'^3} \right) \sin \theta' \hat{\theta}'. \quad (4.26)$$

At the boundary $r' = a$, set $r_< = r'$, $r_> = r$, we have

$$\begin{aligned} \frac{\partial G(\bar{r}, \bar{r}')}{\partial n'} &= - \frac{\partial G(\bar{r}, \bar{r}')}{\partial r'} \\ &= -4\pi \sum_{lm} \frac{Y_{lm}^*(\theta', \phi') Y_{lm}(\theta, \phi)}{(2l+1) \left(1 - \left(\frac{a}{b} \right)^{2l+1} \right)} \left(\frac{1}{r^{l+1}} - \frac{r^l}{b^{2l+1}} \right) \left(lr'^{l+1} + (l+1) \frac{a^{2l+1}}{r'^{l+2}} \right) \end{aligned} \quad (4.27)$$

and at $r' = b$, set $r_< = r$, $r_> = r'$ then

$$\begin{aligned} \frac{\partial G(\bar{r}, \bar{r}')}{\partial n'} &= \frac{\partial G(\bar{r}, \bar{r}')}{\partial r'} \\ &= 4\pi \sum_{lm} \frac{Y_{lm}^*(\theta', \phi') Y_{lm}(\theta, \phi)}{(2l+1) \left(1 - \left(\frac{a}{b} \right)^{2l+1} \right)} \left(r^l - \frac{a^{2l+1}}{r^{l+1}} \right) \left(-\frac{(l+1)}{r'^{l+2}} - \frac{lr'^{l-1}}{b^{2l+1}} \right). \end{aligned} \quad (4.28)$$

Substitute Equations (4.6), (4.26), (4.27) and (4.28) into Equation (4.5) and integrate. We find that

$$\bar{v}_1(\bar{r}) = v_0 [P(r_a, \gamma) \cos \theta \hat{r} + Q(r_a, \gamma) \sin \theta \hat{\theta}], \quad (4.29)$$

where

$$P(r_a, \gamma) = \frac{2}{5(1-\gamma^5)} \left[BT_1 + \frac{5C}{3} \gamma^2 \left(r_a^2 - \frac{1}{r_a^3} \right) \right] - \frac{1}{(1-\gamma)} \left[AT_2 - \frac{D}{3} \left(1 - \frac{1}{r_a} \right) \right], \quad (4.29a)$$

$$Q(r_a, \gamma) = \frac{1}{5(1-\gamma^5)} \left[BT_1 + \frac{5C}{3} \gamma^2 \left(r_a^2 - \frac{1}{r_a^3} \right) \right] + \frac{1}{(1-\gamma)} \left[AT_2 - \frac{D}{3} \left(1 - \frac{1}{r_a} \right) \right], \quad (4.29b)$$

$$T_1 = \frac{5}{6} \left[r_a^2 (\gamma^2 - 1) \gamma^3 + \frac{(1-\gamma^5)}{r_a} - \frac{(1-\gamma^3)}{r_a^3} \right], \quad (4.29c)$$

$$T_2 = \frac{1}{6} \left[-r_a^2 (1-\gamma) + \frac{(1-\gamma^3)}{\gamma^2} + \frac{(1-\gamma^{-2})}{r_a} \right]. \quad (4.29d)$$

The constants A and B are related to C and D by the equations

$$\begin{bmatrix} -\frac{(1-\gamma^5)}{10\gamma^2} & \frac{\gamma}{2}(1-\gamma^2) \\ \frac{(1-\gamma^2)}{2\gamma^2} & -2(1-\gamma) \end{bmatrix} \begin{bmatrix} A \\ B \end{bmatrix} = \begin{bmatrix} C \\ D \end{bmatrix}, \quad (4.30)$$

which arise from the continuity equation $\bar{\nabla} \cdot \bar{v}_1(\bar{r}) = 0$. The relations determining the constants A and B are obtained from the no-slip boundary conditions (4.10) and (4.11). We find that

$$\begin{aligned}
& \begin{bmatrix} \frac{-2 + 3\gamma - \gamma^3}{6\gamma^2(1-\gamma)} & \frac{\gamma(-3 + 5\gamma^2 - 2\gamma^5)}{6(1-\gamma^5)} \\ \frac{1 + \gamma + \gamma^2}{3\gamma^2} & \frac{\gamma(9 - 10\gamma^2 + \gamma^5)}{3(1-\gamma^5)} \end{bmatrix} \begin{bmatrix} A \\ B \end{bmatrix} \\
& + \begin{bmatrix} \frac{6\gamma^5 - 1}{3(1-\gamma^5)} + 2\delta & \frac{-\gamma}{3(1-\gamma)} - \frac{\delta}{2} \\ \frac{-4(2 + 3\gamma^5)}{3(1-\gamma^5)} - 4\delta & \frac{-2\gamma}{3(1-\gamma)} - \frac{\delta}{2} \end{bmatrix} \begin{bmatrix} C \\ D \end{bmatrix} = - \begin{bmatrix} \frac{3\delta}{2} \\ \frac{3\delta}{2} \end{bmatrix}, \quad (4.31)
\end{aligned}$$

where $\delta = \eta^* / \eta$ is the relative effective viscosity.

Happel theory successfully explained the pressure drop through a suspension of spheres. The pressure drop per unit length of the distributed spheres is the drag force per unit cell volume. The drag force on a sphere in a fluid is [14]

$$\vec{f}_D = -4\pi\bar{V}(r^3 p_{-2}), \quad (4.32)$$

where p_{-2} is the term $\eta v_0 a B \cos \theta / r^2$ of the fluid pressure within the fluid shell given by Equation (4.25). Thus

$$\vec{f}_D = -4\pi\eta v_0 a B \hat{z}. \quad (4.33)$$

In the dilute limit, the drag obeys Stokes's law,

$$\vec{f}_{D0} = 6\pi\eta a v_0 \hat{z}. \quad (4.34)$$

The ratio between pressure drop through a single isolated sphere and through each sphere in an assemblage of spheres is

$$\frac{\Delta p_0}{\Delta p} = \frac{f_{D0}}{f_D} = -\frac{3}{2B}. \quad (4.35)$$

Using the values of the reported pressure drop ratio given by Happel, B is determined from the above equation. Then the other parameters, A , C , D and δ are determined from Equations (4.30) and (4.31) as functions of γ ($\gamma^3 =$ volume packing fraction).

By using Mathematica program [15] (see Appendix A) to solve Equations (4.30) and (4.31), we get the constants as follows;

$$A = \frac{10\gamma^3 N_1}{(-1 + \gamma)^3 (1 + \gamma)(2 + \gamma + 2\gamma^2) N_2} \quad (4.36a)$$

$$B = -\frac{(3 + 2\gamma^5)}{2 - 3\gamma + 3\gamma^5 - 2\gamma^6} \quad (4.36b)$$

$$C = -\frac{\gamma(1 - \gamma^2)(3 + 2\gamma^5)}{2(2 - 3\gamma + 3\gamma^5 - 2\gamma^6)} - \frac{\gamma(1 - \gamma^5)N_1}{(-1 + \gamma)^3 (1 + \gamma)(2 + \gamma + 2\gamma^2)N_2} \quad (4.36c)$$

$$D = \frac{2(1 - \gamma)(3 + 2\gamma^5)}{2 - 3\gamma + 3\gamma^5 - 2\gamma^6} + \frac{5\gamma(1 - \gamma^2)N_1}{(-1 + \gamma)^3 (1 + \gamma)(2 + \gamma + 2\gamma^2)N_2} \quad (4.36d)$$

$$\delta = \frac{36 - 30\gamma^2 + 18\gamma^5 - 20\gamma^7 - 4\gamma^{10} - 2\sqrt{3}(-3 + 3\gamma - 2\gamma^5 + 2\gamma^6)N}{2(9 - 30\gamma^2 + 25\gamma^4 + 12\gamma^5 - 20\gamma^7 + 4\gamma^{10})}, \quad (4.36e)$$

where

$$N = (18 + 36\gamma + 14\gamma^2 - 8\gamma^3 - 5\gamma^4 + 2\gamma^5 + 9\gamma^6 + 6\gamma^7 + 3\gamma^8)^{1/2} \quad (4.37a)$$

$$\begin{aligned} N_1 = & 21\gamma^7 + 30\gamma^8 + 24\gamma^9 + 12\gamma^{10} + \gamma^4(21 - 2\sqrt{3}N) + 4\gamma^6(3 + \sqrt{3}N) \\ & + 9(6 + \sqrt{3}N) + 9\gamma(12 + \sqrt{3}N) + 3\gamma^3(30 + \sqrt{3}N) \\ & + 3\gamma^2(33 + \sqrt{3}N) + \gamma^5(-21 + 4\sqrt{3}N) \end{aligned} \quad (4.37b)$$

$$\begin{aligned} N_2 = & 33\gamma^5 + 36\gamma^6 + 24\gamma^7 + 12\gamma^8 + 9(8 + \sqrt{3}N) + 9\gamma(16 + \sqrt{3}N) \\ & + \gamma^3(18 + 4\sqrt{3}N) + \gamma^4(30 + 4\sqrt{3}N) + \gamma^2(81 + 4\sqrt{3}N). \end{aligned} \quad (4.37c)$$

The numerical values of the above constants for various packing fractions (γ^3) are shown in Table 4.1 in agreement with the previous reported results [14]. These confirm the closed form solutions in Equations (4.22) and (4.29) obtained in this research. Figure 4.2 shows the variation of the relative effective viscosity as a function of γ . Inserting these results into Equations (4.22) and (4.29) yields the velocity profile in the effective medium and the shell region respectively. As can be seen that the velocity field

equations are so complicated, thus we determine the approximate closed form solutions for two ranges of γ ; low packing fraction $\gamma^3 < 0.1$ or $\gamma < 0.45$ and the other range $\gamma > 0.45$.

γ^3	A	B	C	D	δ
0.001	-0.0051	-1.765	-0.0361	2.922	4.556
0.01	-0.0649	-2.215	-0.0877	2.809	4.986
0.05	-0.4912	-3.311	-0.1677	2.619	6.396
0.10	-1.386	-4.666	-0.2204	2.478	8.296
0.20	-4.934	-8.460	-0.2837	2.278	13.71
0.30	-12.87	-15.20	-0.3222	2.126	23.28
0.40	-30.73	-28.37	-0.3472	1.999	41.76
0.50	-73.45	-56.86	-0.3633	1.889	81.24
0.60	-188.2	-127.7	-0.3730	1.792	178.3

Table 4.1 The numerical values of relative viscosity ($\delta = \eta^*/\eta$) and constants in Equations (4.30) and (4.31) for various packing fraction (γ^3).

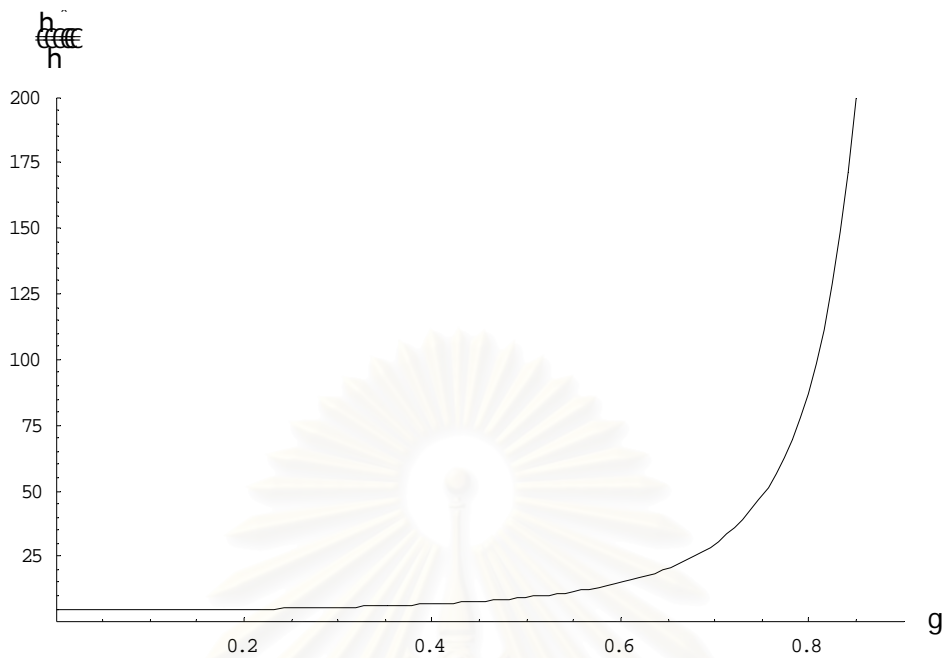


Figure 4.2 The effective viscosity as a function of γ ($\gamma^3 =$ packing fraction).

4.3 Closed Form of Velocity Fields

In the previous section, the closed form of the velocity fields in the effective medium and in the shell region are shown in Equations (4.22) and (4.29), respectively. Now we consider these velocity fields for $\gamma^3 < 0.1$ (dilute packing fraction) and $\gamma^3 > 0.1$ separately in order to reduce the complication.

4.3.1 For Low Packing Fraction

In the range of dilute packing fraction condition ($\gamma^3 < 0.1$), we neglect insignificant γ^n terms for $n > 2$. Thus, the approximate velocity field in the shell region, Equation (4.29), becomes

$$\vec{v}_{II}(\vec{r}) = v_0 [P_1(r_a, \gamma) \cos \theta \hat{r} + Q_1(r_a, \gamma) \sin \theta \hat{\theta}], \quad (4.38)$$

where

$$P_1(r_a, \gamma) = \frac{2}{5} \left[BT_3 + \frac{5}{3} C \gamma^2 \left(r_a^2 - \frac{1}{r_a^3} \right) \right] - \frac{1}{(1-\gamma)} \left[AT_4 - \frac{D}{3} \left(1 - \frac{1}{r_a} \right) \right] \quad (4.39a)$$

$$Q_1(r_a, \gamma) = \frac{1}{5} \left[BT_3 + \frac{5}{3} C \gamma^2 \left(r_a^2 - \frac{1}{r_a^3} \right) \right] + \frac{1}{(1-\gamma)} \left[AT_4 - \frac{D}{3} \left(1 - \frac{1}{r_a} \right) \right] \quad (4.39b)$$

$$T_3 = \frac{5}{6} (-r_a^2 \gamma^3 + r_a^{-1} - r_a^{-3}) \quad (4.39c)$$

$$T_4 = \frac{1}{6} [-r_a^2 (1-\gamma) + \gamma^{-2} + r_a^{-1} (1-\gamma^{-2})] \quad (4.39d)$$

and the velocity field in the effective medium is still Equation (4.22), that is

$$\vec{v}_{2l}(\vec{r}) = v_0 [P_1^*(r_a, \gamma) \cos \theta \hat{r} + Q_1^*(r_a, \gamma) \sin \theta \hat{\theta}], \quad (4.40)$$

where

$$P_1^*(r_a, \gamma) = 1 - \frac{3}{2r_a \gamma} + \frac{1}{2r_a^3 \gamma^3} + \frac{3C}{3r_a^3 \gamma^3} + D \left(\frac{1}{2r_a \gamma} - \frac{1}{6r_a^3 \gamma^3} \right) \quad (4.41a)$$

$$Q_1^*(r_a, \gamma) = -1 + \frac{3}{4r_a \gamma} + \frac{1}{4r_a^3 \gamma^3} + \frac{C}{3r_a^3 \gamma^3} - D \left(\frac{1}{4r_a \gamma} + \frac{1}{12r_a^3 \gamma^3} \right). \quad (4.41b)$$

The constants in the above equations obtained from the continuity equation and no-slip boundary conditions, Equations (4.30) and (4.31) can be reduced to

$$\begin{bmatrix} -\frac{1}{10\gamma^2} & \frac{\gamma}{2} \\ \frac{1}{2\gamma^2} & -2(1-\gamma) \end{bmatrix} \begin{bmatrix} A \\ B \end{bmatrix} = \begin{bmatrix} C \\ D \end{bmatrix} \quad (4.42)$$

and

$$\begin{bmatrix} \frac{3\gamma-2}{6\gamma^2(1-\gamma)} & \frac{\gamma(5\gamma^2-3)}{6} \\ \frac{(1+\gamma)}{3\gamma^2} & 3\gamma \end{bmatrix} \begin{bmatrix} A \\ B \end{bmatrix} + \begin{bmatrix} -\frac{1}{3} + 2\delta & \frac{-\gamma}{3(1-\gamma)} - \frac{\delta}{2} \\ -\frac{8}{3} - 4\delta & \frac{-2\gamma}{3(1-\gamma)} - \frac{\delta}{2} \end{bmatrix} \begin{bmatrix} C \\ D \end{bmatrix} = \begin{bmatrix} -\frac{3\delta}{2} \\ \frac{3\delta}{2} \end{bmatrix}. \quad (4.43)$$

Equations (4.42) and (4.43) are solved for the constants A , B , C , D and δ in terms of γ . The results are

$$A = \frac{6\gamma^3(\sqrt{6} - 1)}{(3\gamma - 2)} \quad (4.44a)$$

$$B = \frac{3}{(3\gamma - 2)} \quad (4.44b)$$

$$C = \frac{3\gamma(7 - 2\sqrt{6})}{10(3\gamma - 2)} \quad (4.44c)$$

$$D = \frac{3(1 + \sqrt{6})\gamma - 6}{(3\gamma - 2)} \quad (4.44d)$$

and
$$\delta = \frac{3(2 + \sqrt{6})}{3 - 10\gamma^2}. \quad (4.44e)$$

Substitute the above constants into Equations (4.38) and (4.40) to obtain the velocity fields for low packing fraction in the shell region and in the effective medium as

$$\vec{v}_{1l}(\vec{r}) = \frac{2v_0}{(2 - 3\gamma)} \begin{bmatrix} \left(1 - \frac{3}{2r_a} + \frac{1}{2r_a^3} - \frac{3(\sqrt{6} - 1)\gamma^3 r_a^2}{10}\right) \cos \theta \hat{r} \\ - \left(1 - \frac{3}{4r_a} - \frac{1}{4r_a^3} - \frac{3(\sqrt{6} - 1)\gamma^3 r_a^2}{5}\right) \sin \theta \hat{\theta} \end{bmatrix} \quad (4.45)$$

and

$$\vec{v}_{2l}(\vec{r}) = \frac{2v_0}{(2 - 3\gamma)} \begin{bmatrix} \left(1 - \frac{3(\sqrt{6} - 2)}{4r_a} - \frac{3(8 - 3\sqrt{6})}{20\gamma^2 r_a^3} - \frac{3\gamma}{2}\right) \cos \theta \hat{r} \\ - \left(1 - \frac{3(\sqrt{6} - 2)}{8r_a} + \frac{3(8 - 3\sqrt{6})}{40\gamma^2 r_a^3} - \frac{3\gamma}{2}\right) \sin \theta \hat{\theta} \end{bmatrix}. \quad (4.46)$$

The above two equations are approximate velocity fields in closed form for low packing fraction.

4.3.2 For Higher Packing Fraction

For $\gamma^3 > 0.1$, the constants A , B , C and D are determined by fitting curve to the value of the constants shown in Table 4.2 which are obtained from Equation (4.36). By minimizing the square error to obtain the best-fitting curve [16], the Equation of each constant in the form of polynomial function of degree m is obtained (see Appendix B). The higher order of polynomial terms used, the better fitting obtained, however it is complicated in the velocity flow field results. Thus we will choose the appropriate value.

γ	A	B	C	D
0.46	-1.3263	-4.5881	-0.2181	2.4843
0.48	-1.6356	-4.9854	-0.2290	2.4530
0.50	-2.0156	-5.4444	-0.2398	2.4211
0.52	-2.4837	-5.9785	-0.2505	2.3885
0.54	-3.0631	-6.6042	-0.2610	2.3553
0.56	-3.7836	-7.3433	-0.2713	2.3214
0.58	-4.6850	-8.2235	-0.2813	2.2869
0.60	-5.8204	-9.2818	-0.2911	2.2518
0.62	-7.2619	-10.567	-0.3005	2.2162

Table 4.2 The numerical values of the constants from Equations (4.36a)-(4.36d) for varying γ .

γ	A	B	C	D
0.64	-9.1089	-12.146	-0.3096	2.1800
0.66	-11.500	-14.108	-0.3182	2.1434
0.68	-14.634	-16.583	-0.3265	2.1062
0.70	-18.796	-19.751	-0.3342	2.0687
0.72	-24.414	-23.878	-0.3415	2.0308
0.74	-32.138	-29.362	-0.3482	1.9926
0.76	-42.986	-36.817	-0.3543	1.9542
0.78	-58.614	-47.225	-0.3598	1.9155
0.80	-81.813	-62.217	-0.3647	1.8767
0.82	-117.53	-84.637	-0.3689	1.8379
0.84	-175.05	-119.74	-0.3725	1.7991

Table 4.2 (continue) The numerical values of the constants from Equations (4.36a)-(4.36d) for various γ .

The curves that fit with numerical values of the constants A , B , C and D in Table 4.2 are shown in Figures 4.3, 4.4, 4.5 and 4.6.

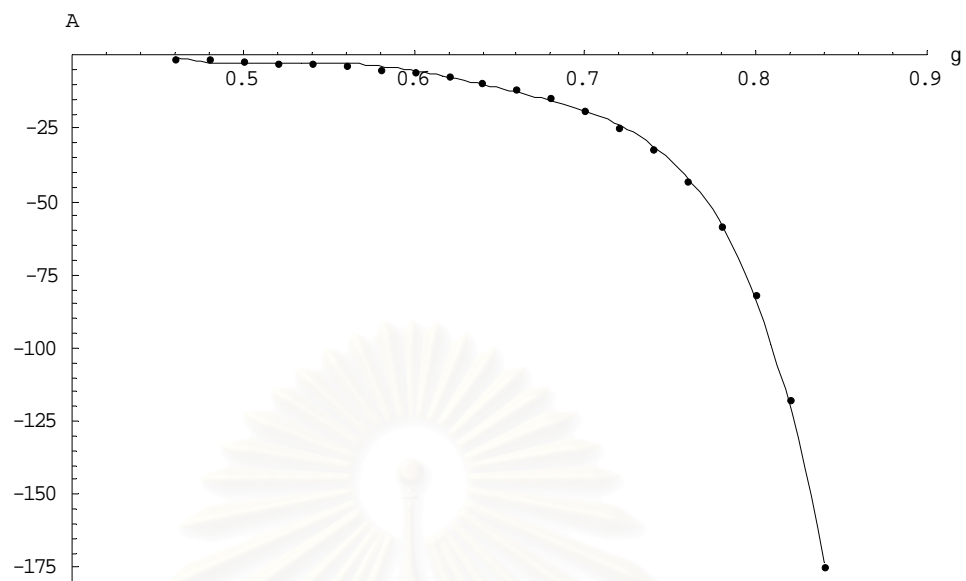


Figure 4.3 The fitted curve of parameter A (solid line) superimposed on the numerical values of A (points).

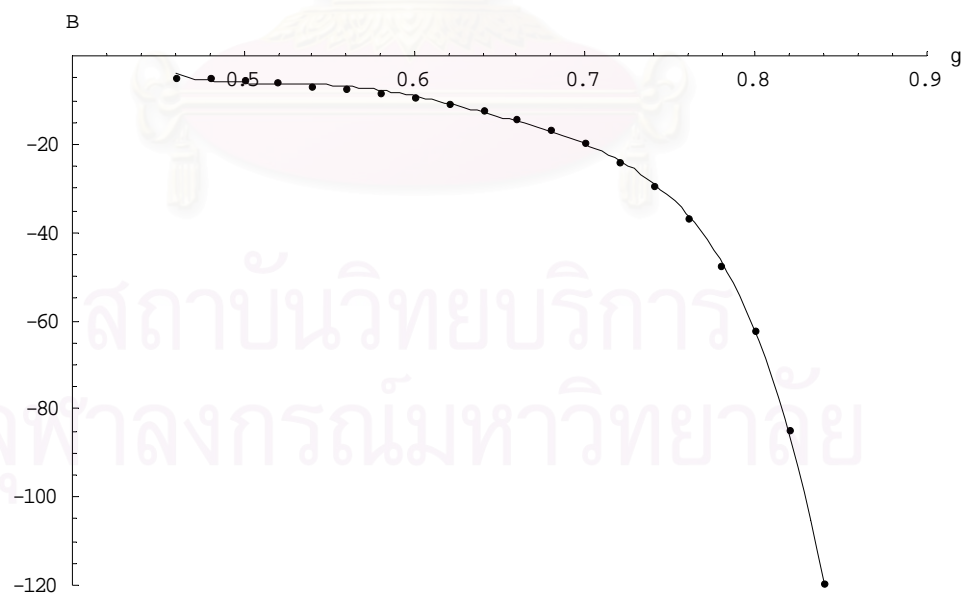


Figure 4.4 The fitted curve of parameter B (solid line) superimposed on the numerical values of B (points).

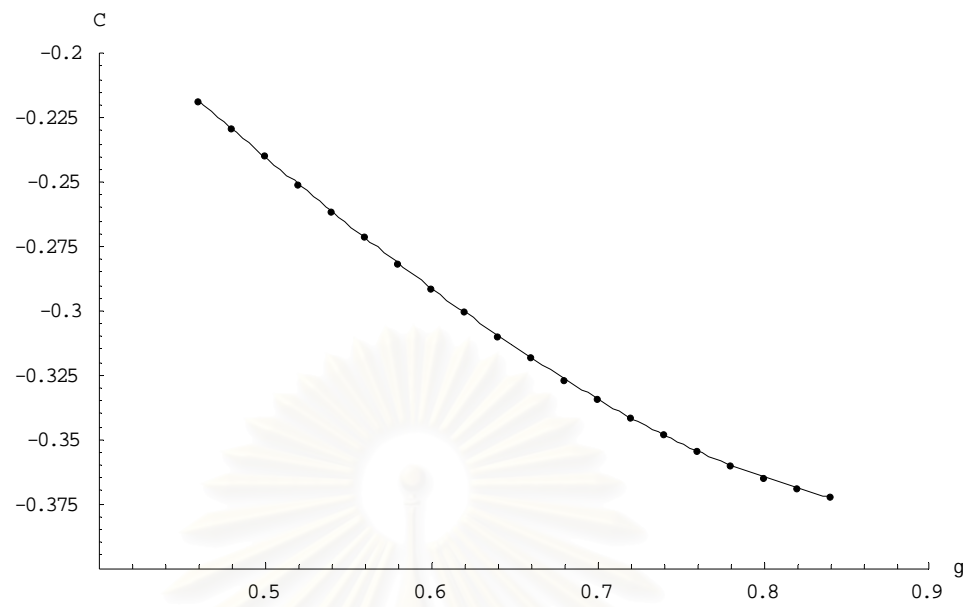


Figure 4.5 The fitted curve of parameter C (solid line) superimposed on the numerical values of C (points).

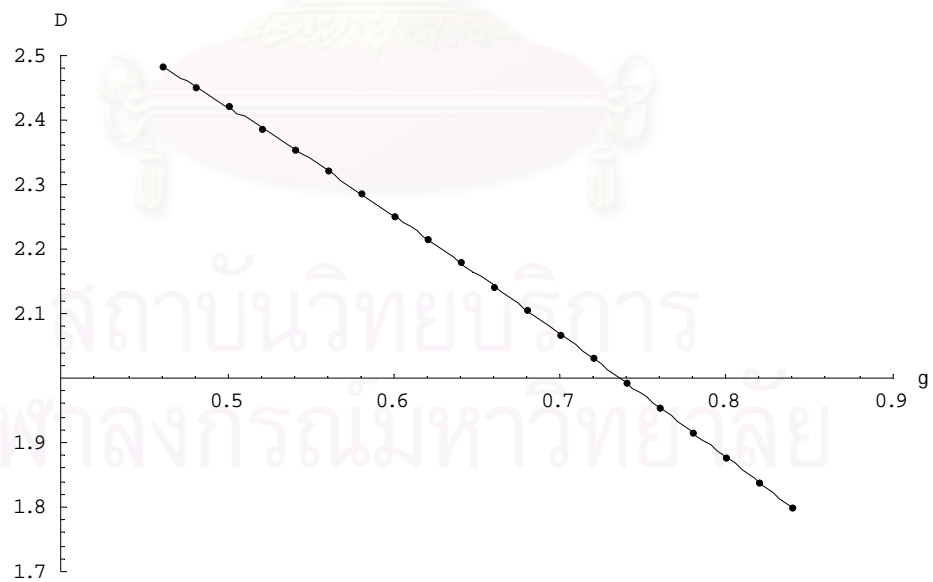


Figure 4.6 The fitted curve of parameter D (solid line) superimposed on the numerical values of D (points).

By curve fitting, the constant parameters are

$$A = [1.68 - (14.3)\gamma + (48.0)\gamma^2 - (80.2)\gamma^3 + (66.6)\gamma^4 - (22.0)\gamma^5] \times 10^4 \quad (4.47a)$$

$$B = [0.955 - (8.10)\gamma + (27.3)\gamma^2 - (45.6)\gamma^3 + (38.0)\gamma^4 - (12.6)\gamma^5] \times 10^4 \quad (4.47b)$$

$$C = -0.0208 - (0.149)\gamma - (0.955)\gamma^2 + (0.755)\gamma^3 \quad (4.47c)$$

$$D = 2.89 - (0.0614)\gamma - (2.17)\gamma^2 + (0.826)\gamma^3. \quad (4.47d)$$

Thus, for higher volume packing fractions ($\gamma^3 > 0.1$), the velocity fields in the shell region and in the effective medium are Equations (4.29) and (4.22) respectively. That is

$$\vec{v}_{1h}(\vec{r}) = v_0 [P_2(r_a, \gamma) \cos \theta \hat{r} + Q_2(r_a, \gamma) \sin \theta \hat{\theta}], \quad (4.48)$$

where

$$P_2(r_a, \gamma) = \frac{2}{5(1-\gamma^5)} \left[BT_5 + \frac{5C\gamma^2}{3} \left(r_a^2 - \frac{1}{r_a^3} \right) \right] - \frac{1}{(1-\gamma)} \left[AT_6 - \frac{D}{3} \left(1 - \frac{1}{r_a} \right) \right] \quad (4.49a)$$

$$Q_2(r_a, \gamma) = \frac{1}{5(1-\gamma^5)} \left[BT_5 + \frac{5C\gamma^2}{3} \left(r_a^2 - \frac{1}{r_a^3} \right) \right] + \frac{1}{(1-\gamma)} \left[AT_6 - \frac{D}{3} \left(1 - \frac{1}{r_a} \right) \right] \quad (4.49b)$$

$$T_5 = \frac{5}{6} \left[r_a^2 (\gamma^2 - 1) \gamma^3 + \frac{(1-\gamma^5)}{r_a} - \frac{(1-\gamma^5)}{r_a^3} \right] \quad (4.49c)$$

$$T_6 = \frac{1}{6} \left[-r_a^2(1-\gamma) + \frac{(1-\gamma^3)}{\gamma^2} + \frac{(1-\gamma^{-2})}{r_a} \right], \quad (4.49d)$$

and

$$\vec{v}_{2h}(\vec{r}) = v_0 [P_2^*(r_a, \gamma) \cos \theta \hat{r} + Q_2^*(r_a, \gamma) \sin \theta \hat{\theta}], \quad (4.50)$$

where

$$P_2^*(r_a, \gamma) = 1 - \frac{3}{2r_a\gamma} + \frac{1}{2r_a^3\gamma^3} + \frac{2C}{3r_a^3\gamma^3} + D \left(\frac{1}{2r_a\gamma} - \frac{1}{6r_a^3\gamma^3} \right), \quad (4.51a)$$

$$Q_2^*(r_a, \gamma) = -1 + \frac{3}{4r_a\gamma} + \frac{1}{4r_a^3\gamma^3} + \frac{C}{3r_a^3\gamma^3} - D \left(\frac{1}{4r_a\gamma} + \frac{1}{12r_a^3\gamma^3} \right) \quad (4.51b)$$

with the constants given by Equations (4.47a)-(4.47d).

4.4 Comparing Velocity Profiles

Using the velocity fields in previous sections, the velocity profiles or the streamlines of fluid flow can be determined. The streamlines or the trajectories of free particles carried by the fluid can be obtained by integration of the fluid velocity field ($\vec{v} = d\vec{r}/dt$). The comparison of Happel and EMT velocity profiles in the fluid shell is presented in this section. Happel flow fields are obtained from Equation (3.23) and the EMT velocity fields in approximate closed form solutions for low packing fraction ($\gamma^3 < 0.1$) and higher packing fraction ($\gamma^3 > 0.1$) are \vec{v}_{1l} and \vec{v}_{1h} given by Equations (4.45) and (4.48), respectively. The velocity profiles for some packing fraction in the shell region are shown in Figures 4.7- 4.12. While, Figures 4.13- 4.18 shown the comparison of the velocity profiles given by Equation (4.29), which is the EMT closed form velocity fields. The results indicate insignificant difference of the two models.

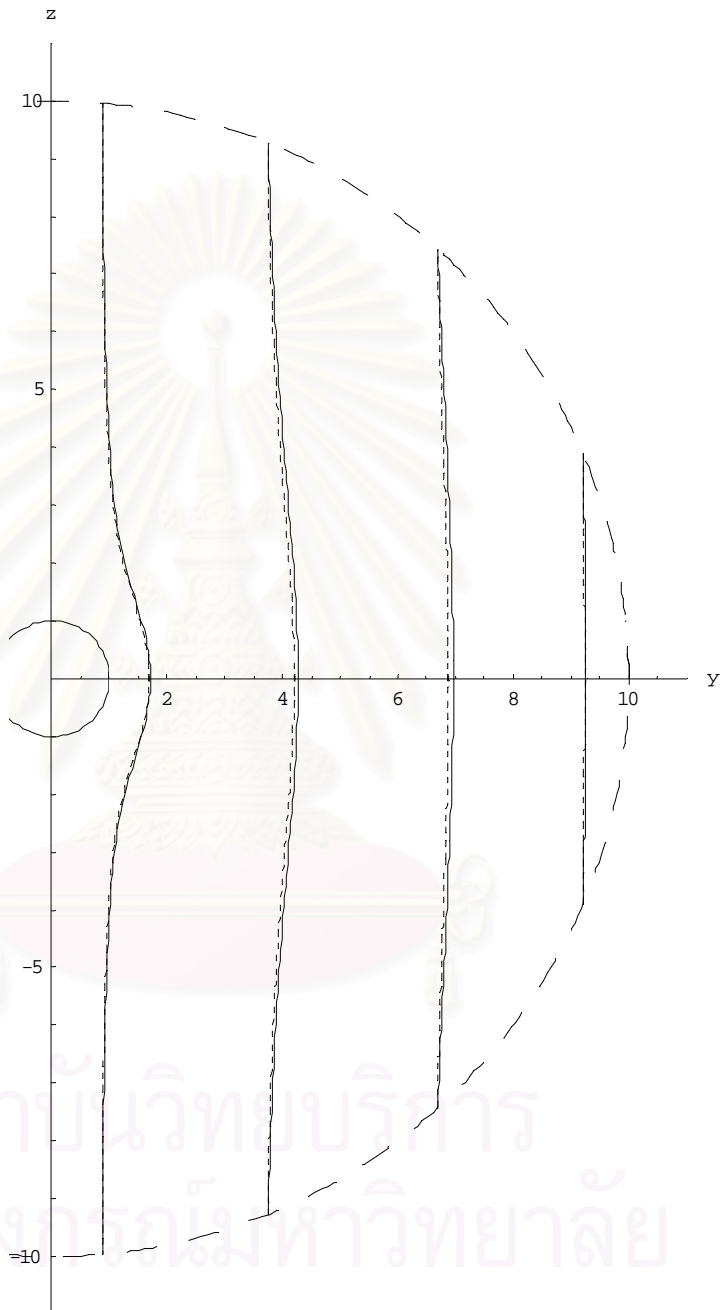
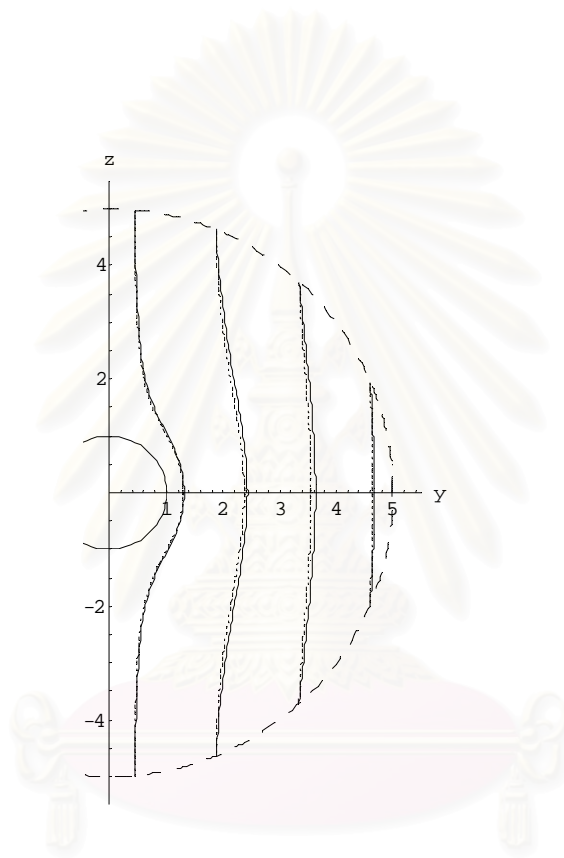


Figure 4.7 Comparison of EMT velocity profiles (dash lines) with Happel flow profile (solid lines) for low packing fraction at $\gamma^3 = 0.001$, and $v_{0a} = 6.65 \text{ s}^{-1}$.



สถาบันวิทยบริการ
จุฬาลงกรณ์มหาวิทยาลัย

Figure 4.8 Comparison of EMT velocity profiles (dash lines) with Happel flow profile (solid lines) for low packing fraction at $\gamma^3 = 0.008$, and $v_{0a} = 6.65 \text{ s}^{-1}$.

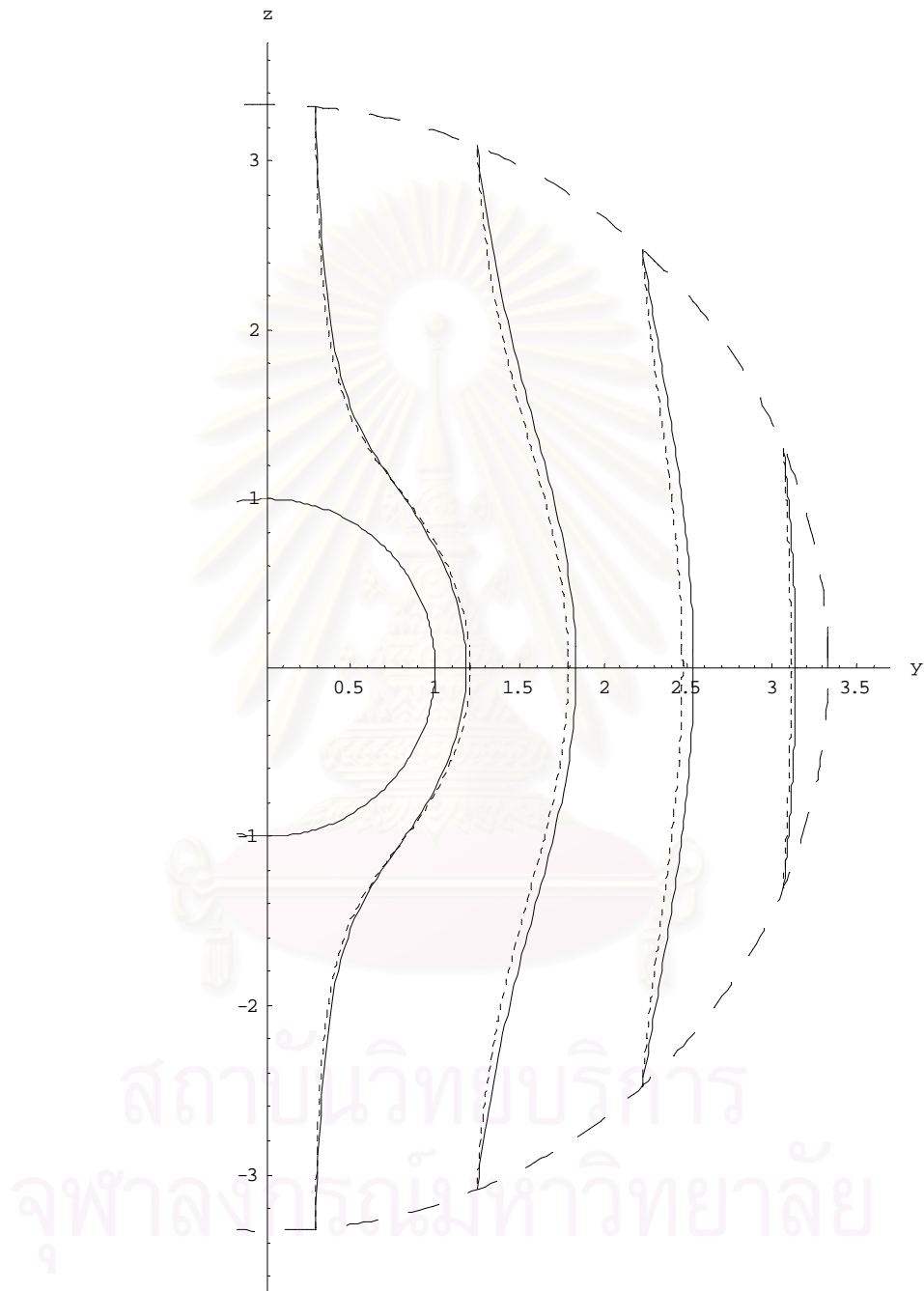
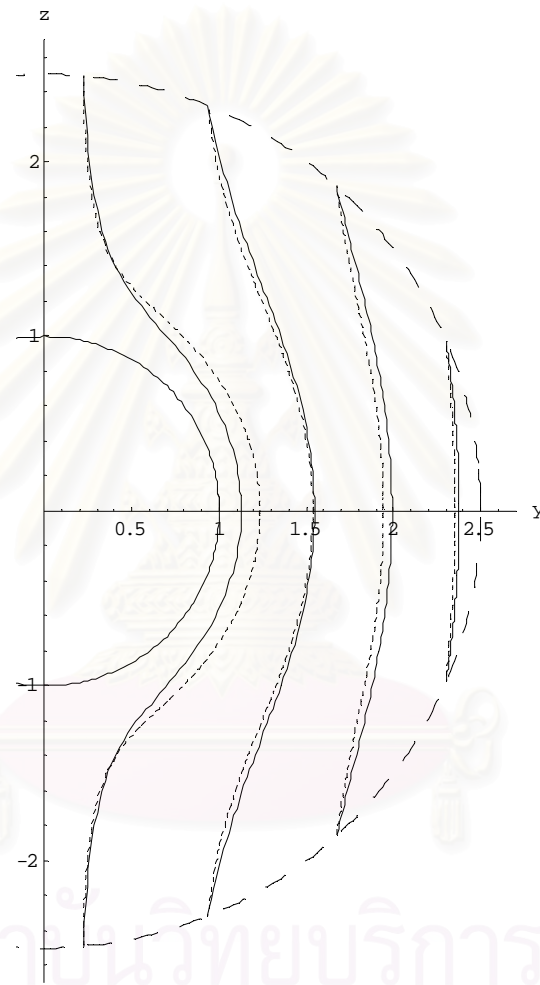


Figure 4.9 Comparison of EMT velocity profiles (dash lines) with Happel flow profile (solid lines) for low packing fraction at $\gamma^3 = 0.027$, and $v_{0a} = 6.65 \text{ s}^{-1}$.



สถาบันวิทยบริการ
จุฬาลงกรณ์มหาวิทยาลัย

Figure 4.10 Comparison of EMT velocity profiles (dash lines) with Happel flow profile (solid lines) for low packing fraction at $\gamma^3 = 0.064$, and $v_{0a} = 6.65 \text{ s}^{-1}$.

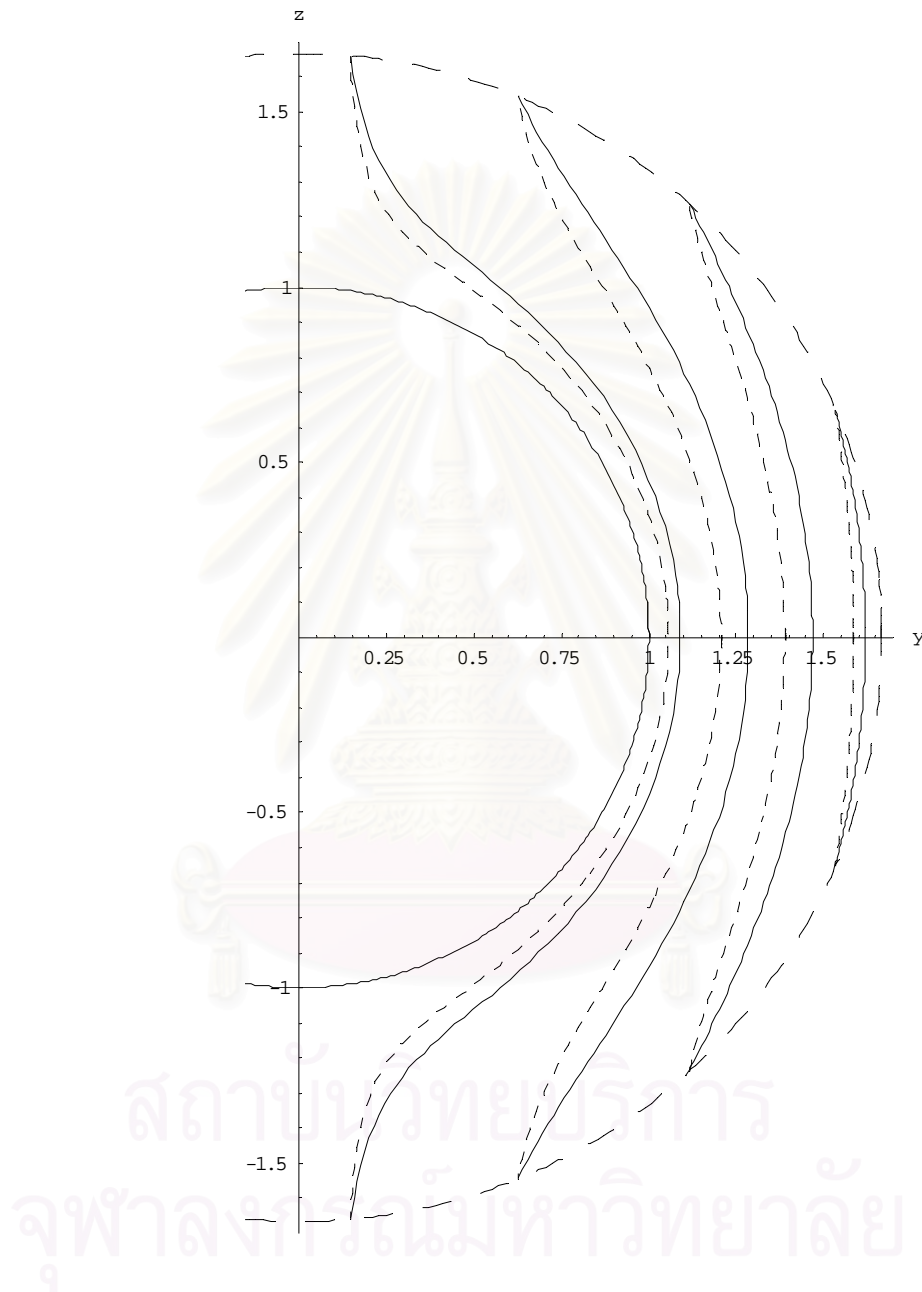


Figure 4.11 Comparison of EMT velocity profiles (dash lines) with Happel flow profile (solid lines) for higher packing fraction at $\gamma^3 = 0.216$, and $v_{0a} = 6.65 \text{ s}^{-1}$.

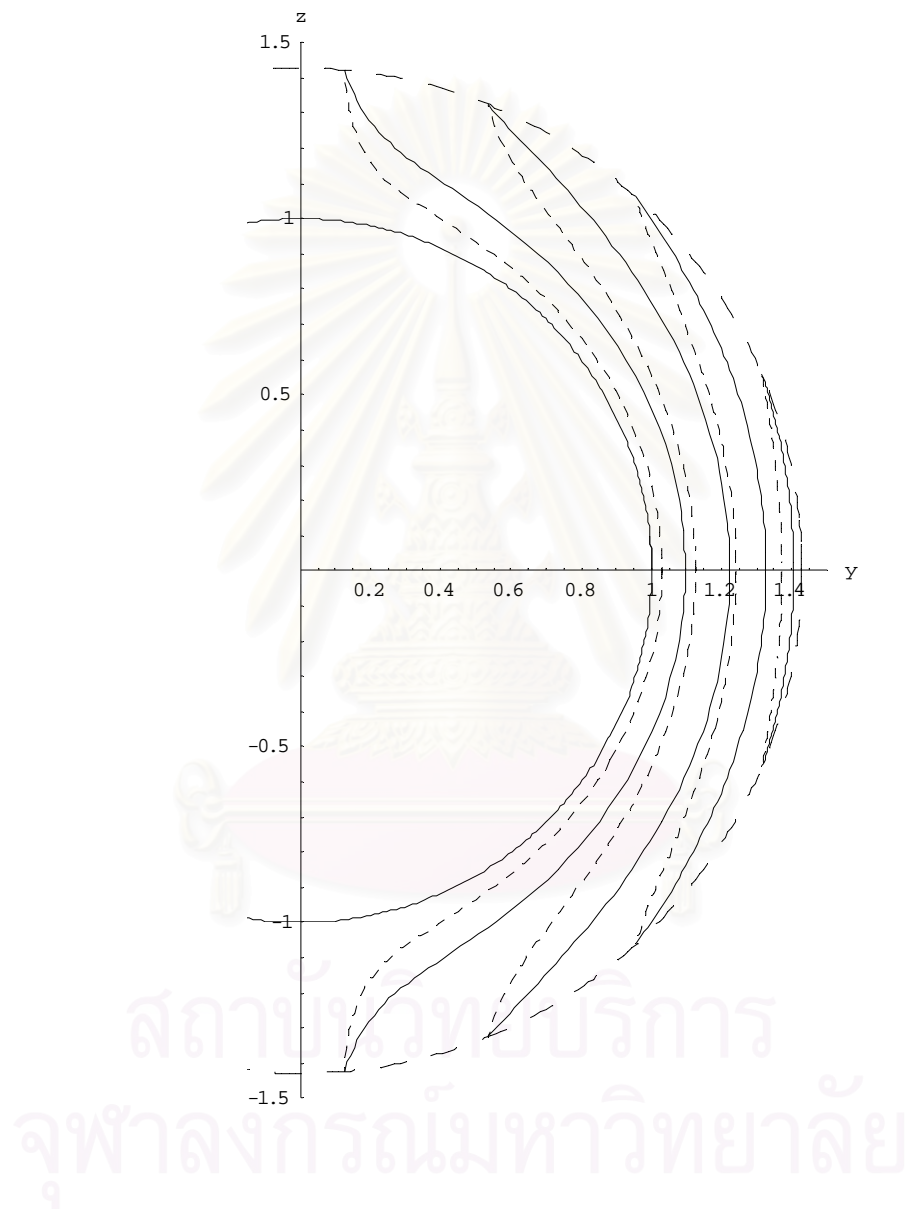


Figure 4.12 Comparison of EMT velocity profiles (dash lines) with Happel flow profile (solid lines) for higher packing fraction at $\gamma^3 = 0.343$, and $v_{0a} = 6.65 \text{ s}^{-1}$.

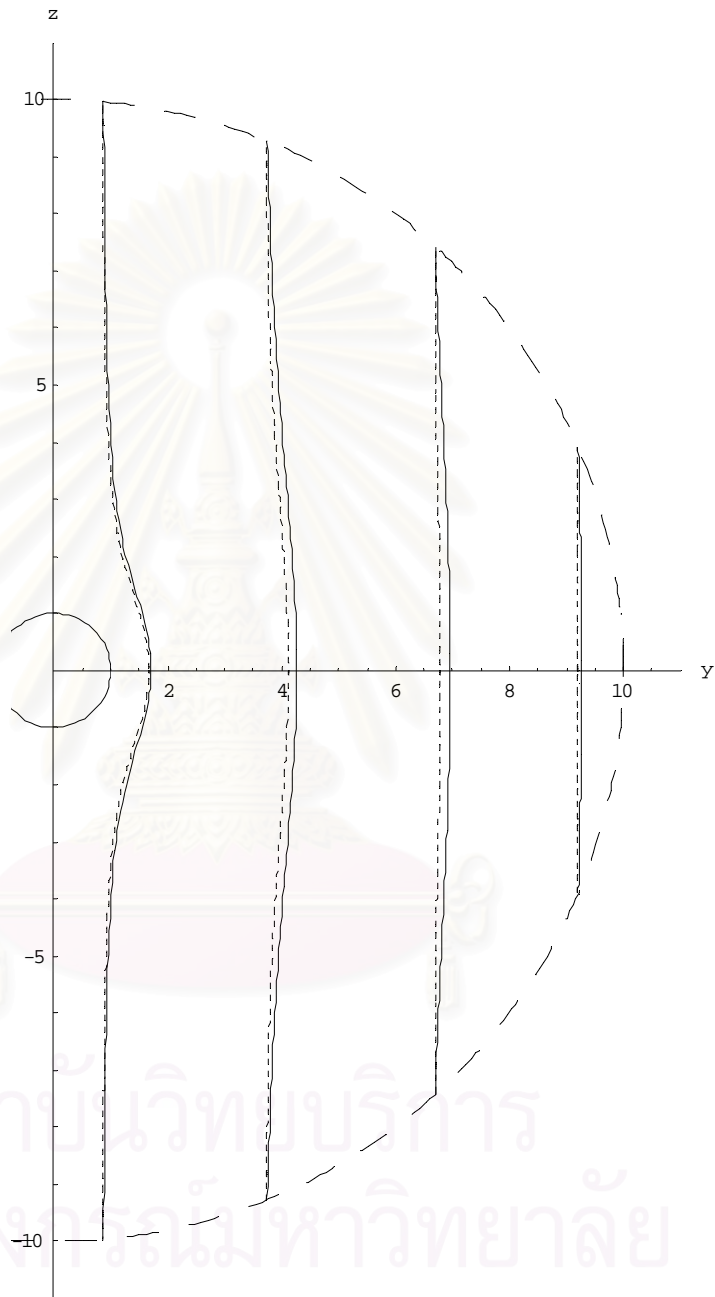
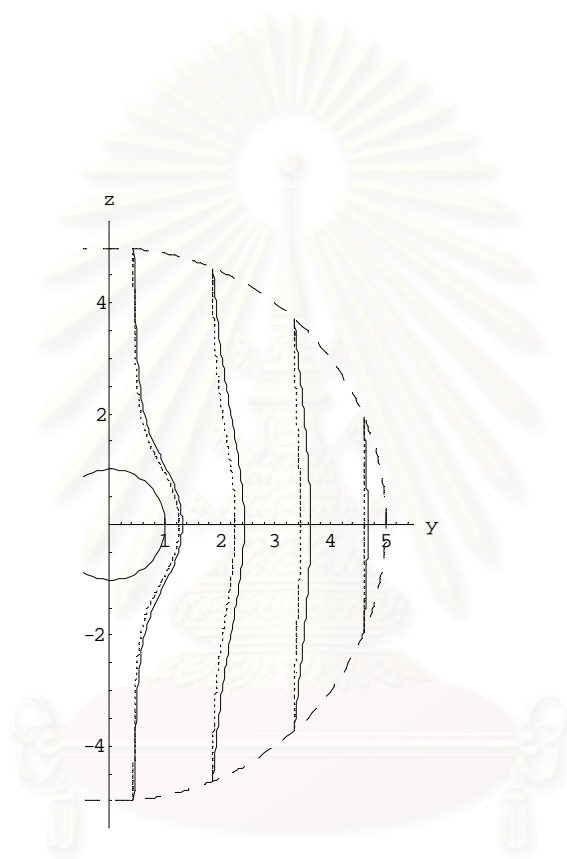


Figure 4.13 Comparison of EMT velocity profiles Equation (4.29) (dash lines) with Happel flow profile (solid lines) at $\gamma^3 = 0.001$, and $v_{0a} = 6.65 \text{ s}^{-1}$.



สถาบันวิทยบริการ
จุฬาลงกรณ์มหาวิทยาลัย

Figure 4.14 Comparison of EMT velocity profiles Equation (4.29) (dash lines) with Happel flow profile (solid lines) at $\gamma^3 = 0.008$, and $v_{0a} = 6.65 \text{ s}^{-1}$.

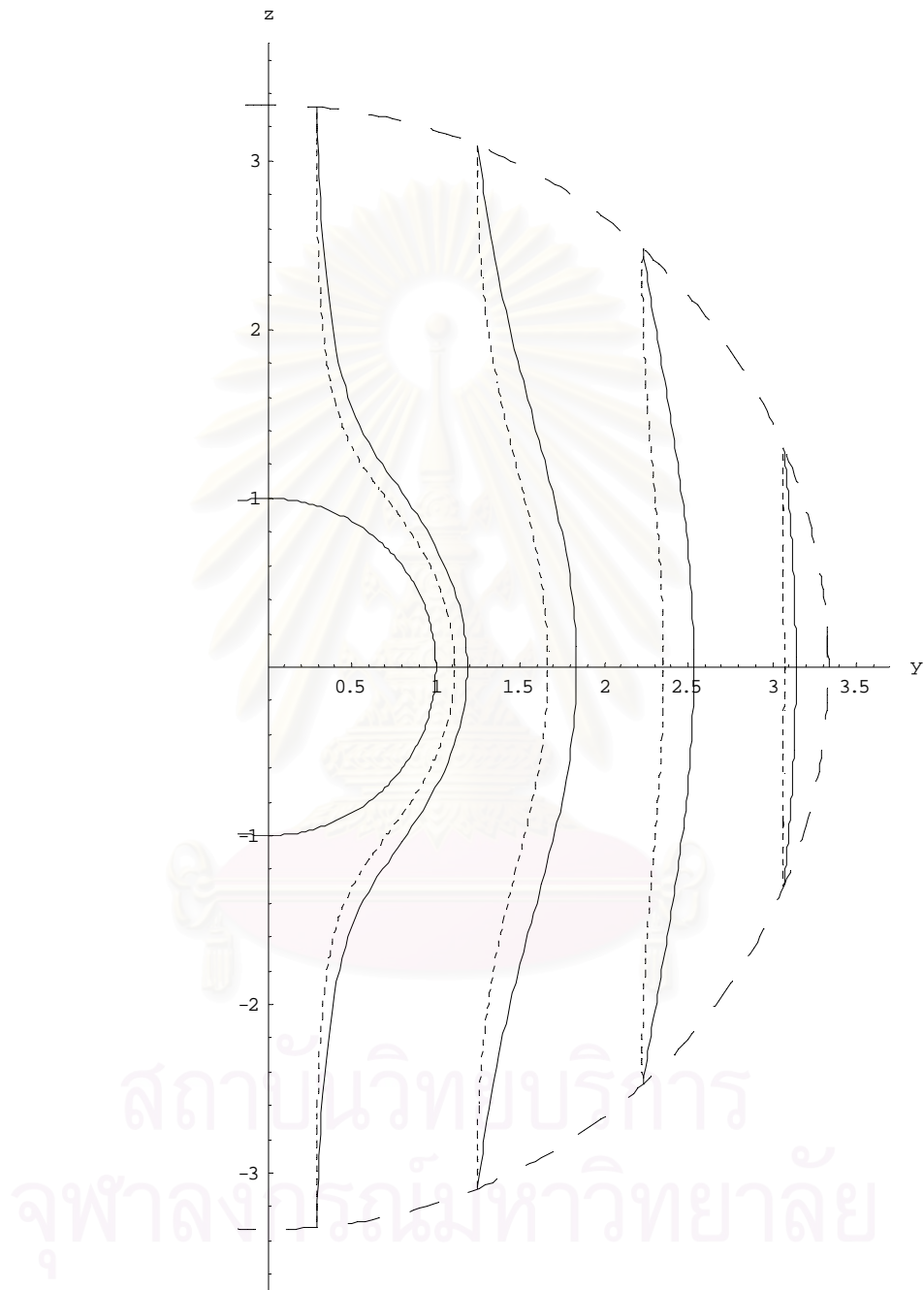
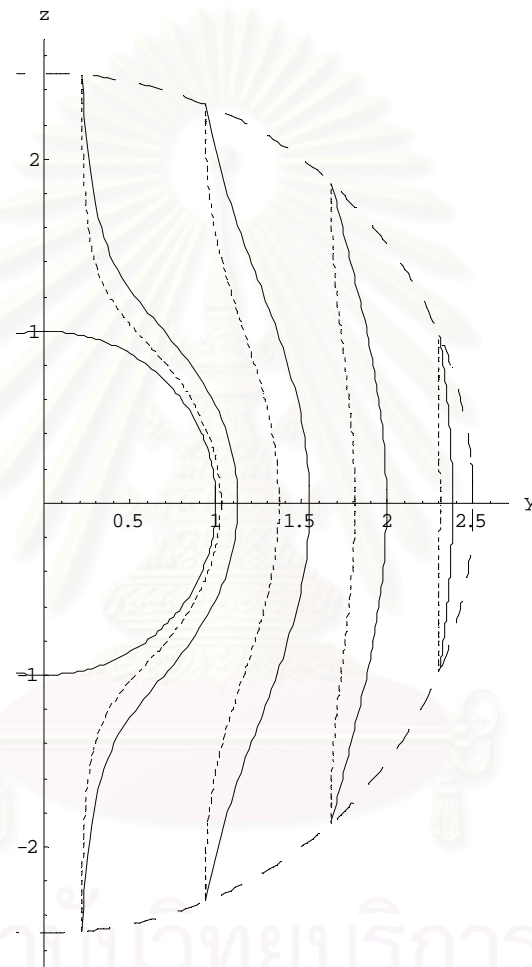


Figure 4.15 Comparison of EMT velocity profiles Equation (4.29) (dash lines) with Happel flow profile (solid lines) at $\gamma^3 = 0.027$, and $v_{0a} = 6.65 \text{ s}^{-1}$.



สถาบันวิทยบริการ
จุฬาลงกรณ์มหาวิทยาลัย

Figure 4.16 Comparison of EMT velocity profiles Equation (4.29) (dash lines) with Happel flow profile (solid lines) at $\gamma^3 = 0.064$, and $v_{0a} = 6.65 \text{ s}^{-1}$.

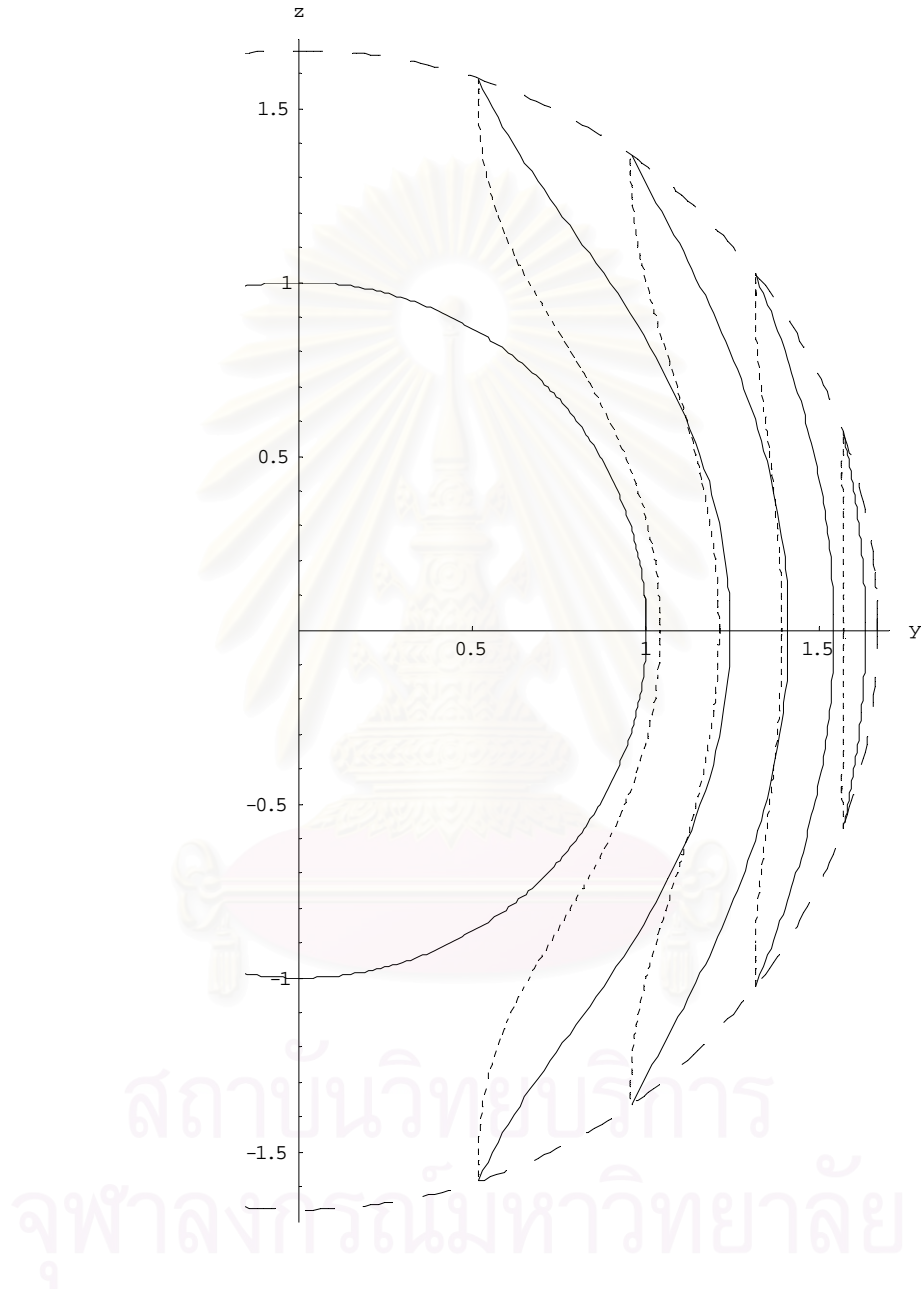


Figure 4.17 Comparison of EMT velocity profiles Equation (4.29) (dash lines) with Happel flow profile (solid lines) at $\gamma^3 = 0.216$, and $v_{0a} = 6.65 \text{ s}^{-1}$.

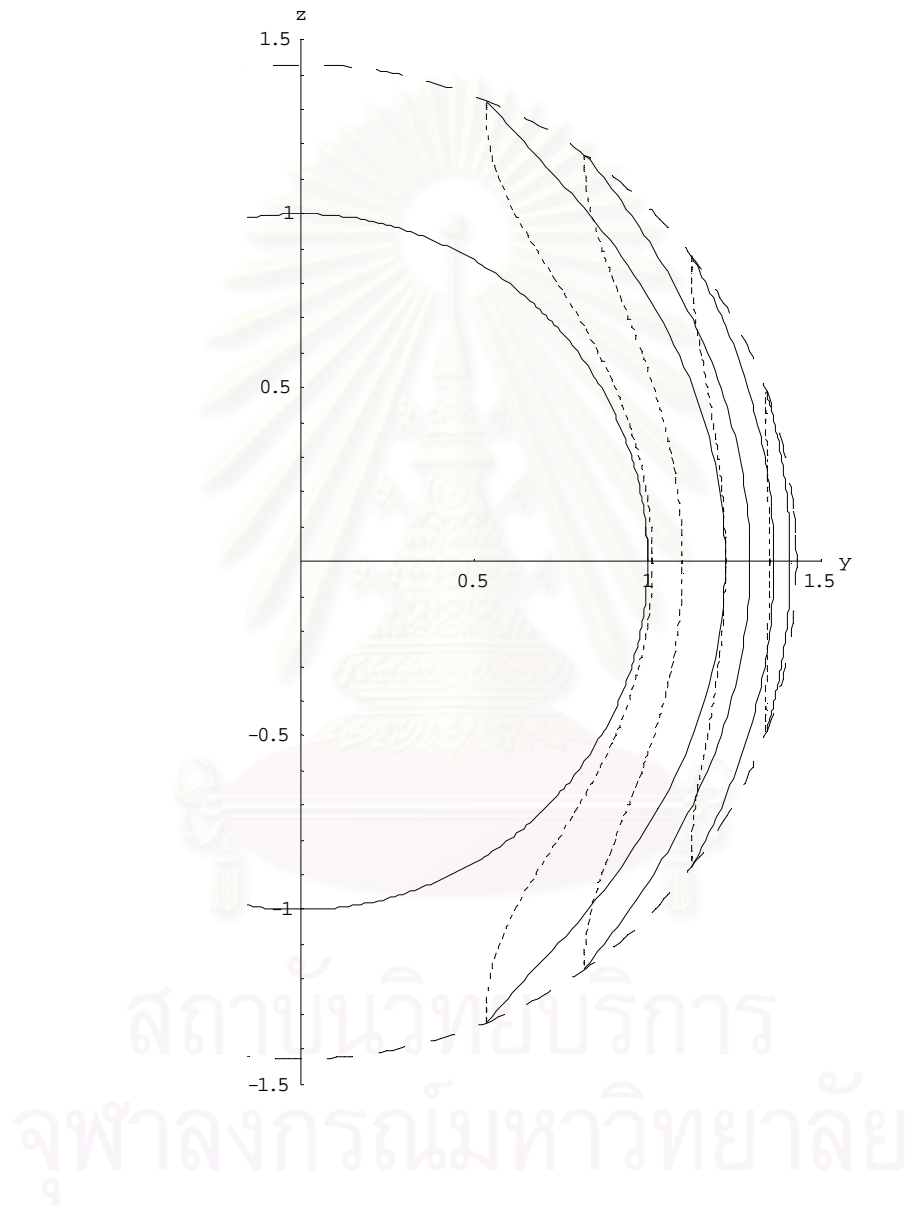


Figure 4.18 Comparison of EMT velocity profiles Equation (4.29) (dash lines) with Happel flow profile (solid lines) at $\gamma^3 = 0.343$, and $v_{0a} = 6.65 \text{ s}^{-1}$.

CHAPTER V

CAPTURE OF MAGNETIC PARTICLES IN LAMINAR FLOW

The fluid velocity fields in closed form are obtained in Chapter 4 both in the effective medium and the fluid shell regions. Now we apply these results to determine the trajectories of magnetic microscopic particles suspended in the fluid flow through randomly distributed magnetic spheres (collectors) in the presence of a uniform external magnetic field (\vec{H}_0). The magnetization of particles and collectors occurs and thus the magnetic particles are attracted to the collectors by magnetic force (\vec{f}_m) which is the dominant force. This process is called the capture of magnetic particles. The critical capture distance is defined as capture radius (r_c). There are two type of magnetic field (\vec{H}_0) and fluid flow (\vec{v}_0) direction alignment considered here; longitudinal mode for \vec{H}_0 and \vec{v}_0 parallel and transverse mode for \vec{H}_0 and \vec{v}_0 perpendicular. The longitudinal mode is symmetric around the polar axis but the transverse mode is not. For the transverse mode, the trajectories of particles on (\vec{H}_0, \vec{v}_0) plane is considered. Remember that for low packing fraction ($\gamma^3 < 0.1$), the fluid velocity fields \vec{v}_{1l} and \vec{v}_{2l} in Equations (4.45) and (4.46) are used, but it is \vec{v}_{1h} and \vec{v}_{2h} in Equations (4.48) and (4.50) for higher packing fraction ($\gamma^3 > 0.1$). Finally, the capture radius as a function of γ is obtained.

5.1 Equation of Motion

We consider the capture of paramagnetic and diamagnetic particles by the randomly distributed spheres in a uniform external magnetic field. Particles of microscopic size ($> 1 \mu m$) in a fluid described by laminar flow undergo capture process by interception. For particles less than $200 \mu m$ in diameter, the inertia and gravitational forces are insignificant. The dominant forces acting upon the individual particle are the viscous drag force (\vec{f}_D) and the magnetic force (\vec{f}_m), depending on the situation of the spheres, whose elements have high magnetic permeability, in a uniform field \vec{H}_0 . The viscous drag force is assumed to obey Stokes's law,

$$\vec{f}_D = -6\pi\eta r_p (\vec{v} - \vec{v}_f), \quad (5.1)$$

where \vec{v} is the particle velocity, \vec{v}_f the fluid velocity, η the viscosity, and r_p the particle radius. For a small particle with specific susceptibility χ_p immersed in a fluid of susceptibility χ_f and subjected to a magnetic field \vec{H} , the magnetic force is

$$\vec{f}_m = \left(\frac{2\pi}{3}\right) r_p^3 \mu_0 (\chi_p - \chi_f) \vec{\nabla} H^2. \quad (5.2)$$

The particle is said to be paramagnetic if $\chi_p > \chi_f$ and diamagnetic if $\chi_p < \chi_f$.

Using the velocity field \vec{v}_f and the magnetic field \vec{H} given by Moyer and coworkers [17], the drag force and the magnetic force can be determined. The equation of motion for microscopic particles is

$$\vec{f}_D + \vec{f}_m = 0 \quad (5.3)$$

and this can be solved for the particle velocity ($\vec{v} = d\vec{r}/dt$) which is subsequently integrated to obtain the particle trajectories as a function of the sphere volume packing fraction.

The equations of motion for microscopic particles in spherical coordinates with the polar axis along the applied magnetic field \vec{H}_0 are obtained from equation (5.3) as

$$\frac{dr_a}{dt} = v_{0a} P^*(r_a, \gamma) \cos \theta_v, \quad (5.4a)$$

$$\frac{d\theta}{dt} = v_{0a} r_a^{-1} Q^*(r_a, \gamma) \sin \theta_v, \quad (5.4b)$$

for $r_a > 1/\gamma$, since in this model H is uniform for $r > b$, and

$$\frac{dr_a}{dt} = v_{0a} P(r_a, \gamma) \cos \theta_v - v_{ma}^* r_a^{-4} [1 + 3 \cos 2\theta + K_s r_a^{-3} (5 + 3 \cos 2\theta)] / 2, \quad (5.5a)$$

$$\frac{d\theta}{dt} = v_{0a} r_a^{-1} Q(r_a, \gamma) \sin \theta_v - v_{ma}^* r_a^{-5} \left(1 + K_s \frac{r_a^{-3}}{2} \right) \sin 2\theta, \quad (5.5b)$$

for $1 < r_a < 1/\gamma$. Above $v_{0a} = v_0/a$, P^* , Q^* , P and Q are respectively given by Equations (4.23), (4.24), (4.29a), (4.29b), $\theta_v = \theta$ or $\theta - \pi/2$ for interception in longitudinal ($\vec{H}_0 // \vec{v}_0$) or transverse ($\vec{H}_0 \perp \vec{v}_0$) design, respectively, $v_{ma}^* = v_{ma} A^2$ with

$$v_{ma} = \frac{2\chi\mu_0 K_s H_0^2 r_p^2}{3\eta a^2} = \text{magnetic velocity},$$

where we defined $\chi = \chi_p - \chi_f$, $A = (2 + \nu)/[2 + \gamma^3 + \nu(1 - \gamma^3)]$, $\nu = \mu_p / \mu_f$ (relative permeability of collector and fluid) and $K_s = (\nu - 1)/(\nu + 2)$.

5.2 Mathematica Program for Particle Trajectories

Equations (5.4a), (5.4b), (5.5a) and (5.5b) can be solved by using Mathematica program [15] (see Appendix C) to obtain particle trajectories as a function of γ . Inspection of the particle trajectories yields the critical capture trajectory or capture distance called capture radius r_c as shown in Figure 5.1.

We determine the capture radius as a function of γ in both longitudinal fields ($\vec{H}_0 // \vec{v}_0$) and transverse fields ($\vec{H}_0 \perp \vec{v}_0$) for both paramagnetic and diamagnetic particles with characteristic constants magnetic velocity = 571.5 s^{-1} , fluid entrance velocity = 6.65 s^{-1} and $K_s = 0.58$ which are taken from the work of Friedlaender et al. for the single collector model [18].

By integration of Equations (5.4a), (5.4b), (5.5a) and (5.5b), we obtain the trajectories of particles. The figures below illustrate some particle trajectories and a capture radius (r_c).

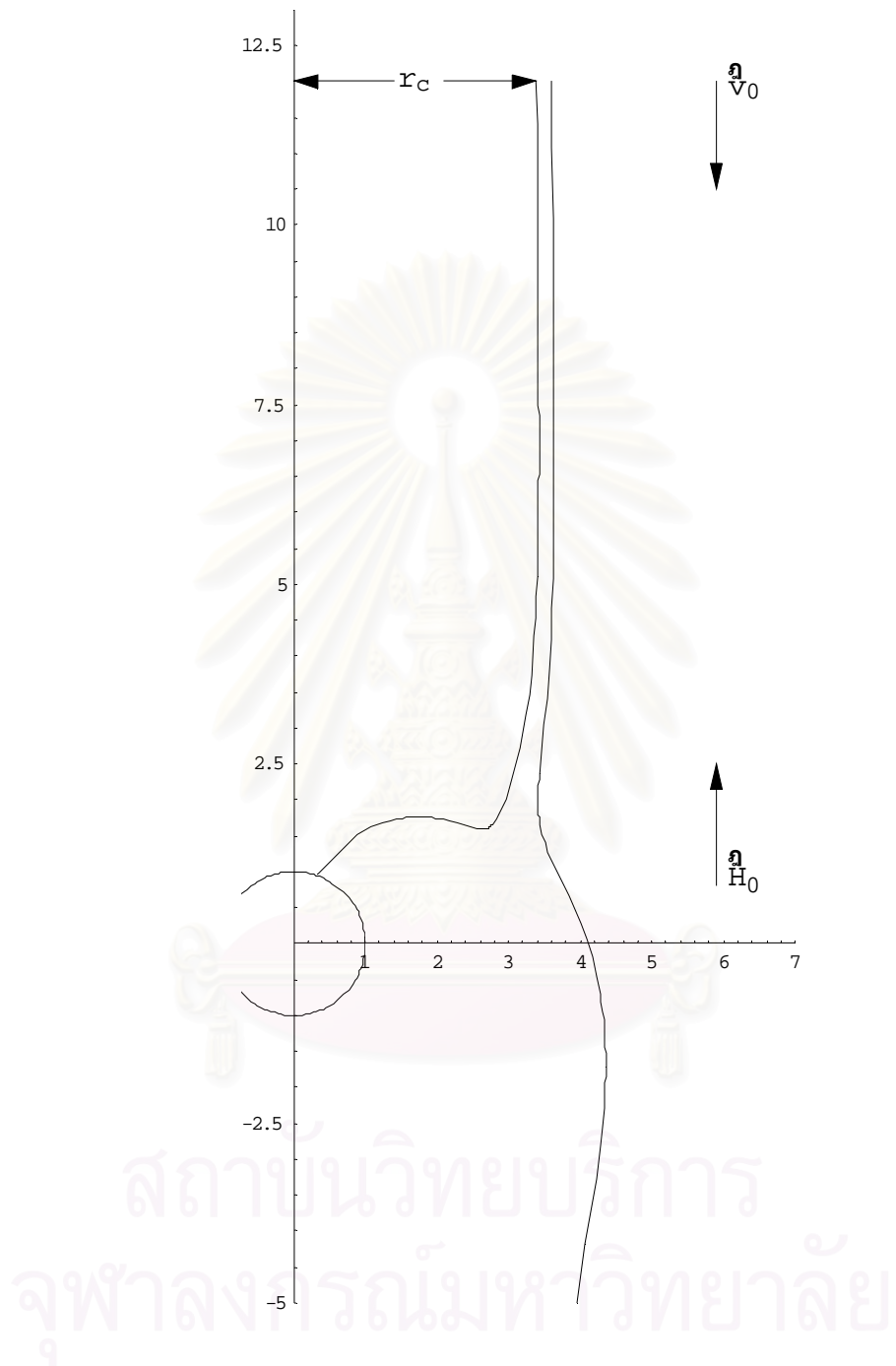


Figure 5.1 Capture radius r_c and particle trajectories of paramagnetic particles for a longitudinal mode ($\vec{H}_0 // \vec{v}_0$) with $\gamma^3 = 0.001$, $v_{0a} = 6.65 \text{ s}^{-1}$, $v_{ma}^* = 572.16 \text{ s}^{-1}$ and $K_s = 0.58$.

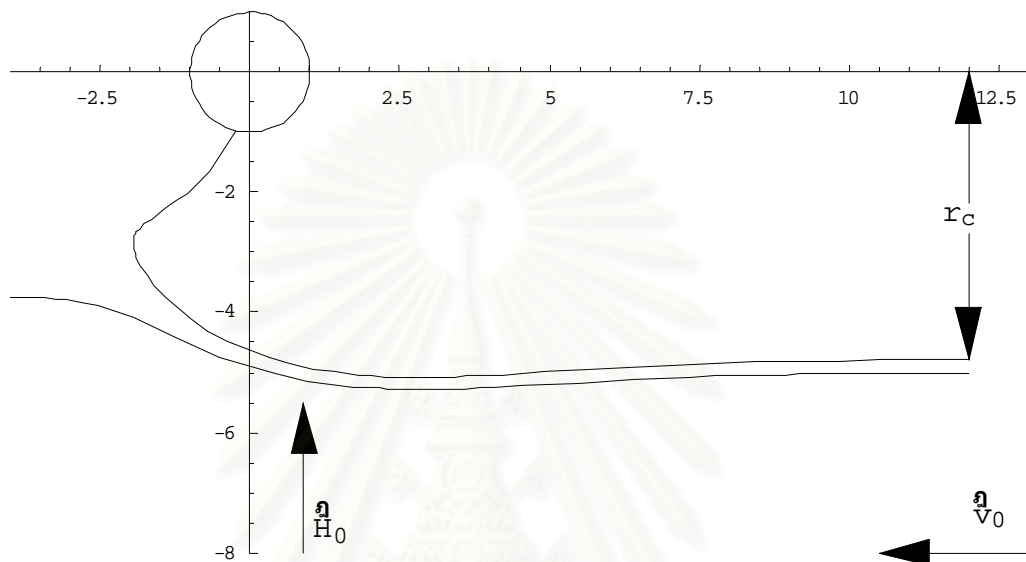


Figure 5.2 Capture radius r_c and particle trajectories of paramagnetic particles for a transverse mode ($\vec{H}_0 \perp \vec{v}_0$) with $\gamma^3 = 0.001$, $v_{0a} = 6.65 \text{ s}^{-1}$, $v_{ma}^* = 572.16 \text{ s}^{-1}$ and $K_s = 0.58$.

สถาบันวิทยบริการ
จุฬาลงกรณ์มหาวิทยาลัย

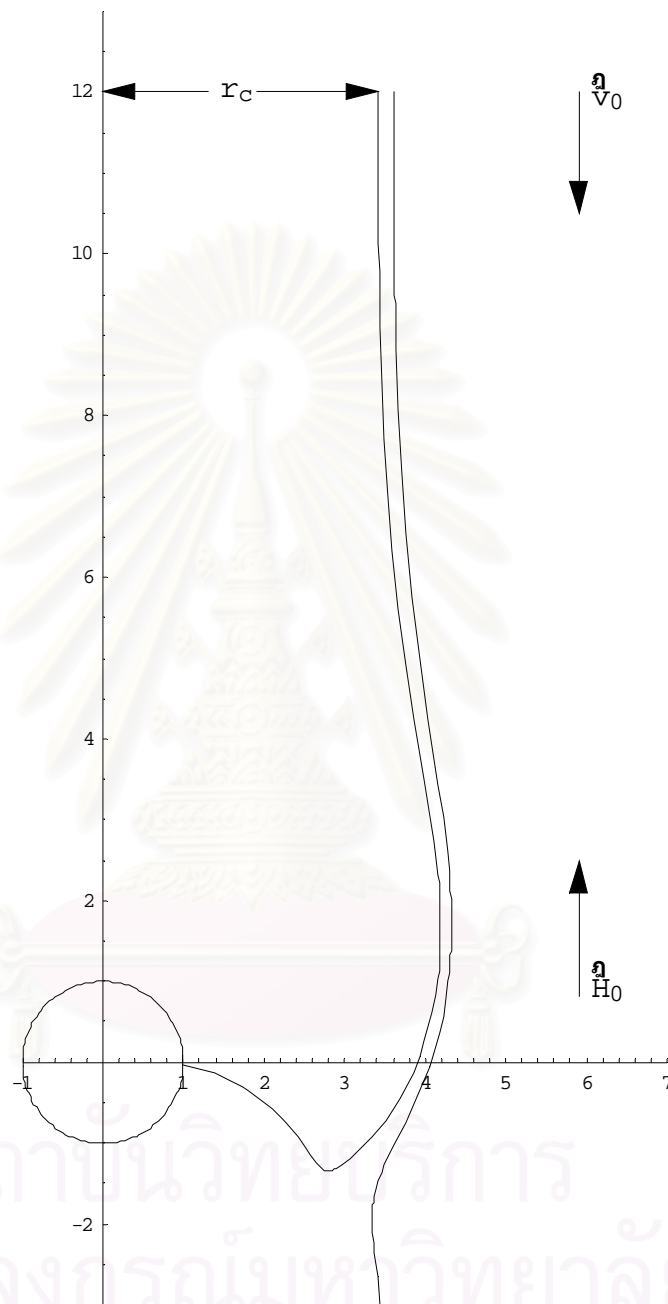


Figure 5.3 Capture radius r_c and particle trajectories of diamagnetic particles for a longitudinal mode ($\vec{H}_0 // \vec{v}_0$) with $\gamma^3 = 0.001$, $v_{0a} = 6.65 \text{ s}^{-1}$, $v_{ma}^* = -572.16 \text{ s}^{-1}$ and $K_s = 0.58$.

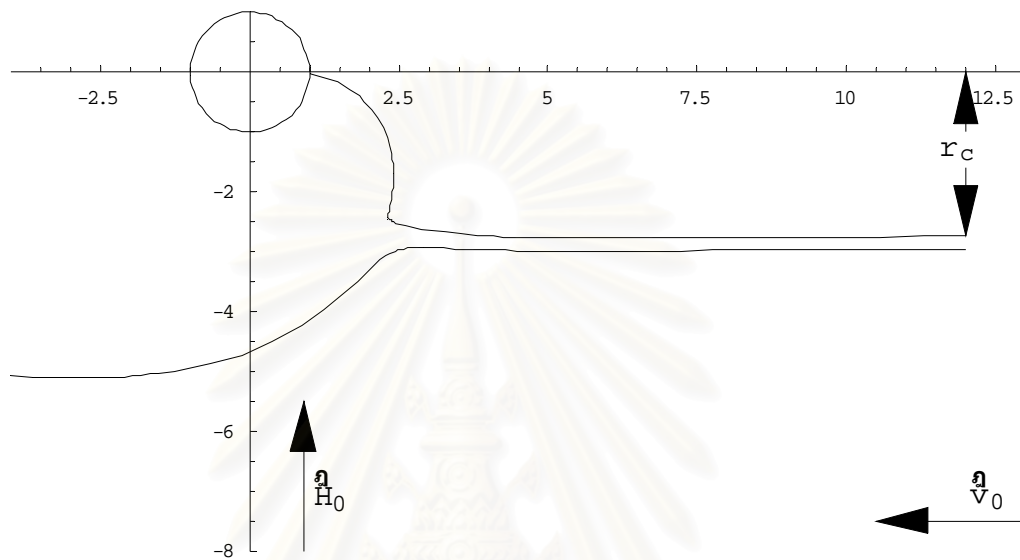


Figure 5.4 Capture radius r_c and particle trajectories of diamagnetic particles for a transverse mode ($\vec{H}_0 \perp \vec{v}_0$) with $\gamma^3 = 0.001$, $v_{0a} = 6.65 \text{ s}^{-1}$, $v_{ma}^* = -572.16 \text{ s}^{-1}$ and $K_s = 0.58$.

สถาบันวิทยบริการ
จุฬาลงกรณ์มหาวิทยาลัย

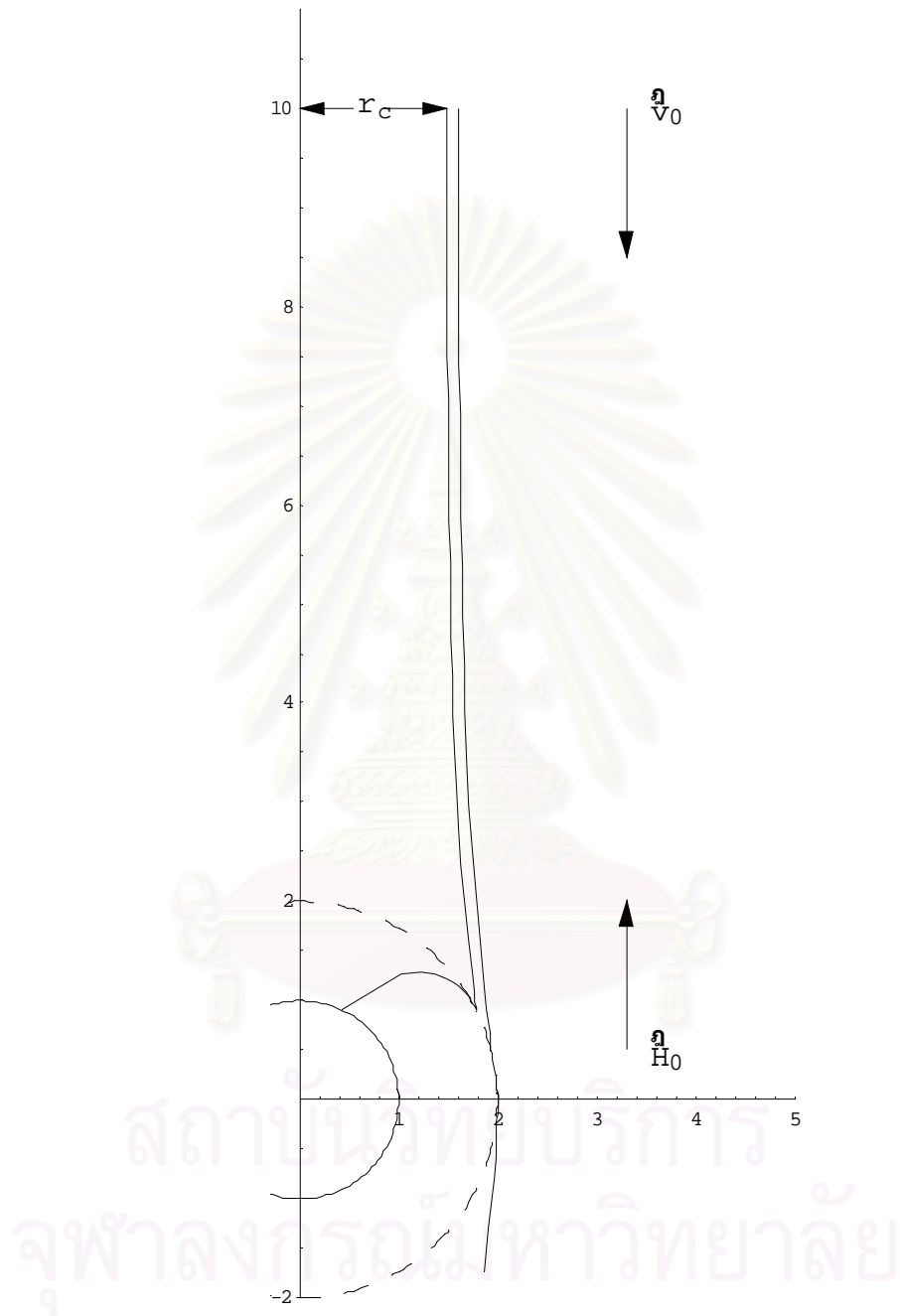


Figure 5.5 Capture radius r_c and particle trajectories of paramagnetic particles for a longitudinal mode ($\vec{H}_0 \parallel \vec{v}_0$) with $\gamma^3 = 0.125$, $v_{0a} = 6.65 \text{ s}^{-1}$, $v_{ma}^* = 664.34 \text{ s}^{-1}$ and $K_s = 0.58$.

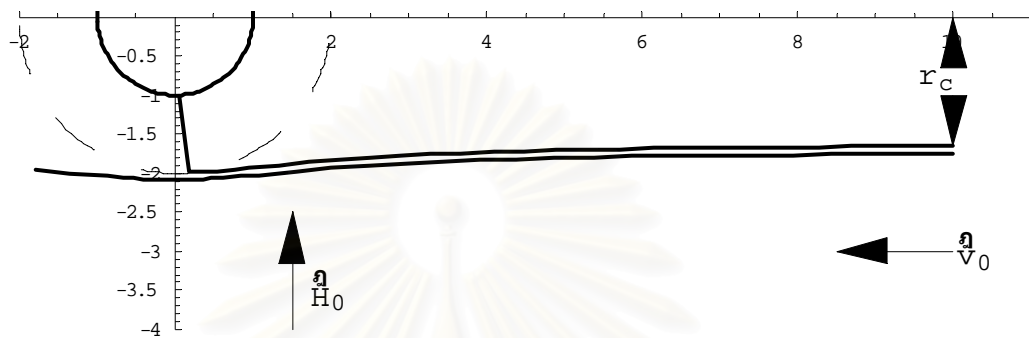


Figure 5.6 Capture radius r_c and particle trajectories of paramagnetic particles for a transverse mode ($\vec{H}_0 \perp \vec{v}_0$) with $\gamma^3 = 0.125$, $v_{0a} = 6.65 \text{ s}^{-1}$, $v_{ma}^* = 664.34 \text{ s}^{-1}$ and $K_s = 0.58$.

The pattern of particle's trajectory of diamagnetic particle in transverse mode is similar to that of paramagnetic particle in longitudinal mode; the particle moves toward the front of collector sphere. Note that the pattern of diamagnetic particle trajectory in longitudinal mode similar to that of the paramagnetic particle in transverse mode; the collection of magnetic particles occurs beside the collector sphere.

5.3 Capture Radius

The randomly distributed spheres in a nonmagnetic canister is one type of magnetic filter. The magnetic filter has been used to remove weakly magnetic particles from fluid systems. Capture radius describes the capture boundary which indicates the filtration efficiency. High capture radius means the extensive capture distance.

By solving Equations (5.4a), (5.4b), (5.5a) and (5.5b) with the use of the EMT velocity fields in the approximate closed form from this research, the critical capture distances or capture radii are obtained. The capture radii are show in Table 5.1 for various γ .



γ	Capture Radius (r_c)			
	paramagnetic		diamagnetic	
	$(\vec{H}_0 // \vec{v}_0)$	$(\vec{H}_0 \perp \vec{v}_0)$	$(\vec{H}_0 // \vec{v}_0)$	$(\vec{H}_0 \perp \vec{v}_0)$
0.10	3.39	4.78	3.41	2.74
0.20	3.19	4.67	3.88	2.64
0.30	2.58	3.00	3.00	2.26
0.40	1.74	1.96	1.96	1.41
0.50	1.48	1.65	1.65	1.18
0.60	1.16	1.29	1.29	0.88
0.70	0.93	1.01	1.01	0.65
0.80	0.75	0.80	0.80	0.47

Table 5.1 Capture radii of magnetic particles for varying γ taken from the EMT velocity field in closed form. Characteristic constants are $v_{ma} = 571.5 \text{ s}^{-1}$, $v_{0a} = 6.65 \text{ s}^{-1}$ and $K_s = 0.58$. $\vec{H}_0 // \vec{v}_0$ and $\vec{H}_0 \perp \vec{v}_0$ denote longitudinal and transverse mode design, respectively.

The comparisons of the capture radius from our results with the results taken from the previous publication based on the Happel flow fields are shown in Figures (5.5) and (5.6).

In the figures,

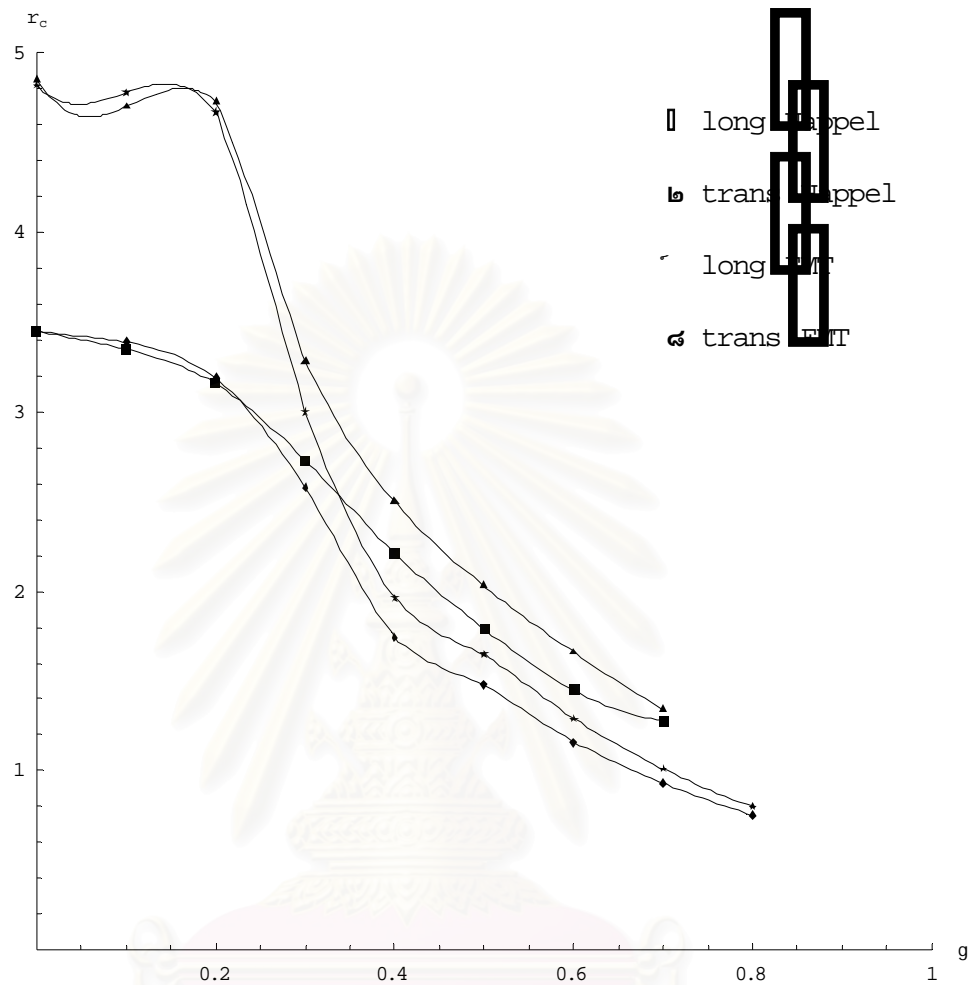


Figure 5.7 Capture radius for paramagnetic particles as a function of γ based on Happel and EMT flow fields in closed form. Characteristic constants are $v_{ma} = 571.5 \text{ s}^{-1}$, $v_{0a} = 6.65 \text{ s}^{-1}$ and $K_s = 0.58$.

long/Happel and trans/Happel denote longitudinal ($\vec{H}_0 // \vec{v}_0$) and transverse ($\vec{H}_0 \perp \vec{v}_0$) mode design, respectively, with Happel flow fields, while long/EMT and trans/EMT denote longitudinal ($\vec{H}_0 // \vec{v}_0$) and transverse ($\vec{H}_0 \perp \vec{v}_0$) mode design, respectively, with EMT flow fields in closed form.

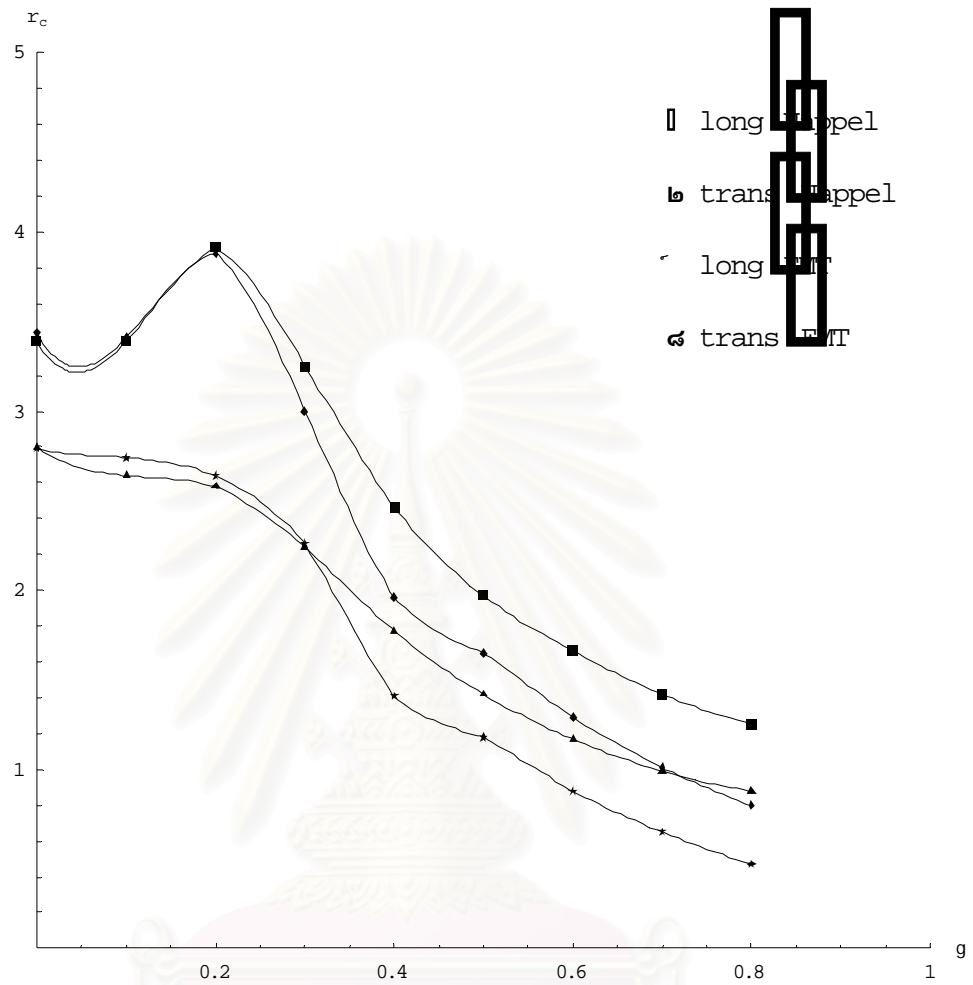


Figure 5.8 Capture radius for diamagnetic particles as a function of γ based on Happel and EMT flow fields in closed form. Characteristic constants are $v_{ma} = -571.5 \text{ s}^{-1}$, $v_{0a} = 6.65 \text{ s}^{-1}$ and $K_s = 0.58$.

The general features of the variation of r_c with γ in this research and Happel flow fields are very similar. We find the maximum value of r_c at $\gamma \approx 0.2$ in transverse design for paramagnetic particles and in longitudinal design for diamagnetic particles. For $\gamma > 0.3$, the effect of neighboring spheres is always to diminish r_c , since r_c is confined to the fluid shell which, itself, shrinks with increasing γ . For all cases we studied, the EMT results for r_c at $\gamma > 0.4$ are lower than the corresponding Happel model results reported previously.



สถาบันวิทยบริการ
จุฬาลงกรณ์มหาวิทยาลัย

CHAPTER VI

CONCLUSION AND DISCUSSION

Laminar flow occurs when the fluid stream around the solid object is smooth. This type of fluid flow occurs at low Reynolds number, $\text{Re} = \rho v_0 a / \eta < 1$, where ρ , v_0 , η , and a are the fluid density, entrance velocity, viscosity, and sphere radius, respectively. The determination of the velocity flow fields in closed form for the laminar flow passing randomly-distributed spheres is an objective of this research. These velocity fields are then used to predict the capture radii of microscopic magnetic particles carried by laminar flow in high gradient magnetic field (HGMF). The HGMF occurs when random paramagnetic or ferromagnetic spheres of diameter $\sim 100 \mu\text{m}$ are placed in an external uniform magnetic field.

In this research, the method used to model the system of fluid passing an assemblage of random spheres is called an effective medium treatment (EMT). In the EMT, the system of fluid and distributed spheres are replaced by a concentric sphere; a representative solid sphere enclosed by a fluid shell, embedded in an effective medium as described in detail in Section 4.1. The velocity flow fields in the effective medium (\vec{v}_2) and the fluid shell (\vec{v}_1) were determined by using Green's theorem as shown in Chapter 4. The results are Equations (4.22) and (4.29), respectively, with the constants in the expression of fluid velocity given by Equations (4.36a)-(4.36d). These equations are so complicated and impractical to apply in further research. Therefore, the approximate solutions for dilute sphere packing $\gamma^3 < 0.1$ are evaluated to reduce its complication by omitting some insignificant terms. The velocity fields in closed form, \vec{v}_{2l} and \vec{v}_{1l} , are obtained as shown in Equations (4.46) and (4.45). For the other range of packing fraction, the curve fitting was used to represent the constants A , B , C and D whose numerical values are shown in Table 4.2. The velocity fields for this case are \vec{v}_{2h} and \vec{v}_{1h} as shown in Equations (4.50) and (4.48) with the curve fitting results of these constants given by Equations (4.47a)-(4.47d).

The most successful model to determine laminar velocity profiles in an assemblage of random spheres is the free surface model due to Happel. In Happel theory, the cell model was used similar to a concentric composite sphere in the EMT model. However, the outside surface of each cell in the free surface model was assumed to be frictionless and prohibit fluid interchange between the cells. To ensure the accuracy of our results, the comparison of the streamlines obtained in this research with those of Happel flow fields, Equation (3.23), which successfully predicted the pressure drop experimental data, was shown in Figures 4.7-4.18.

The streamlines that begin at some point on the outer surface of the fluid shell will end on the outer surface at the same point too. At low packing fraction ($\gamma^3 < 0.1$), the streamlines of EMT flow fields are quite similar to the Happel flow fields. The streamlines of EMT for this case, tend to leave the inner sphere compared with Happel's results, especially for the region near the solid sphere. For higher packing fraction ($\gamma^3 > 0.1$), the streamlines of EMT flow fields are closer to the inner sphere than those of Happel for all positions in the fluid shell.

Furthermore, the EMT velocity fields obtained in this research was applied to study the capture of magnetic particles carried by the laminar flow in high gradient magnetic fields. The trajectories of magnetic particles are determined by using Mathematica program and shown in Figures 5.1-5.6. The capture radii (r_c) as a function of γ were compared with the previous results based on Happel's theory [9] as shown in Figures 5.7 and 5.8 for paramagnetic particles and diamagnetic particles, respectively. The general features of the variation of r_c with γ for the EMT and Happel flow fields are very similar. We find the maximum value of r_c at $\gamma \approx 0.2$ for both in the transverse design for paramagnetic particles and in the longitudinal design for diamagnetic particles. For other cases, r_c is maximum at γ approaching to zero and decreases for increasing γ . For all cases we studied, the EMT results for r_c at $\gamma > 0.4$ are lower than the corresponding Happel model results. This is because the calculation of r_c by Happel model assumed the flow field outside the fluid shell to be uniform (\vec{v}_0), which allows magnetic particles to arrive at the outer shell surface with a greater velocity in the

radial inward captured direction. This resulted in a larger value of r_c than those obtained from this study. Comparison of the EMT radial velocity at the outer fluid shell calculated from Equation (4.22) with the previously used [9] $v_0 \cos\theta$ shows that the EMT radial velocity is smaller, especially for higher packing fractions, and the difference in r_c increases with increasing γ as seen in Figures 5.7 and 5.8.

In conclusion, Happel flow fields is less complicated and most accepted, with over hundreds of citation in current research papers [19]. For the EMT velocity fields in this research, with the less physical assumption the more complicated results are obtained. Thus, if the mathematical complication of the equation is not a problem, it is an alternative for application in some research problems, such as in the theory of magnetic filtration based on the EMT magnetic field, which the knowledge of the velocity fields outside the fluid shell is required and not given in Happel's theory. It is of interest that the EMT streamlines agree with Happel's theory, which gives good results for predicting pressure drop of experimental data. Therefore, EMT velocity fields may also be useful in the development of the application employed in fluid mechanics problems.



สถาบันวิทยบริการ
จุฬาลงกรณ์มหาวิทยาลัย

References

1. Toll, S. A solution technique for longitudinal Stokes flow around multiple aligned cylinders. J. Fluid Mech. 439 (2001): 199-216.
2. Nakanishi, M.; Kida, T.; and Nakajima, T. Asymptotic solutions for two dimensional low Reynolds number flow around an impulsively started circular cylinder. J. Fluid Mech. 334 (1997): 31-59.
3. Cheng, H.; and Papanicolaou, G. Flow past periodic arrays of spheres at low Reynolds number. J. Fluid Mech. 335 (1997): 189-212.
4. Shame, I. H. Mechanics of fluids. 2nd ed. New York: McGraw-Hill, 1985.
5. Umnova, O.; Attenborough, K.; and Li, K. M. A cell model for the acoustical properties of packing of spheres. Acustica. 87 (2001): 226-235.
6. Wei, Y. K.; and Keh, H. J. Diffusiophoresis and electrophoresis in concentrated suspensions of charged colloidal spheres. Langmuir. 17 (2001): 1437-1447.
7. Chen, S. K.; and Yang, C. Y. Boundary and concentration effects on sedimentation of a liquid aerosol dispersion. Journal of the Chinese Institute of Chemical Engineers. 31 (2000): 545-560.
8. Tu, H. J.; and Keh, H. J. Some solutions of a cell model for a suspension of spherical vesicles in osmophoresis. Colloids and Surfaces B-Biointerfaces. 20 (2001): 177-187.
9. Happel, J. Viscous flow in multiparticle system: Slow motion of fluid relative to beds of spherical particles. AIChE J. 4 (1958): 197-201.
10. Balanis, C. A. Advanced engineering electromagnetics. New York: John Wiley & Sons, 1989.
11. Jackson, J. D. Classical electrodynamics. 3rd ed. New York: John Wiley & Sons, 1999.
12. Hassani, S. Mathematical physics: A modern introduction to its foundations. New York: Springer-Verlag, 1999.
13. Lamb, H. Hydrodynamics. 6th ed. Cambridge Univ. Press, 1932. Cited in Happel, J. Viscous flow in multiparticle system: Slow motion of fluids relative to beds of spherical particles. AIChE J. 4 (1958): 197-201.

14. Natenapit, M. Effective medium treatment of laminar flow in magnetic filtration. J. Appl. Phys. 78 (1995): 4353-4359.
15. Wolfram, S. The mathematica book. 4th ed. Champaign: Wolfram Media, 1999.
16. Spiegel, M. R.; and Liu, J. Mathematical handbook of formulas and tables. 2nd ed. Singapore: McGraw-Hill, 1999.
17. Moyer, C.; Natenapit, M.; and Arajs, S. Magnetic filtration of particles in laminar flow through a bed of spheres. J. Magn. Mater. 44 (1984): 99-104. Cited in Natenapit, M. Effective medium treatment of laminar flow in magnetic filtration. J. Appl. Phys. 78 (1995): 4353-4359.
18. Friedlaender, F. J.; Takayasu, M.; Nakan, T.; and McNeese, W. H. IEEE Trans. Magn. 15 (1979): 1526. Cited in Natenapit, M. Effective medium treatment of laminar flow in magnetic filtration. J. Appl. Phys. 78 (1995): 4353-4359.
19. Center of Academic Resources Chulalongkorn University. CU Reference databases [Online]. Institute for Scientific Information, 2003. Available from: [http://isinew.car.chula.ac.th/WoS/CIW.cgi\[2003](http://isinew.car.chula.ac.th/WoS/CIW.cgi[2003), March 23]



APPENDICES

สถาบันวิทยบริการ
จุฬาลงกรณ์มหาวิทยาลัย

Appendix A

Solution for the constants A, B, C, D and δ

This appendix shows the determination of the constants in Equations (4.30) and (4.31).

■ Set M1 to be a square matrix in equation (4.30) .

$$M1 = \left\{ \left\{ \frac{-(1-\gamma^5)}{10\gamma^2}, \frac{\gamma(1-\gamma^2)}{2} \right\}, \left\{ \frac{(1-\gamma^2)}{2\gamma^2}, -2(1-\gamma) \right\} \right\}$$

$$\left\{ \left\{ -\frac{1-\gamma^5}{10\gamma^2}, \frac{1}{2}\gamma(1-\gamma^2) \right\}, \left\{ \frac{1-\gamma^2}{2\gamma^2}, -2(1-\gamma) \right\} \right\}$$

■ The matrix multiplication of M1 and column matrix of the constants A and B set equal to matrix M2. Thus,

M2 is a column matrix of the constants C and D (see equation (4.30)) .

$$M2 = M1 \cdot \{A\}, \{B\}$$

$$\left\{ \left\{ \frac{1}{2} B\gamma(1-\gamma^2) - \frac{A(1-\gamma^5)}{10\gamma^2} \right\}, \left\{ -2B(1-\gamma) + \frac{A(1-\gamma^2)}{2\gamma^2} \right\} \right\}$$

■ Matrix M3 is the first term in the left hand side of equation (4.31) . It is the matrix multiplication of square matrix and matrix of constants A and B.

$$M3 = \left\{ \left\{ \frac{3\gamma - 2 - \gamma^3}{6\gamma^2(1-\gamma)}, \frac{\gamma(5\gamma^2 - 2\gamma^5 - 3)}{6(1-\gamma^5)} \right\}, \left\{ \frac{1+\gamma+\gamma^2}{3\gamma^2}, \frac{\gamma(9-10\gamma^2+\gamma^5)}{3(1-\gamma^5)} \right\} \right\} \cdot \{A\}, \{B\}$$

$$\left\{ \left\{ \frac{A(-2+3\gamma-\gamma^3)}{6(1-\gamma)\gamma^2} + \frac{B\gamma(-3+5\gamma^2-2\gamma^5)}{6(1-\gamma^5)} \right\}, \left\{ \frac{A(1+\gamma+\gamma^2)}{3\gamma^2} + \frac{B\gamma(9-10\gamma^2+\gamma^5)}{3(1-\gamma^5)} \right\} \right\}$$

■ Matrix M4 is the second term in the left hand side of equation (4.31) . It is the matrix multiplication of square matrix and matrix of constants C and D.

$$M4 = \left\{ \left\{ \frac{6\gamma^5 - 1}{3(1-\gamma^5)} + 2\delta, \frac{-\gamma}{3(1-\gamma)} - \frac{\delta}{2} \right\}, \left\{ \frac{-4(2+3\gamma^5)}{3(1-\gamma^5)} - 4\delta, \frac{-2\gamma}{3(1-\gamma)} - \frac{\delta}{2} \right\} \right\}$$

$$\left\{ \left\{ \frac{1}{2} B\gamma(1-\gamma^2) - \frac{A(1-\gamma^5)}{10\gamma^2} \right\}, \left\{ -2B(1-\gamma) + \frac{A(1-\gamma^2)}{2\gamma^2} \right\} \right\}$$

$$\left\{ \left\{ \left(-2B(1-\gamma) + \frac{A(1-\gamma^2)}{2\gamma^2} \right) \left(-\frac{\gamma}{3(1-\gamma)} - \frac{\delta}{2} \right) + \left(\frac{1}{2} B\gamma(1-\gamma^2) - \frac{A(1-\gamma^5)}{10\gamma^2} \right) \left(\frac{-1+6\gamma^5}{3(1-\gamma^5)} + 2\delta \right) \right\}, \right. \\ \left. \left\{ \left(\frac{1}{2} B\gamma(1-\gamma^2) - \frac{A(1-\gamma^5)}{10\gamma^2} \right) \left(-\frac{4(2+3\gamma^5)}{3(1-\gamma^5)} - 4\delta \right) + \left(-2B(1-\gamma) + \frac{A(1-\gamma^2)}{2\gamma^2} \right) \left(-\frac{2\gamma}{3(1-\gamma)} - \frac{\delta}{2} \right) \right\} \right\}$$

■ Set matrices M3 plus M4 equal to M5,
which is the left hand side of equation (4.31).

$$M5 = M3 + M4$$

$$\left\{ \left\{ \frac{A(-2+3\gamma-\gamma^3)}{6(1-\gamma)\gamma^2} + \frac{B\gamma(-3+5\gamma^2-2\gamma^5)}{6(1-\gamma^5)} + \left(-2B(1-\gamma) + \frac{A(1-\gamma^2)}{2\gamma^2} \right) \left(-\frac{\gamma}{3(1-\gamma)} - \frac{\delta}{2} \right) + \left(\frac{1}{2} B\gamma(1-\gamma^2) - \frac{A(1-\gamma^5)}{10\gamma^2} \right) \left(\frac{-1+6\gamma^5}{3(1-\gamma^5)} + 2\delta \right) \right\}, \right. \\ \left. \left\{ \frac{A(1+\gamma+\gamma^2)}{3\gamma^2} + \frac{B\gamma(9-10\gamma^2+\gamma^5)}{3(1-\gamma^5)} + \left(\frac{1}{2} B\gamma(1-\gamma^2) - \frac{A(1-\gamma^5)}{10\gamma^2} \right) \left(-\frac{4(2+3\gamma^5)}{3(1-\gamma^5)} - 4\delta \right) + \left(-2B(1-\gamma) + \frac{A(1-\gamma^2)}{2\gamma^2} \right) \left(-\frac{2\gamma}{3(1-\gamma)} - \frac{\delta}{2} \right) \right\} \right\}$$

■ Substitute the constant B into matrix M5 and set to be M6. The constant B obtained from Happel's results [9].

$$M6 = M5 / \left\{ B \rightarrow \frac{-(3+2\gamma^5)}{2-3\gamma+3\gamma^5-2\gamma^6} \right\}$$

$$\left\{ \left\{ \frac{A(-2+3\gamma-\gamma^3)}{6(1-\gamma)\gamma^2} - \frac{\gamma(-3+5\gamma^2-2\gamma^5)(3+2\gamma^5)}{6(1-\gamma^5)(2-3\gamma+3\gamma^5-2\gamma^6)} + \left(\frac{A(1-\gamma^2)}{2\gamma^2} + \frac{2(1-\gamma)(3+2\gamma^5)}{2-3\gamma+3\gamma^5-2\gamma^6} \right) \left(-\frac{\gamma}{3(1-\gamma)} - \frac{\delta}{2} \right) + \left(\frac{A(1-\gamma^5)}{10\gamma^2} - \frac{\gamma(1-\gamma^2)(3+2\gamma^5)}{2(2-3\gamma+3\gamma^5-2\gamma^6)} \right) \left(\frac{-1+6\gamma^5}{3(1-\gamma^5)} + 2\delta \right) \right\}, \right. \\ \left. \left\{ \frac{A(1+\gamma+\gamma^2)}{3\gamma^2} - \frac{\gamma(9-10\gamma^2+\gamma^5)(3+2\gamma^5)}{3(1-\gamma^5)(2-3\gamma+3\gamma^5-2\gamma^6)} + \left(\frac{A(1-\gamma^5)}{10\gamma^2} - \frac{\gamma(1-\gamma^2)(3+2\gamma^5)}{2(2-3\gamma+3\gamma^5-2\gamma^6)} \right) \left(-\frac{4(2+3\gamma^5)}{3(1-\gamma^5)} - 4\delta \right) + \left(\frac{A(1-\gamma^2)}{2\gamma^2} + \frac{2(1-\gamma)(3+2\gamma^5)}{2-3\gamma+3\gamma^5-2\gamma^6} \right) \left(-\frac{2\gamma}{3(1-\gamma)} - \frac{\delta}{2} \right) \right\} \right\}$$

The matrix M6 is a left hand side of equation (4.31), which is a column matrix. Now, we have two equations obtained from equality of two column matrices in equation (4.31);

upper element and lower element.

■ Set Q1 to be the upper element of matrix M6.

$$\begin{aligned}
 Q1 = & \frac{A(-2+3\gamma-\gamma^3)}{6(1-\gamma)\gamma^2} - \frac{\gamma(-3+5\gamma^2-2\gamma^5)(3+2\gamma^5)}{6(1-\gamma^5)(2-3\gamma+3\gamma^5-2\gamma^6)} + \\
 & \left(\frac{A(1-\gamma^2)}{2\gamma^2} + \frac{2(1-\gamma)(3+2\gamma^5)}{2-3\gamma+3\gamma^5-2\gamma^6} \right) \left(-\frac{\gamma}{3(1-\gamma)} - \frac{\delta}{2} \right) + \\
 & \left(-\frac{A(1-\gamma^5)}{10\gamma^2} - \frac{\gamma(1-\gamma^2)(3+2\gamma^5)}{2(2-3\gamma+3\gamma^5-2\gamma^6)} \right) \left(\frac{-1+6\gamma^5}{3(1-\gamma^5)} + 2\delta \right) \\
 A(-2+3\gamma-\gamma^3) & - \frac{\gamma(-3+5\gamma^2-2\gamma^5)(3+2\gamma^5)}{6(1-\gamma^5)(2-3\gamma+3\gamma^5-2\gamma^6)} + \\
 \left(\frac{A(1-\gamma^2)}{2\gamma^2} + \frac{2(1-\gamma)(3+2\gamma^5)}{2-3\gamma+3\gamma^5-2\gamma^6} \right) & \left(-\frac{\gamma}{3(1-\gamma)} - \frac{\delta}{2} \right) + \\
 \left(-\frac{A(1-\gamma^5)}{10\gamma^2} - \frac{\gamma(1-\gamma^2)(3+2\gamma^5)}{2(2-3\gamma+3\gamma^5-2\gamma^6)} \right) & \left(\frac{-1+6\gamma^5}{3(1-\gamma^5)} + 2\delta \right)
 \end{aligned}$$

■ Set the upper element of the left hand side column matrix equal to the upper element on the right hand side in equation (4.31) and solve for the constant A. The answer represent the constant A as a function of γ and δ .

$$\text{Solve} \left[\left\{ Q1 = -\frac{3\delta}{2} \right\}, \{A\} \right]$$

$$\begin{aligned}
 \left\{ A \rightarrow - \left[\frac{\gamma(-3+5\gamma^2-2\gamma^5)(3+2\gamma^5)}{6(1-\gamma^5)(2-3\gamma+3\gamma^5-2\gamma^6)} + \right. \right. \\
 \left. \frac{2(1-\gamma)(3+2\gamma^5) \left(-\frac{\gamma}{3(1-\gamma)} - \frac{\delta}{2} \right)}{2-3\gamma+3\gamma^5-2\gamma^6} + \frac{3\delta}{2} - \frac{\gamma(1-\gamma^2)(3+2\gamma^5) \left(\frac{-1+6\gamma^5}{3(1-\gamma^5)} + 2\delta \right)}{2(2-3\gamma+3\gamma^5-2\gamma^6)} \right] \right. \\
 \left. \left(-\frac{2+3\gamma-\gamma^3}{6(1-\gamma)\gamma^2} + \frac{(1-\gamma^2) \left(-\frac{\gamma}{3(1-\gamma)} - \frac{\delta}{2} \right)}{2\gamma^2} - \frac{(1-\gamma^5) \left(\frac{-1+6\gamma^5}{3(1-\gamma^5)} + 2\delta \right)}{10\gamma^2} \right) \right\}
 \end{aligned}$$

■ Set Q2 to be the lower element of matrix M6.

$$\begin{aligned}
 Q2 = & \frac{A(1+\gamma+\gamma^2)}{3\gamma^2} - \frac{\gamma(9-10\gamma^2+\gamma^5)(3+2\gamma^5)}{3(1-\gamma^5)(2-3\gamma+3\gamma^5-2\gamma^6)} + \\
 & \left(-\frac{A(1-\gamma^5)}{10\gamma^2} - \frac{\gamma(1-\gamma^2)(3+2\gamma^5)}{2(2-3\gamma+3\gamma^5-2\gamma^6)} \right) \left(-\frac{4(2+3\gamma^5)}{3(1-\gamma^5)} - 4\delta \right) + \\
 & \left(\frac{A(1-\gamma^2)}{2\gamma^2} + \frac{2(1-\gamma)(3+2\gamma^5)}{2-3\gamma+3\gamma^5-2\gamma^6} \right) \left(-\frac{2\gamma}{3(1-\gamma)} - \frac{\delta}{2} \right)
 \end{aligned}$$

$$\frac{A(1+\gamma+\gamma^2)}{3\gamma^2} - \frac{\gamma(9-10\gamma^2+\gamma^5)(3+2\gamma^5)}{3(1-\gamma^5)(2-3\gamma+3\gamma^5-2\gamma^6)} +$$

$$\left(\frac{A(1-\gamma^5)}{10\gamma^2} - \frac{\gamma(1-\gamma^2)(3+2\gamma^5)}{2(2-3\gamma+3\gamma^5-2\gamma^6)} \right) \left(-\frac{4(2+3\gamma^5)}{3(1-\gamma^5)} - 4\delta \right) +$$

$$\left(\frac{A(1-\gamma^2)}{2\gamma^2} + \frac{2(1-\gamma)(3+2\gamma^5)}{2-3\gamma+3\gamma^5-2\gamma^6} \right) \left(-\frac{2\gamma}{3(1-\gamma)} - 2\delta \right)$$

■ Substitute the constant A obtained in the previous result, to the lower element of matrix M6 (Q2) and set to be Q3.

Q3 =

Q2 / .

{A ->

$$\frac{\gamma(-3+5\gamma^2-2\gamma^5)(3+2\gamma^5)}{6(1-\gamma^5)(2-3\gamma+3\gamma^5-2\gamma^6)} + \frac{2(1-\gamma)(3+2\gamma^5)\left(-\frac{\gamma}{3(1-\gamma)} - 2\delta\right)}{2-3\gamma+3\gamma^5-2\gamma^6} + \frac{3\delta}{2} - \frac{\gamma(1-\gamma^2)(3+2\gamma^5)\left(\frac{-1+6\gamma^5}{3(1-\gamma^5)} + 2\delta\right)}{2(2-3\gamma+3\gamma^5-2\gamma^6)}$$

$$\frac{-2+3\gamma-\gamma^3}{6(1-\gamma)\gamma^2} + \frac{(1-\gamma^2)\left(-\frac{\gamma}{3(1-\gamma)} - 2\delta\right)}{2\gamma^2} - \frac{(1-\gamma^5)\left(\frac{-1+6\gamma^5}{3(1-\gamma^5)} + 2\delta\right)}{10\gamma^2}$$

สถาบันวิทยบริการ
จุฬาลงกรณ์มหาวิทยาลัย

$$\begin{aligned}
& \frac{\gamma (9 - 10\gamma^2 + \gamma^5) (3 + 2\gamma^5)}{3(1 - \gamma^5) (2 - 3\gamma + 3\gamma^5 - 2\gamma^6)} \\
& \left((1 + \gamma + \gamma^2) \left(-\frac{\gamma (-3 + 5\gamma^2 - 2\gamma^5) (3 + 2\gamma^5)}{6(1 - \gamma^5) (2 - 3\gamma + 3\gamma^5 - 2\gamma^6)} + \frac{2(1 - \gamma) (3 + 2\gamma^5) \left(-\frac{\gamma}{3(1 - \gamma)} - \frac{\delta}{2} \right)}{2 - 3\gamma + 3\gamma^5 - 2\gamma^6} \right) \right. \\
& \quad \left. \frac{3\delta}{2} \frac{\gamma (1 - \gamma^2) (3 + 2\gamma^5) \left(\frac{-1 + 6\gamma^5}{3(1 - \gamma^5)} + 2\delta \right)}{2(2 - 3\gamma + 3\gamma^5 - 2\gamma^6)} \right) / \\
& \left(3\gamma^2 \left(\frac{-2 + 3\gamma - \gamma^3}{6(1 - \gamma)\gamma^2} + \frac{(1 - \gamma^2) \left(-\frac{\gamma}{3(1 - \gamma)} - \frac{\delta}{2} \right)}{2\gamma^2} - \frac{(1 - \gamma^5) \left(\frac{-1 + 6\gamma^5}{3(1 - \gamma^5)} + 2\delta \right)}{10\gamma^2} \right) \right) + \\
& \left(-\frac{2\gamma}{3(1 - \gamma)} - \frac{\delta}{2} \right) \left(\frac{2(1 - \gamma) (3 + 2\gamma^5)}{2 - 3\gamma + 3\gamma^5 - 2\gamma^6} - \right. \\
& \left. (1 - \gamma^2) \left(-\frac{\gamma (-3 + 5\gamma^2 - 2\gamma^5) (3 + 2\gamma^5)}{6(1 - \gamma^5) (2 - 3\gamma + 3\gamma^5 - 2\gamma^6)} + \frac{2(1 - \gamma) (3 + 2\gamma^5) \left(-\frac{\gamma}{3(1 - \gamma)} - \frac{\delta}{2} \right)}{2 - 3\gamma + 3\gamma^5 - 2\gamma^6} \right) \right. \\
& \quad \left. \frac{3\delta}{2} \frac{\gamma (1 - \gamma^2) (3 + 2\gamma^5) \left(\frac{-1 + 6\gamma^5}{3(1 - \gamma^5)} + 2\delta \right)}{2(2 - 3\gamma + 3\gamma^5 - 2\gamma^6)} \right) / \\
& \left(2\gamma^2 \left(\frac{-2 + 3\gamma - \gamma^3}{6(1 - \gamma)\gamma^2} + \frac{(1 - \gamma^2) \left(-\frac{\gamma}{3(1 - \gamma)} - \frac{\delta}{2} \right)}{2\gamma^2} - \frac{(1 - \gamma^5) \left(\frac{-1 + 6\gamma^5}{3(1 - \gamma^5)} + 2\delta \right)}{10\gamma^2} \right) \right) + \\
& \left(-\frac{4(2 + 3\gamma^5)}{3(1 - \gamma^5)} - 4\delta \right) \left(-\frac{\gamma (1 - \gamma^2) (3 + 2\gamma^5)}{2(2 - 3\gamma + 3\gamma^5 - 2\gamma^6)} + \right. \\
& \left. (1 - \gamma^5) \left(-\frac{\gamma (-3 + 5\gamma^2 - 2\gamma^5) (3 + 2\gamma^5)}{6(1 - \gamma^5) (2 - 3\gamma + 3\gamma^5 - 2\gamma^6)} + \frac{2(1 - \gamma) (3 + 2\gamma^5) \left(-\frac{\gamma}{3(1 - \gamma)} - \frac{\delta}{2} \right)}{2 - 3\gamma + 3\gamma^5 - 2\gamma^6} \right) \right. \\
& \quad \left. \frac{3\delta}{2} \frac{\gamma (1 - \gamma^2) (3 + 2\gamma^5) \left(\frac{-1 + 6\gamma^5}{3(1 - \gamma^5)} + 2\delta \right)}{2(2 - 3\gamma + 3\gamma^5 - 2\gamma^6)} \right) / \\
& \left(10\gamma^2 \left(\frac{-2 + 3\gamma - \gamma^3}{6(1 - \gamma)\gamma^2} + \frac{(1 - \gamma^2) \left(-\frac{\gamma}{3(1 - \gamma)} - \frac{\delta}{2} \right)}{2\gamma^2} - \frac{(1 - \gamma^5) \left(\frac{-1 + 6\gamma^5}{3(1 - \gamma^5)} + 2\delta \right)}{10\gamma^2} \right) \right)
\end{aligned}$$

■ Set the lower element of the left hand side column matrix equal to the lower element on right hand side in equation (4.31) and solve for δ . This give two solutions of δ . By investigate with previous research [14], the results indicate that the first solution is a justifiably answer. Thus, we use first answer as shown in equation (4.36 e).

$$\text{Solve}[\{Q3 == \frac{-3\delta}{2}\}, \{\delta\}]$$

$$\left\{ \left\{ \delta \rightarrow \left(\frac{36 - 30\gamma^2 + 18\gamma^5 - 20\gamma^7 - 4\gamma^{10} - 2\sqrt{3}(-3 + 3\gamma - 2\gamma^5 + 2\gamma^6)}{\sqrt{18 + 36\gamma + 14\gamma^2 - 8\gamma^3 - 5\gamma^4 + 2\gamma^5 + 9\gamma^6 + 6\gamma^7 + 3\gamma^8}} \right) / \right. \right. \\ \left. \left. (2(9 - 30\gamma^2 + 25\gamma^4 + 12\gamma^5 - 20\gamma^7 + 4\gamma^{10})) \right\}, \right. \\ \left. \left\{ \delta \rightarrow \left(\frac{36 - 30\gamma^2 + 18\gamma^5 - 20\gamma^7 - 4\gamma^{10} + 2\sqrt{3}(-3 + 3\gamma - 2\gamma^5 + 2\gamma^6)}{\sqrt{18 + 36\gamma + 14\gamma^2 - 8\gamma^3 - 5\gamma^4 + 2\gamma^5 + 9\gamma^6 + 6\gamma^7 + 3\gamma^8}} \right) / \right. \right. \\ \left. \left. (2(9 - 30\gamma^2 + 25\gamma^4 + 12\gamma^5 - 20\gamma^7 + 4\gamma^{10})) \right\} \right\}$$

■ Let Q4 equal to the constant A as a function of γ and δ .

$$Q4 = - \frac{\gamma(-3+5\gamma^2-2\gamma^5)(3+2\gamma^5)}{6(1-\gamma^5)(2-3\gamma+3\gamma^5-2\gamma^6)} + \frac{2(1-\gamma)(3+2\gamma^5)\left(-\frac{\gamma}{3(1-\gamma)} - \frac{\delta}{2}\right)}{2-3\gamma+3\gamma^5-2\gamma^6} + \frac{3\delta}{2} - \frac{\gamma(1-\gamma^2)(3+2\gamma^5)\left(\frac{-1+6\gamma^5}{3(1-\gamma^5)} + 2\delta\right)}{2(2-3\gamma+3\gamma^5-2\gamma^6)}$$

$$= - \frac{-2+3\gamma-\gamma^3}{6(1-\gamma)\gamma^2} + \frac{(1-\gamma^2)\left(-\frac{\gamma}{3(1-\gamma)} - \frac{\delta}{2}\right)}{2\gamma^2} - \frac{(1-\gamma^5)\left(\frac{-1+6\gamma^5}{3(1-\gamma^5)} + 2\delta\right)}{10\gamma^2}$$

$$= - \frac{\gamma(-3+5\gamma^2-2\gamma^5)(3+2\gamma^5)}{6(1-\gamma^5)(2-3\gamma+3\gamma^5-2\gamma^6)} + \frac{2(1-\gamma)(3+2\gamma^5)\left(-\frac{\gamma}{3(1-\gamma)} - \frac{\delta}{2}\right)}{2-3\gamma+3\gamma^5-2\gamma^6} + \frac{3\delta}{2} - \frac{\gamma(1-\gamma^2)(3+2\gamma^5)\left(\frac{-1+6\gamma^5}{3(1-\gamma^5)} + 2\delta\right)}{2(2-3\gamma+3\gamma^5-2\gamma^6)}$$

$$= - \frac{-2+3\gamma-\gamma^3}{6(1-\gamma)\gamma^2} + \frac{(1-\gamma^2)\left(-\frac{\gamma}{3(1-\gamma)} - \frac{\delta}{2}\right)}{2\gamma^2} - \frac{(1-\gamma^5)\left(\frac{-1+6\gamma^5}{3(1-\gamma^5)} + 2\delta\right)}{10\gamma^2}$$

■ Substitute δ into the constant A (Q4), obtain the solution of A as a function of γ .

$$Q41 =$$

$$Q4 / .$$

$$\{\delta \rightarrow$$

$$\left(\frac{36 - 30\gamma^2 + 18\gamma^5 - 20\gamma^7 - 4\gamma^{10} - 2\sqrt{3}(-3 + 3\gamma - 2\gamma^5 + 2\gamma^6)}{\sqrt{18 + 36\gamma + 14\gamma^2 - 8\gamma^3 - 5\gamma^4 + 2\gamma^5 + 9\gamma^6 + 6\gamma^7 + 3\gamma^8}} \right) / \\ (2(9 - 30\gamma^2 + 25\gamma^4 + 12\gamma^5 - 20\gamma^7 + 4\gamma^{10})) \}$$

$$\begin{aligned}
& \left(-\frac{\gamma(-3+5\gamma^2-2\gamma^5)(3+2\gamma^5)}{6(1-\gamma^5)(2-3\gamma+3\gamma^5-2\gamma^6)} + \right. \\
& \left. \left(3 \left(36-30\gamma^2+18\gamma^5-20\gamma^7-4\gamma^{10}-2\sqrt{3}(-3+3\gamma-2\gamma^5+2\gamma^6) \right. \right. \right. \\
& \left. \left. \left. \sqrt{18+36\gamma+14\gamma^2-8\gamma^3-5\gamma^4+2\gamma^5+9\gamma^6+6\gamma^7+3\gamma^8} \right) \right) \right) / \\
& (4(9-30\gamma^2+25\gamma^4+12\gamma^5-20\gamma^7+4\gamma^{10})) + \frac{1}{2-3\gamma+3\gamma^5-2\gamma^6} \\
& \left(2(1-\gamma)(3+2\gamma^5) \left(-\frac{\gamma}{3(1-\gamma)} - \left(36-30\gamma^2+18\gamma^5-20\gamma^7-4\gamma^{10}-2\sqrt{3}(-3+3\gamma \right. \right. \right. \\
& \left. \left. \left. \gamma-2\gamma^5+2\gamma^6) \sqrt{18+36\gamma+14\gamma^2-8\gamma^3-5\gamma^4+2\gamma^5+9\gamma^6+6\gamma^7+3\gamma^8} \right) \right) \right) / \\
& (4(9-30\gamma^2+25\gamma^4+12\gamma^5-20\gamma^7+4\gamma^{10})) \left. \right) - \frac{1}{2(2-3\gamma+3\gamma^5-2\gamma^6)} \\
& \left(\gamma(1-\gamma^2)(3+2\gamma^5) \left(\frac{-1+6\gamma^5}{3(1-\gamma^5)} + \left(36-30\gamma^2+18\gamma^5-20\gamma^7-4\gamma^{10}-2\sqrt{3}(-3+3\gamma \right. \right. \right. \\
& \left. \left. \left. \gamma-2\gamma^5+2\gamma^6) \sqrt{18+36\gamma+14\gamma^2-8\gamma^3-5\gamma^4+2\gamma^5+9\gamma^6+6\gamma^7+3\gamma^8} \right) \right) \right) / \\
& (9-30\gamma^2+25\gamma^4+12\gamma^5-20\gamma^7+4\gamma^{10}) \left. \right) \left. \right) / \left(\frac{-2+3\gamma-\gamma^3}{6(1-\gamma)\gamma^2} + \frac{1}{2\gamma^2} \right. \\
& \left. \left((1-\gamma^2) \left(-\frac{\gamma}{3(1-\gamma)} - \left(36-30\gamma^2+18\gamma^5-20\gamma^7-4\gamma^{10}-2\sqrt{3}(-3+3\gamma-2\gamma^5+2\gamma^6) \right. \right. \right. \right. \\
& \left. \left. \left. \sqrt{18+36\gamma+14\gamma^2-8\gamma^3-5\gamma^4+2\gamma^5+9\gamma^6+6\gamma^7+3\gamma^8} \right) \right) \right) / \\
& (4(9-30\gamma^2+25\gamma^4+12\gamma^5-20\gamma^7+4\gamma^{10})) \left. \right) \left. \right) - \frac{1}{10\gamma^2} \\
& \left((1-\gamma^5) \left(\frac{-1+6\gamma^5}{3(1-\gamma^5)} + \left(36-30\gamma^2+18\gamma^5-20\gamma^7-4\gamma^{10}-2\sqrt{3}(-3+3\gamma-2\gamma^5+2\gamma^6) \right. \right. \right. \right. \\
& \left. \left. \left. \sqrt{18+36\gamma+14\gamma^2-8\gamma^3-5\gamma^4+2\gamma^5+9\gamma^6+6\gamma^7+3\gamma^8} \right) \right) \right) / \\
& (9-30\gamma^2+25\gamma^4+12\gamma^5-20\gamma^7+4\gamma^{10}) \left. \right) \left. \right) \left. \right)
\end{aligned}$$

สถาบันวิทยบริการ
จุฬาลงกรณ์มหาวิทยาลัย

$$\begin{aligned}
& \frac{2(1-\gamma)(3+2\gamma^5)}{2-3\gamma+3\gamma^5-2\gamma^6} + \left(5\gamma(1-\gamma^2) \left(21\gamma^7 + 30\gamma^8 + 24\gamma^9 + 12\gamma^{10} + \right. \right. \\
& \quad \gamma^4 \left(21 - 2\sqrt{3} \sqrt{18+36\gamma+14\gamma^2-8\gamma^3-5\gamma^4+2\gamma^5+9\gamma^6+6\gamma^7+3\gamma^8} \right) + \\
& \quad 4\gamma^6 \left(3 + \sqrt{3} \sqrt{18+36\gamma+14\gamma^2-8\gamma^3-5\gamma^4+2\gamma^5+9\gamma^6+6\gamma^7+3\gamma^8} \right) + \\
& \quad 9 \left(6 + \sqrt{3} \sqrt{18+36\gamma+14\gamma^2-8\gamma^3-5\gamma^4+2\gamma^5+9\gamma^6+6\gamma^7+3\gamma^8} \right) + \\
& \quad 9\gamma \left(12 + \sqrt{3} \sqrt{18+36\gamma+14\gamma^2-8\gamma^3-5\gamma^4+2\gamma^5+9\gamma^6+6\gamma^7+3\gamma^8} \right) + \\
& \quad 3\gamma^3 \left(30 + \sqrt{3} \sqrt{18+36\gamma+14\gamma^2-8\gamma^3-5\gamma^4+2\gamma^5+9\gamma^6+6\gamma^7+3\gamma^8} \right) + \\
& \quad \left. \left. \left. \left. \left. 3\gamma^2 \left(33 + \sqrt{3} \sqrt{18+36\gamma+14\gamma^2-8\gamma^3-5\gamma^4+2\gamma^5+9\gamma^6+6\gamma^7+3\gamma^8} \right) + \right. \right. \right. \right. \\
& \quad \left. \left. \left. \left. \left. \left. \left. \left. \left. \left. \left. \gamma^5 \left(-21 + 4\sqrt{3} \sqrt{18+36\gamma+14\gamma^2-8\gamma^3-5\gamma^4+2\gamma^5+9\gamma^6+6\gamma^7+3\gamma^8} \right) \right) \right) \right) \right) \right) \right) \right) \right) / \\
& \left((-1+\gamma)^3 (1+\gamma) (2+\gamma+2\gamma^2) \left(33\gamma^5 + 36\gamma^6 + 24\gamma^7 + 12\gamma^8 + \right. \right. \\
& \quad 9 \left(8 + \sqrt{3} \sqrt{18+36\gamma+14\gamma^2-8\gamma^3-5\gamma^4+2\gamma^5+9\gamma^6+6\gamma^7+3\gamma^8} \right) + \\
& \quad 9\gamma \left(16 + \sqrt{3} \sqrt{18+36\gamma+14\gamma^2-8\gamma^3-5\gamma^4+2\gamma^5+9\gamma^6+6\gamma^7+3\gamma^8} \right) + \\
& \quad \gamma^3 \left(18 + 4\sqrt{3} \sqrt{18+36\gamma+14\gamma^2-8\gamma^3-5\gamma^4+2\gamma^5+9\gamma^6+6\gamma^7+3\gamma^8} \right) + \\
& \quad \gamma^4 \left(30 + 4\sqrt{3} \sqrt{18+36\gamma+14\gamma^2-8\gamma^3-5\gamma^4+2\gamma^5+9\gamma^6+6\gamma^7+3\gamma^8} \right) + \\
& \quad \left. \left. \left. \left. \left. \left. \left. \left. \left. \left. \left. \gamma^2 \left(81 + 4\sqrt{3} \sqrt{18+36\gamma+14\gamma^2-8\gamma^3-5\gamma^4+2\gamma^5+9\gamma^6+6\gamma^7+3\gamma^8} \right) \right) \right) \right) \right) \right) \right) \right) \right) \right)
\end{aligned}$$



 สถาบันวิทยบริการ
 จุฬาลงกรณ์มหาวิทยาลัย

Appendix B

Curve Fitting of the Constants

The curve fitting presented here are polynomial fits of the constants A , B , C and D for varying γ from 0.46 to 0.84. The numerical values of these constants shown in Table 4.2 are obtained from Equations (4.36a)-(4.36d).

■ This gives a table of the data points (γ, A) .

```
Q1 = {{0.46, -1.3263133488145251}, {0.48, -1.6356461385855632},  
      {0.50, -2.015556331471041}, {0.52, -2.483724589999957},  
      {0.54, -3.0630653844891573}, {0.56, -3.7835749238236422},  
      {0.58, -4.684949871895356}, {0.60, -5.820353499371482},  
      {0.62, -7.261920091185831}, {0.64, -9.108943593532711},  
      {0.66, -11.500299711248235}, {0.68, -14.633702609549237},  
      {0.70, -18.796286303069426}, {0.72, -24.41450531830003},  
      {0.74, -32.138094179198205}, {0.76, -42.9863580397327},  
      {0.78, -58.613539164586896}, {0.80, -81.81328617701911},  
      {0.82, -117.53221794015806}, {0.84, -175.04606133285031}}  
{(0.46, -1.32631), (0.48, -1.63565), (0.5, -2.01556), (0.52, -2.48372),  
(0.54, -3.06307), (0.56, -3.78357), (0.58, -4.68495), (0.6, -5.82035),  
(0.62, -7.26192), (0.64, -9.10894), (0.66, -11.5003), (0.68, -14.6337),  
(0.7, -18.7963), (0.72, -24.4145), (0.74, -32.1381), (0.76, -42.9864),  
(0.78, -58.6135), (0.8, -81.8133), (0.82, -117.532), (0.84, -175.046)}
```

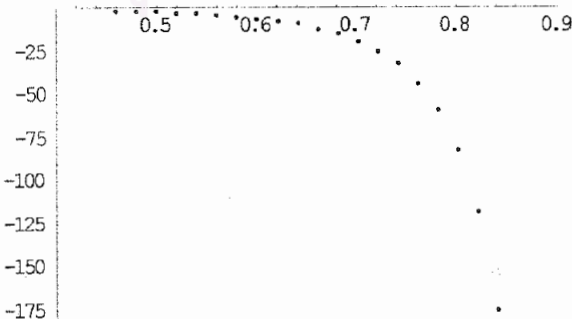
■ This gives a degree 5 polynomial fit to the above data. This answer shown in equation (4.47 a).

```
FA1 = Fit[Q1, {1, x, x^2, x^3, x^4, x^5}, x]
```

```
16832.1 - 142559. x + 479630. x^2 - 801664. x^3 + 666117. x^4 - 220400. x^5
```

■ Here is a plot of the data points (γ, A) .

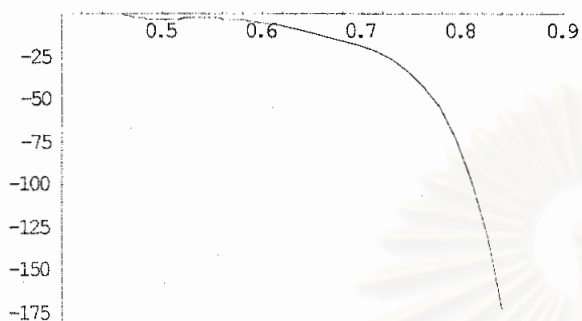
```
GA1 = ListPlot[Q1, PlotRange -> {{0.4, 0.9}, {-180, 0}}]
```



- Graphics -

■ Here is a plot of the fit of the data points (γ, A) .

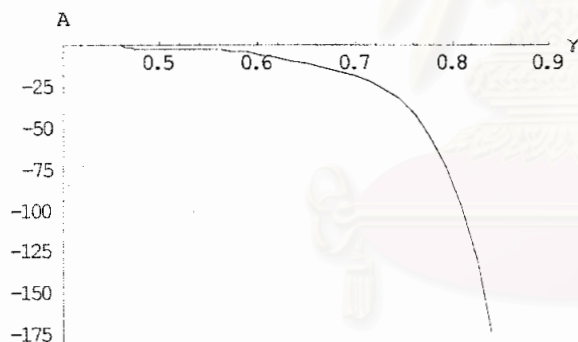
```
GA2 = Plot[FA1, {x, 0.46, 0.84}, PlotRange -> {{0.4, 0.9}, {-180, 0}}]
```



- Graphics -

■ Here is the fit superimposed on the original data (γ, A) , shown in figure 4.3.

```
GA3 = Show[GA1, GA2, AxesLabel -> {"\gamma", "A"}]
```



- Graphics -

สถาบันวิทยบริการ
จุฬาลงกรณ์มหาวิทยาลัย

■ This gives a table of the data points (γ , B).

```
Q2 = {{0.46, -4.5881226590347906`}, {0.48, -4.985392899078987`},
      {0.50, -5.444444444444444`}, {0.52, -5.978467046098359`},
      {0.54, -6.6042273746592635`}, {0.56, -7.343259599495289`},
      {0.58, -8.223531975702157`}, {0.60, -9.281814759036148`},
      {0.62, -10.567099769522867`}, {0.64, -12.145627613412298`},
      {0.66, -14.108425250196015`}, {0.68, -16.582856559144684`},
      {0.70, -19.75075779103909`}, {0.72, -23.877698721929946`},
      {0.74, -29.361671799838554`}, {0.76, -36.817002997211`},
      {0.78, -47.224924774741446`}, {0.80, -62.21677559912864`},
      {0.82, -84.6370148909241`}, {0.84, -119.73945527912402`}}
{{0.46, -4.58812}, {0.48, -4.98539}, {0.5, -5.44444}, {0.52, -5.97847},
 {0.54, -6.60423}, {0.56, -7.34326}, {0.58, -8.22353}, {0.6, -9.28181},
 {0.62, -10.5671}, {0.64, -12.1456}, {0.66, -14.1084}, {0.68, -16.5829},
 {0.7, -19.7508}, {0.72, -23.8777}, {0.74, -29.3617}, {0.76, -36.817},
 {0.78, -47.2249}, {0.8, -62.2168}, {0.82, -84.637}, {0.84, -119.739}}
```

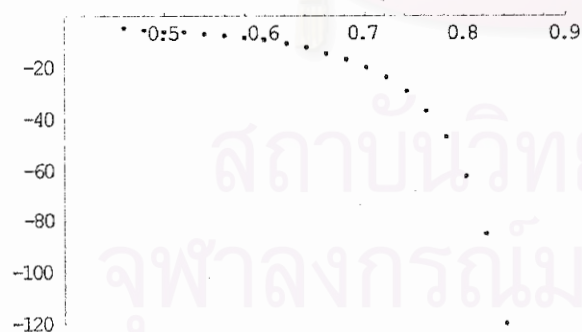
■ This gives a degree 5 polynomial fit to the data points (γ , B). This answer shown in equation (4.47 b).

```
FB1 = Fit[Q2, {1, x, x^2, x^3, x^4, x^5}, x]
```

```
9554.46 - 80995.3 x + 272728. x^2 - 456328. x^3 + 379657. x^4 - 125839. x^5
```

■ Here is a plot of the data points (γ , B).

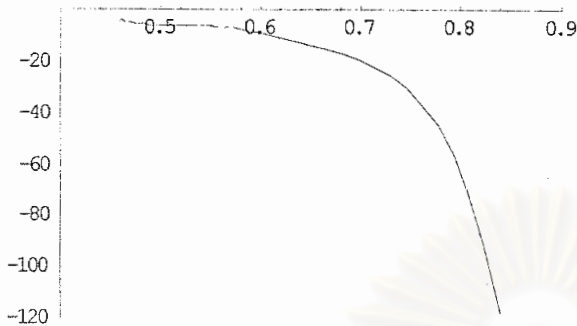
```
GB1 = ListPlot[Q2, PlotRange -> {{0.4, 0.9}, {-120, 0}}]
```



- Graphics -

■ Here is a plot of the fit of the data points (γ, B) .

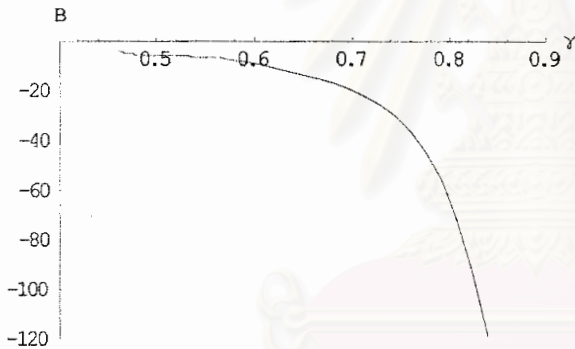
```
GB2 = Plot[FB1, {x, 0.46, 0.84}, PlotRange -> {{0.4, 0.9}, {-120, 0}}]
```



- Graphics -

■ Here is the fit superimposed on the original data (γ, B) , shown in figure 4.4.

```
GB3 = Show[GB1, GB2, AxesLabel -> {"\gamma", "B"}]
```



- Graphics -

■ This gives a table of the data points (γ, C) .

```
Q3 = {{0.46, -0.21808111189680723`}, {0.48, -0.2289950890462359`},
      {0.50, -0.23980525488830473`}, {0.52, -0.2504772390479748`},
      {0.54, -0.26097566896858315`}, {0.56, -0.27126427251730933`},
      {0.58, -0.2813060057604948`}, {0.60, -0.29106320838484234`},
      {0.62, -0.3004977890526046`}, {0.64, -0.3095714426702407`},
      {0.66, -0.3182459010970571`}, {0.68, -0.3264832181998787`},
      {0.70, -0.33424608935097666`}, {0.72, -0.3414982044531438`},
      {0.74, -0.3482046323503418`}, {0.76, -0.35433223304949735`},
      {0.78, -0.3598500925581387`}, {0.80, -0.3647299733786671`},
      {0.82, -0.3689467718520625`}, {0.84, -0.3724789717146013`}}
```

```
{ {0.46, -0.218081}, {0.48, -0.228995}, {0.5, -0.239805}, {0.52, -0.250477},
  {0.54, -0.260976}, {0.56, -0.271264}, {0.58, -0.281306}, {0.6, -0.291063},
  {0.62, -0.300498}, {0.64, -0.309571}, {0.66, -0.318246}, {0.68, -0.326483},
  {0.7, -0.334246}, {0.72, -0.341498}, {0.74, -0.348205}, {0.76, -0.354332},
  {0.78, -0.35985}, {0.8, -0.36473}, {0.82, -0.368947}, {0.84, -0.372479} }
```

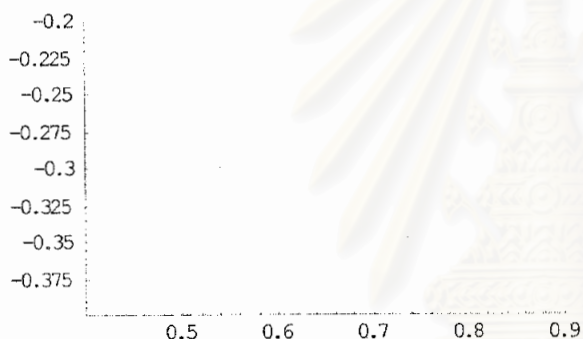
■ This gives a degree 3 polynomial fit to the data points (γ, C) . This answer shown in equation (4.47 c).

```
FC1 = Fit[Q3, {1, x, x^2, x^3}, x]
```

```
-0.0207887 - 0.149388 x - 0.954971 x^2 + 0.755306 x^3
```

■ Here is a plot of the data points (γ, C) .

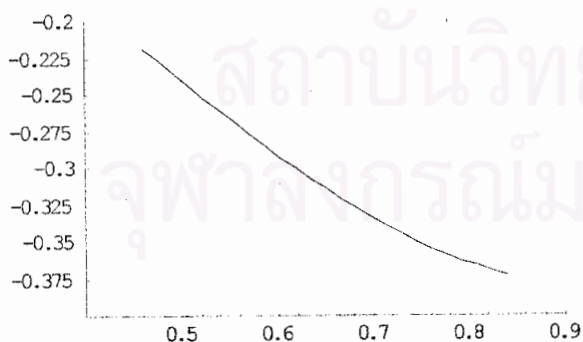
```
GC1 = ListPlot[Q3, PlotRange -> {{0.4, 0.9}, {-0.4, -0.2}}]
```



- Graphics -

■ Here is a plot of the fit of the data points (γ, C) .

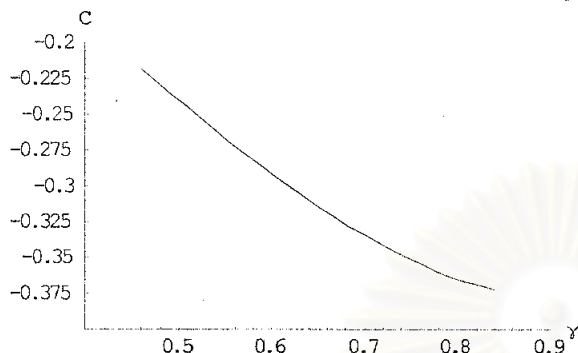
```
GC2 = Plot[FC1, {x, 0.46, 0.84}, PlotRange -> {{0.4, 0.9}, {-0.4, -0.2}}]
```



- Graphics -

■ Here is the fit superimposed on the original data (γ , C), shown in figure 4.5.

GC3 = Show[GC1, GC2, AxesLabel → {" γ ", "C"}]



- Graphics -

■ This gives a table of the data points (γ , D).

```
Q4 = {{0.46, 2.4843183975482837`}, {0.48, 2.453052390529454`},
      {0.50, 2.421109947237882`}, {0.52, 2.3885046570355484`},
      {0.54, 2.3552521504407764`}, {0.56, 2.321370380412124`},
      {0.58, 2.2868799169772105`}, {0.60, 2.2518042522320485`},
      {0.62, 2.216170111863918`}, {0.64, 2.1800077683490997`},
      {0.66, 2.1433513498526393`}, {0.68, 2.1062391376302063`},
      {0.70, 2.0687138434342582`}, {0.72, 2.0308228571074505`},
      {0.74, 1.992618453274277`}, {0.76, 1.9541579449086015`},
      {0.78, 1.9155037706658007`}, {0.80, 1.876723502364836`},
      {0.82, 1.8378897590106575`}, {0.84, 1.7990800144393333`}}
{{0.46, 2.48432}, {0.48, 2.45305}, {0.5, 2.42111}, {0.52, 2.3885},
 {0.54, 2.35525}, {0.56, 2.32137}, {0.58, 2.28688}, {0.6, 2.2518},
 {0.62, 2.21617}, {0.64, 2.18001}, {0.66, 2.14335}, {0.68, 2.10624},
 {0.7, 2.06871}, {0.72, 2.03082}, {0.74, 1.99262}, {0.76, 1.95416},
 {0.78, 1.9155}, {0.8, 1.87672}, {0.82, 1.83789}, {0.84, 1.79908}}
```

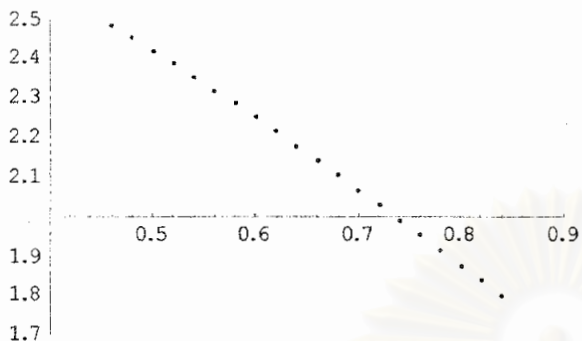
■ This gives a degree 3 polynomial fit to the data points (γ , D). This answer shown in equation (4.47 d).

FD1 = Fit[Q4, {1, x, x², x³}, x]

2.89074 - 0.0613565 x - 2.16837 x² + 0.826108 x³

■ Here is a plot of the data points (γ , D).

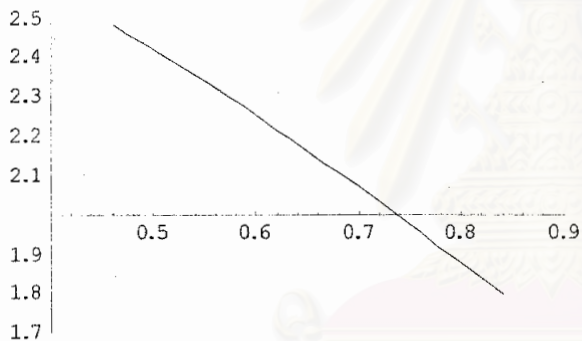
```
GD1 = ListPlot[Q4, PlotRange -> {{0.4, 0.9}, {1.7, 2.5}}]
```



- Graphics -

■ Here is a plot of the fit of the data points (γ , D).

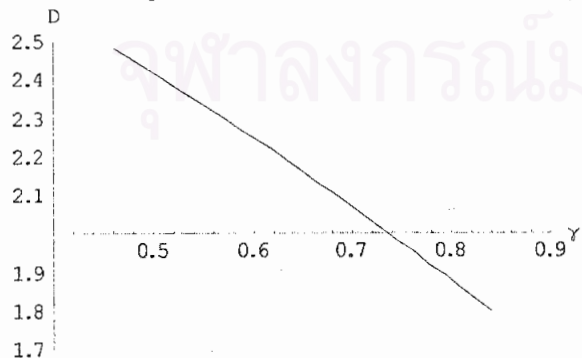
```
GD2 = Plot[FD1, {x, 0.46, 0.84}, PlotRange -> {{0.4, 0.9}, {1.7, 2.5}}]
```



- Graphics -

■ Here is the fit superimposed on the original data (γ , D), shown in figure 4.6.

```
GD3 = Show[GD1, GD2, AxesLabel -> {"gamma", "D"}]
```



- Graphics -

Appendix C

Particle Trajectories by Mathematica Program

The differential equations (5.4a), (5.4b), (5.5a) and (5.5b) have no explicit closed form solution. Thus, we find the numerical solutions in terms of InterpolatingFunction objects. The procedure below gives the solution for the trajectories of paramagnetic and diamagnetic particles in longitudinal and transverse mode design at $\gamma=0.1$.

■ Set $\frac{dr_a}{dt}$ in equation (5.5 a) and $\frac{d\theta}{dt}$ in equation (5.5 b) to be d1 and d2, respectively. This obtained from the velocity field in the fluid shell.

$$d1 = \frac{2V}{2-3\gamma} \left(1 - \frac{3}{2r[t]} + \frac{1}{2(r[t])^3} - \frac{3(\sqrt{6}-1)\gamma^3(r[t])^2}{10} \right) \text{Cos}[\theta[t]] - \frac{v^*}{2(r[t])^4} \left(1 + 3\text{Cos}[2\theta[t]] + K_s(5+3\text{Cos}[2\theta[t]]) \frac{1}{(r[t])^3} \right)$$

$$d2 = -\frac{2V}{(2-3\gamma)r[t]} \left(1 - \frac{3}{4r[t]} - \frac{1}{4(r[t])^3} - \frac{3(\sqrt{6}-1)\gamma^3(r[t])^2}{5} \right) \text{Sin}[\theta[t]] - \frac{v^*}{r[t]^5} \left(1 + \frac{K_s}{2(r[t])^3} \right) \text{Sin}[2\theta[t]]$$

$$\frac{2V\text{Cos}[\theta[t]] \left(1 + \frac{1}{2r[t]^3} - \frac{3}{2r[t]} - \frac{3(-1+\sqrt{6})\gamma^3 r[t]^2}{10} \right)}{2-3\gamma} - \frac{\left(1 + 3\text{Cos}[2\theta[t]] + \frac{(5+3\text{Cos}[2\theta[t]))K_s}{r[t]^3} \right) v^*}{2r[t]^4}$$

$$\frac{2V \left(1 - \frac{1}{4r[t]^3} - \frac{3}{4r[t]} - \frac{3(-1+\sqrt{6})\gamma^3 r[t]^2}{5} \right) \text{Sin}[\theta[t]]}{(2-3\gamma)r[t]} - \frac{\text{Sin}[2\theta[t]] \left(1 + \frac{K_s}{2r[t]^3} \right) v^*}{r[t]^5}$$

■ Set $\frac{dr_a}{dt}$ in equation (5.4 a) and $\frac{d\theta}{dt}$ in equation (5.4 b) to be d3 and d4, respectively. This obtained from the velocity field in the effective medium.

$$d3 = \frac{2V}{2-3\gamma} \left(1 - \frac{3(\sqrt{6}-2)}{4r[t]} - \frac{3(8-3\sqrt{6})}{20\gamma^2(r[t])^3} - \frac{3\gamma}{2} \right) \text{Cos}[\theta[t]]$$

$$d4 = -\frac{2V}{(2-3\gamma)r[t]} \left(1 - \frac{3(\sqrt{6}-2)}{8r[t]} + \frac{3(8-3\sqrt{6})}{40\gamma^2(r[t])^3} - \frac{3\gamma}{2} \right) \text{Sin}[\theta[t]]$$

$$\frac{2V\text{Cos}[\theta[t]] \left(1 - \frac{3\gamma}{2} - \frac{3(8-3\sqrt{6})}{20\gamma^2 r[t]^3} - \frac{3(-2+\sqrt{6})}{4r[t]} \right)}{2-3\gamma}$$

$$\frac{2V \left(1 - \frac{3\gamma}{2} + \frac{3(8-3\sqrt{6})}{40\gamma^2 r[t]^3} - \frac{3(-2+\sqrt{6})}{8r[t]} \right) \sin[\theta[t]]}{(2-3\gamma) r[t]}$$

■ Substitute the parameters for paramagnetic particle in longitudinal mode.

$$u11 = d1 /. \{V \rightarrow -6.65, \gamma \rightarrow 0.1, v^* \rightarrow 572.16, K_s \rightarrow 0.58\}$$

$$w11 = d2 /. \{V \rightarrow -6.65, \gamma \rightarrow 0.1, v^* \rightarrow 572.16, K_s \rightarrow 0.58\}$$

$$u12 = d3 /. \{V \rightarrow -6.65, \gamma \rightarrow 0.1\}$$

$$w12 = d4 /. \{V \rightarrow -6.65, \gamma \rightarrow 0.1\}$$

$$\frac{286.08 \left(1 + 3 \cos[2\theta[t]] + \frac{0.58(5+3\cos[2\theta[t]])}{r[t]^3} \right)}{r[t]^4}$$

$$7.82353 \cos[\theta[t]] \left(1 + \frac{1}{2r[t]^3} - \frac{3}{2r[t]} - 0.000434847 r[t]^2 \right)$$

$$\frac{7.82353 \left(1 - \frac{1}{4r[t]^3} - \frac{3}{4r[t]} - 0.000869694 r[t]^2 \right) \sin[\theta[t]]}{r[t]}$$

$$\frac{572.16 \left(1 + \frac{0.29}{r[t]^3} \right) \sin[2\theta[t]]}{r[t]^5}$$

$$-7.82353 \cos[\theta[t]] \left(0.85 - \frac{9.77296}{r[t]^3} - \frac{3(-2+\sqrt{6})}{4r[t]} \right)$$

$$\frac{7.82353 \left(0.85 + \frac{4.88648}{r[t]^3} - \frac{3(-2+\sqrt{6})}{8r[t]} \right) \sin[\theta[t]]}{r[t]}$$

สถาบันวิทยบริการ
จุฬาลงกรณ์มหาวิทยาลัย

■ This find solution for $r(t)$ and $\theta(t)$ as InterpolatingFunction objects. For $\gamma = 0.1$, the fluid shell radius is 10 a (set $a = 1$). Thus, using the velocity field in the effective medium or u_{l2} , w_{l2} for $r > 10$, and the velocity field in the fluid shell or u_{l1} , w_{l1} for $r < 10$. The conditions specify for captured magnetic particle.

n11 =

```
NDSolve[
  {r'[t] == If[r[t] < 10, -
    
$$\frac{286.08 (1 + 3 \cos[2\theta[t]] + \frac{0.58 (5 + 3 \cos[2\theta[t]])}{r[t]^3}}{r[t]^4} -$$

    
$$7.823529 \cos[\theta[t]] \left( 1 + \frac{1}{2 r[t]^3} - \frac{3}{2 r[t]} - 0.000435 r[t]^2 \right),$$

    
$$-7.823529 \cos[\theta[t]] \left( 0.85 - \frac{9.772962}{r[t]^3} - \frac{3(-2 + \sqrt{6})}{4 r[t]} \right)],$$

    
$$\theta'[t] == \text{If}[r[t] < 10, \frac{7.823529 \left( 1 - \frac{1}{4 r[t]^3} - \frac{3}{4 r[t]} - 0.000870 r[t]^2 \right) \sin[\theta[t]]}{r[t]} -$$

    
$$\frac{572.16 \left( 1 + \frac{0.29}{r[t]^3} \right) \sin[2\theta[t]]}{r[t]^5},$$

    
$$\frac{7.823529 \left( 0.85 + \frac{4.886481}{r[t]^3} - \frac{3(-2 + \sqrt{6})}{8 r[t]} \right) \sin[\theta[t]]}{r[t]}], r[0] == 12.469647,$$

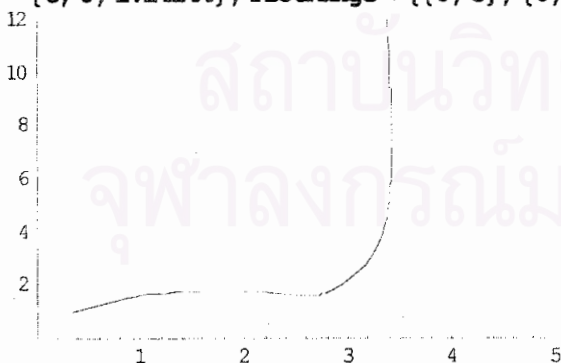
    
$$\theta[0] == 0.275325], \{r, \theta\}, \{t, 0, 2.2425\}]$$

```

{{r -> InterpolatingFunction[{{0., 2.2425}}, <>],
 θ -> InterpolatingFunction[{{0., 2.2425}}, <>]}}

■ This plots the solution obtained.

```
n12 = ParametricPlot[Evaluate[{r[t] Sin[ $\theta$ [t]], r[t] Cos[ $\theta$ [t]]} /. n11],
  {t, 0, 2.24244}, PlotRange -> {{0, 5}, {0, 12}}]
```



- Graphics -

- This find the solution for the trajectory of magnetic particle which don't move toward the solid sphere.

n13 =

```
NDSolve[
  {r'[t] == If[r[t] < 10, -
    
$$\frac{286.08 \left(1 + 3 \cos[2\theta[t]] + \frac{0.58(5+3\cos[2\theta[t]])}{r[t]^3}\right)}{r[t]^4} -$$

    
$$7.823529 \cos[\theta[t]] \left(1 + \frac{1}{2r[t]^3} - \frac{3}{2r[t]} - 0.000435 r[t]^2\right),$$

    
$$-7.823529 \cos[\theta[t]] \left(0.85 - \frac{9.772962}{r[t]^3} - \frac{3(-2+\sqrt{6})}{4r[t]}\right)],$$

    
$$\theta'[t] == If[r[t] < 10, \frac{7.823529 \left(1 - \frac{1}{4r[t]^3} - \frac{3}{4r[t]} - 0.000870 r[t]^2\right) \sin[\theta[t]]}{r[t]} -$$

    
$$\frac{572.16 \left(1 + \frac{0.29}{r[t]^3}\right) \sin[2\theta[t]]}{r[t]^5},$$

    
$$\frac{7.823529 \left(0.85 + \frac{4.886481}{r[t]^3} - \frac{3(-2+\sqrt{6})}{8r[t]}\right) \sin[\theta[t]]}{r[t]}], r[0] == 12.472369,$$

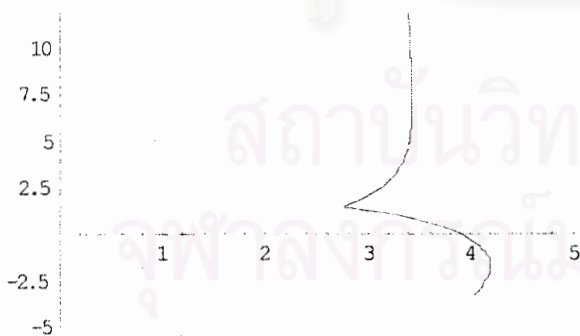
    
$$\theta[0] == 0.276097\}, \{r, \theta\}, \{t, 0, 3.5\}$$

  }, {r -> InterpolatingFunction[{{0., 3.5}}, <>],
    
$$\theta \rightarrow \text{InterpolatingFunction}[\{0., 3.5\}, \langle \rangle]}$$


```

- This plot the solution obtained.

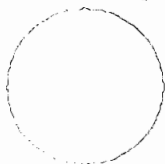
```
n14 = ParametricPlot[Evaluate[{r[t] Sin[θ[t]], r[t] Cos[θ[t]]} /. n13],
  {t, 0, 3.5}, PlotRange -> {{0, 5}, {-5, 12}}]
```



- Graphics -

- This show the solid sphere radius a, set a = 1.

```
n10 = Show[Graphics[Circle[{0, 0}, 1], AspectRatio -> Automatic]]
```



- Graphics -

- This show the outer surface of the fluid shell radius b, b = 10.

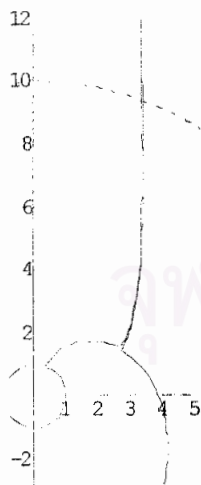
```
n20 = Show[Graphics[{Dashing[{0.05, 0.05}], Circle[{0, 0}, 10]},  
AspectRatio -> Automatic]]
```



- Graphics -

- This show the trajectories of paramagnetic particles in longitudinal mode as shown in figure 5.1. Dash line is the outer surface of the fluid shell.

```
fig01 = Show[n12, n14, n10, n20, PlotRange -> {{0, 5}, {-3, 12}},  
AspectRatio -> Automatic]
```



- Graphics -

■ Substitute the parameters for paramagnetic particle in transverse mode.

$$u21 = d1 /. \{V \rightarrow -6.65, \gamma \rightarrow 0.1, v^* \rightarrow 572.16313, K_g \rightarrow 0.58\}$$

$$w21 = d2 /. \{V \rightarrow -6.65, \gamma \rightarrow 0.1, v^* \rightarrow 572.16313, K_g \rightarrow 0.58\}$$

$$u22 = d3 /. \{V \rightarrow -6.65, \gamma \rightarrow 0.1\}$$

$$w22 = d4 /. \{V \rightarrow -6.65, \gamma \rightarrow 0.1\}$$

$$\frac{286.082 \left(1 + 3 \cos[2\theta[t]] + \frac{0.58 (5 + 3 \cos[2\theta[t]])}{r[t]^3} \right)}{r[t]^4}$$

$$\frac{7.82353 \cos[\theta[t]] \left(1 + \frac{1}{2 r[t]^3} - \frac{3}{2 r[t]} - 0.000434847 r[t]^2 \right)}{r[t]}$$

$$\frac{7.82353 \left(1 - \frac{1}{4 r[t]^3} - \frac{3}{4 r[t]} - 0.000869694 r[t]^2 \right) \sin[\theta[t]]}{r[t]}$$

$$\frac{572.163 \left(1 + \frac{0.29}{r[t]^3} \right) \sin[2\theta[t]]}{r[t]^5}$$

$$-7.82353 \cos[\theta[t]] \left(0.85 - \frac{9.77296}{r[t]^3} - \frac{3(-2 + \sqrt{6})}{4 r[t]} \right)$$

$$\frac{7.82353 \left(0.85 + \frac{4.88648}{r[t]^3} - \frac{3(-2 + \sqrt{6})}{8 r[t]} \right) \sin[\theta[t]]}{r[t]}$$

■ This find the solution for captured particle of paramagnetic particle in transverse mode.

n21 =

NDSolve[

$$\{r'[t] = \text{If}[r[t] < 10, - \frac{286.081565 \left(1 + 3 \cos[2\theta[t]] + \frac{0.58 (5 + 3 \cos[2\theta[t]])}{r[t]^3} \right)}{r[t]^4}$$

$$7.823529 \left(1 + \frac{1}{2 r[t]^3} - \frac{3}{2 r[t]} - 0.000435 r[t]^2 \right) \sin[\theta[t]],$$

$$-7.823529 \left(0.85 - \frac{9.772962}{r[t]^3} - \frac{3(-2 + \sqrt{6})}{4 r[t]} \right) \sin[\theta[t]],$$

$$\theta'[t] = \text{If}[r[t] < 10, - \frac{7.823529 \cos[\theta[t]] \left(1 - \frac{1}{4 r[t]^3} - \frac{3}{4 r[t]} - 0.000870 r[t]^2 \right)}{r[t]}$$

$$\frac{572.16313 \left(1 + \frac{0.29}{r[t]^3} \right) \sin[2\theta[t]]}{r[t]^5},$$

$$- \frac{7.823529 \cos[\theta[t]] \left(0.85 + \frac{4.886481}{r[t]^3} - \frac{3(-2 + \sqrt{6})}{8 r[t]} \right)}{r[t]} \}, r[0] = 12.916981,$$

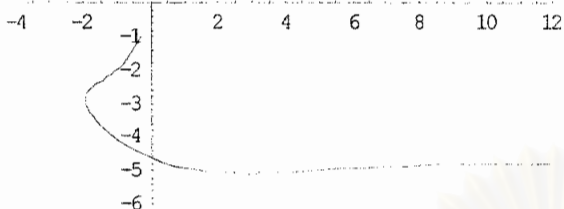
$$\theta[0] = 1.949865, \{r, \theta\}, \{t, 0, 2.654746\}]$$

{r → InterpolatingFunction[{{0., 2.65475}}, <>],

\theta → InterpolatingFunction[{{0., 2.65475}}, <>]]}

■ This plots the solution obtained.

```
n22 = ParametricPlot[Evaluate[{r[t] Sin[θ[t]], r[t] Cos[θ[t]]} /. n21],
  {t, 0, 2.654746}, PlotRange → {{-4, 12}, {-6, 0}}, AspectRatio → Automatic]
```



- Graphics -

■ This find the solution for the trajectory of paramagnetic particle in transverse mode. The conditions specify for the particle which don't move toward the solid sphere.

n23 =

NDSolve[

$$r'[t] = \text{If}[r[t] < 10, -\frac{286.081565 (1 + 3 \cos[2\theta[t]] + \frac{0.58 (5.3 \cos[2\theta[t]])}{r[t]^3})}{r[t]^4} - 7.823529 \left(1 + \frac{1}{2r[t]^3} - \frac{3}{2r[t]} - 0.000435 r[t]^2\right) \sin[\theta[t]],$$

$$-7.823529 \left(0.85 - \frac{9.772962}{r[t]^3} - \frac{3(-2 + \sqrt{6})}{4r[t]}\right) \sin[\theta[t]],$$

$$\theta'[t] = \text{If}[r[t] < 10, -\frac{7.823529 \cos[\theta[t]] \left(1 - \frac{1}{4r[t]^3} - \frac{3}{4r[t]} - 0.000870 r[t]^2\right)}{r[t]}$$

$$-\frac{572.16313 \left(1 + \frac{0.29}{r[t]^3}\right) \sin[2\theta[t]]}{r[t]^5},$$

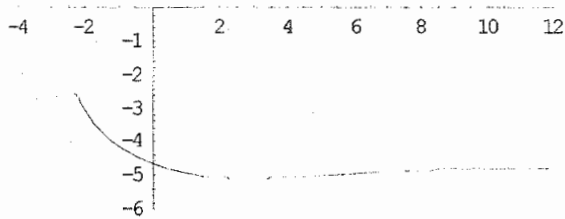
$$-\frac{7.823529 \cos[\theta[t]] \left(0.85 + \frac{4.886481}{r[t]^3} - \frac{3(-2 + \sqrt{6})}{8r[t]}\right)}{r[t]}, r[0] == 12.920685,$$

$$\theta[0] == 1.950584], \{r, \theta\}, \{t, 0, 3.5\}$$

```
{r → InterpolatingFunction[{{0., 3.5}}, <>],
  θ → InterpolatingFunction[{{0., 3.5}}, <>]}
```

■ This plots the solution obtained

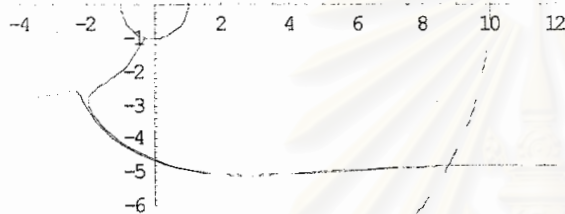
```
n24 = ParametricPlot[Evaluate[{r[t] Sin[θ[t]], r[t] Cos[θ[t]]} /. n23],
  {t, 0, 3.5}, PlotRange → {{-4, 12}, {-6, 0}}, AspectRatio → Automatic]
```



- Graphics -

■ This show the trajectories of paramagnetic particles in transverse mode as shown in figure 5.2. Dash line is the outer surface of the fluid shell.

```
fig02 = Show[n22, n24, n10, n20, PlotRange -> {{-4, 12}, {-6, 0}},
  AspectRatio -> Automatic]
```



- Graphics -

■ Substitute the parameters for diamagnetic particle in longitudinal mode.

```
u31 = d1 /. {V -> -6.65, γ -> 0.1, v* -> -572.16313, Ks -> 0.58}
```

```
w31 = d2 /. {V -> -6.65, γ -> 0.1, v* -> -572.16313, Ks -> 0.58}
```

```
u32 = d3 /. {V -> -6.65, γ -> 0.1}
```

```
w32 = d4 /. {V -> -6.65, γ -> 0.1}
```

$$286.082 \left(1 + 3 \cos[2\theta[t]] + \frac{0.58(5+3\cos[2\theta[t]])}{r[t]^3} \right) r[t]^4$$

$$7.82353 \cos[\theta[t]] \left(1 + \frac{1}{2r[t]^3} - \frac{3}{2r[t]} - 0.000434847 r[t]^2 \right)$$

$$7.82353 \left(1 - \frac{1}{4r[t]^3} - \frac{3}{4r[t]} - 0.000869694 r[t]^2 \right) \sin[\theta[t]] r[t]$$

$$\frac{572.163 \left(1 + \frac{0.29}{r[t]^3} \right) \sin[2\theta[t]]}{r[t]^5}$$

$$-7.82353 \cos[\theta[t]] \left(0.85 - \frac{9.77296}{r[t]^3} - \frac{3(-2+\sqrt{6})}{4r[t]} \right)$$

$$7.82353 \left(0.85 + \frac{4.88648}{r[t]^3} - \frac{3(-2+\sqrt{6})}{8r[t]} \right) \sin[\theta[t]] r[t]$$

■ This find the solution for the trajectory of diamagnetic particle in longitudinal mode. The conditions specify for the particle which don't move toward the solid sphere.

n33 =

```
NDSolve[
  {r'[t] == If[r[t] < 10,
    
$$\frac{286.081565 (1 + 3 \cos[2\theta[t]] + \frac{0.58 (5 + 3 \cos[2\theta[t]])}{r[t]^3})}{r[t]^4}$$

    
$$7.823529 \cos[\theta[t]] \left(1 + \frac{1}{2 r[t]^3} - \frac{3}{2 r[t]} - 0.000435 r[t]^2\right),$$

    
$$-7.823529 \cos[\theta[t]] \left(0.85 - \frac{9.772962}{r[t]^3} - \frac{3(-2 + \sqrt{6})}{4 r[t]}\right)],$$

    
$$\theta'[t] == \text{If}[r[t] < 10, \frac{7.823529 \left(1 - \frac{1}{4 r[t]^3} - \frac{3}{4 r[t]} - 0.000870 r[t]^2\right) \sin[\theta[t]]}{r[t]}$$

    
$$\frac{572.16313 \left(1 + \frac{0.29}{r[t]^3}\right) \sin[2\theta[t]]}{r[t]^5},$$

    
$$\frac{7.823529 \left(0.85 + \frac{4.886481}{r[t]^3} - \frac{3(-2 + \sqrt{6})}{8 r[t]}\right) \sin[\theta[t]]}{r[t]}], r[0] = 12.477836,$$

    
$$\theta[0] = 0.277639], \{r, \theta\}, \{t, 0, 3\}$$

  }, {r → InterpolatingFunction[{{0., 3.}}, <>],
    
$$\theta \rightarrow \text{InterpolatingFunction}[\{0., 3.\}, \langle \rangle]}$$


```

■ This plots the solution obtained.

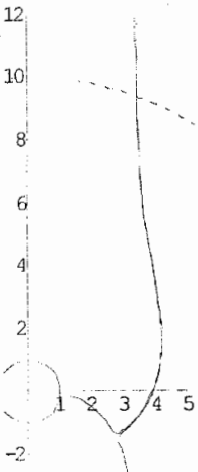
```
n34 = ParametricPlot[Evaluate[{r[t] Sin[θ[t]], r[t] Cos[θ[t]]} /. n33],
  {t, 0, 3}, PlotRange → {{0, 5}, {-4, 12}}
```



- Graphics -

■ This show the trajectories of diamagnetic particles in longitudinal mode as shown in figure 5.3. Dash line is the outer surface of the fluid shell.

```
fig03 = Show[n32, n34, n10, n20, PlotRange -> {{0, 5}, {-3, 12}},
  AspectRatio -> Automatic]
```



- Graphics -

■ Substitute the parameters for diamagnetic particle in transverse mode.

```
u41 = d1 /. {V -> -6.65, γ -> 0.1, v* -> -572.16313, Ks -> 0.58}
```

```
w41 = d2 /. {V -> -6.65, γ -> 0.1, v* -> -572.16313, Ks -> 0.58}
```

```
u42 = d3 /. {V -> -6.65, γ -> 0.1}
```

```
w42 = d4 /. {V -> -6.65, γ -> 0.1}
```

$$286.082 \left(1 + 3 \cos[2\theta[t]] + \frac{0.58(5+3\cos[2\theta[t]])}{r[t]^3} \right) r[t]^4$$

$$7.82353 \cos[\theta[t]] \left(1 + \frac{1}{2r[t]^3} - \frac{3}{2r[t]} - 0.000434847 r[t]^2 \right)$$

$$7.82353 \left(1 - \frac{1}{4r[t]^3} - \frac{3}{4r[t]} - 0.000869694 r[t]^2 \right) \sin[\theta[t]] r[t]$$

$$572.163 \left(1 + \frac{0.29}{r[t]^3} \right) \sin[2\theta[t]] r[t]^5$$

$$-7.82353 \cos[\theta[t]] \left(0.85 - \frac{9.77296}{r[t]^3} - \frac{3(-2+\sqrt{6})}{4r[t]} \right)$$

$$7.82353 \left(0.85 + \frac{4.88648}{r[t]^3} - \frac{3(-2+\sqrt{6})}{8r[t]} \right) \sin[\theta[t]] r[t]$$

■ This find the solution for captured particle of diamagnetic particle in transverse mode.

n41 =

NDSolve[

$$\begin{aligned}
 r'[t] = & \text{If}[r[t] < 10, \frac{286.081565 \left(1 + 3 \cos[2\theta[t]] + \frac{0.58(5+3\cos[2\theta[t]])}{r[t]^3}\right)}{r[t]^4} - \\
 & 7.823529 \left(1 + \frac{1}{2r[t]^3} - \frac{3}{2r[t]} - 0.000435 r[t]^2\right) \sin[\theta[t]], \\
 & -7.823529 \left(0.85 - \frac{9.772962}{r[t]^3} - \frac{3(-2+\sqrt{6})}{4r[t]}\right) \sin[\theta[t]], \\
 \theta'[t] = & \text{If}[r[t] < 10, \frac{7.823529 \cos[\theta[t]] \left(1 - \frac{1}{4r[t]^3} - \frac{3}{4r[t]} - 0.000870 r[t]^2\right)}{r[t]} - \\
 & \frac{572.16313 \left(1 + \frac{0.29}{r[t]^3}\right) \sin[2\theta[t]]}{r[t]^5}, \\
 & \frac{7.823529 \cos[\theta[t]] \left(0.85 + \frac{4.886481}{r[t]^3} - \frac{3(-2+\sqrt{6})}{8r[t]}\right)}{r[t]}, r[0] == 12.308842,
 \end{aligned}$$

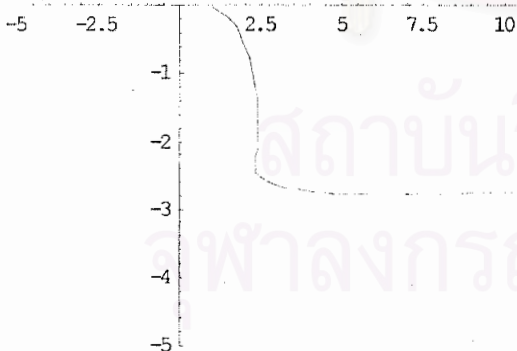
$$\theta[0] = 1.795281, \{r, \theta\}, \{t, 0, 2.7\}]$$

{r → InterpolatingFunction[{{0., 2.7}}, <>],

θ → InterpolatingFunction[{{0., 2.7}}, <>]}

■ This plots the solution obtained.

n42 = ParametricPlot[Evaluate[{r[t] Sin[θ[t]], r[t] Cos[θ[t]]} /. n41],
 {t, 0, 2.6675}, PlotRange → {{-5, 12}, {-5, 0}}]



- Graphics -

■ This find the solution for the trajectory of diamagnetic particle in transverse mode. The conditions specify for the particle which don't move toward the solid sphere.

n43 =

NDSolve[

$$r'[t] = \text{If}[r[t] < 10, \frac{286.081565 \left(1 + 3 \cos[2\theta[t]] + \frac{0.58 (5 + 3 \cos[2\theta[t]])}{r[t]^3}\right)}{r[t]^4} - 7.823529 \left(1 + \frac{1}{2r[t]^3} - \frac{3}{2r[t]} - 0.000435 r[t]^2\right) \sin[\theta[t]],$$

$$-7.823529 \left(0.85 - \frac{9.772962}{r[t]^3} - \frac{3(-2 + \sqrt{6})}{4r[t]}\right) \sin[\theta[t]],$$

$$\theta'[t] = \text{If}[r[t] < 10, -\frac{7.823529 \cos[\theta[t]] \left(1 - \frac{1}{4r[t]^3} - \frac{3}{4r[t]} - 0.000870 r[t]^2\right)}{r[t]},$$

$$\frac{572.16313 \left(1 + \frac{0.29}{r[t]^3}\right) \sin[2\theta[t]]}{r[t]^5},$$

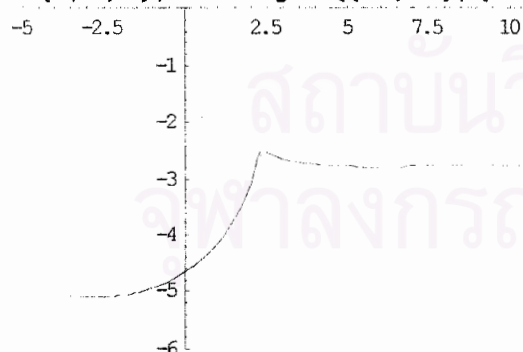
$$-\frac{7.823529 \cos[\theta[t]] \left(0.85 + \frac{4.886481}{r[t]^3} - \frac{3(-2 + \sqrt{6})}{8r[t]}\right)}{r[t]}, r[0] = 12.311072,$$

$$\theta[0] = 1.796073], \{r, \theta\}, \{t, 0, 4\}$$

{{r → InterpolatingFunction[{{0., 4.}}, <>],
 $\theta \rightarrow$ InterpolatingFunction[{{0., 4.}}, <>]}

■ This plots the solution obtained.

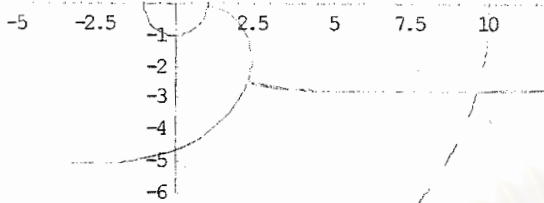
n44 = ParametricPlot[Evaluate[{r[t] Sin[θ [t]], r[t] Cos[θ [t]]} /. n43],
 {t, 0, 4}, PlotRange → {{-5, 12}, {-6, 0}}



- Graphics -

■ This show the trajectories of diamagnetic particles in transverse mode as shown in figure 5.4. Dash line is the outer surface of the fluid shell.

```
fig04 = Show[n42, n44, n10, n20, PlotRange -> {{-5, 12}, {-6, 0}},
  AspectRatio -> Automatic]
```



- Graphics -



สถาบันวิทยบริการ
จุฬาลงกรณ์มหาวิทยาลัย

Biography

Mr. Sakon Sansongsiri was born on May 6, 1974 in Chiangmai, Thailand. From 1993 to 1996 he was a student supported by the Development and Promotion of Science and Technology Talents Project (DPST) to study at Chiangmai University. He graduated with a Bachelor Degree in Physics from the Faculty of Science in 1996. Since 2000 he has been a graduate student in the Physics Department at Chulalongkorn University with the scholarship under the Lecturer Development Project of the Ministry of University Affairs.

Mr. Sakon presented posters based on his research papers in the 24th and 28th Congress on Science and Technology of Thailand entitled “High Power Trigger” in 1998 and “Laminar Flow Velocity Field from a Green’s Function” in 2002, respectively, at Queen Sirikit National Convention Center, Bangkok.



สถาบันวิทยบริการ
จุฬาลงกรณ์มหาวิทยาลัย